Durham E-Theses

Galactic gamma bays and the origin of cosmic rays
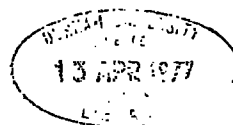
Dodds, D.

How to cite:

GALACTIC GAMMA RAYS AND THE ORIGIN OF

COSMIC RAYS

A Thesis submitted to the University of Durham
for the Degree of Doctor of Philosophy.

by

D. DODDS B.Sc.

GREY COLLEGE

13 APR 1977

FEBRUARY 1977

ABSTRACT

The question of the origin of the cosmic radiation is a fundamental problem in high energy astrophysics, this thesis is concerned with one particular aspect of this question namely, whether or not the cosmic ray sources are Galactic or Extragalactic. This problem is investigated through the results of Galactic Gamma-ray astronomy.

The main mechanism for gamma ray production are discussed. The observational results of Galactic Gamma ray astronomy are described. Theories about the Galactic cosmic ray sources and the distribution of these sources are described and related to the resulting distribution of cosmic rays in various propagation models. The distribution of gas in the galaxy is described.

Calculations are presented which indicate that the role of Inverse Compton Scattering in producing the observed Galactic Gamma ray intensity is small. The reason for the disagreement of this result with earlier results is analysed.

The distribution of cosmic rays in the inner Galaxy (0-10 kpc from the Galactic Centre) is determined from a comparison of the distribution of Gamma ray emissivity and the hydrogen distribution, this is found to follow the distribution of sources between 6 - 10 kpc. The penetration of dense molecular clouds by cosmic rays is investigated. It is concluded that the uncertainties in the hydrogen distribution do not permit us to rule out an Extragalactic origin, from the inner Galaxy data .

The distribution of gamma ray intensity in the Galactic anticentre is modelled on Galactic and Extragalactic theories and the predictions of the Galactic model are found to be in excellent agreement with observation. The cosmic ray distribution is found to be consistent with the origin in Supernovae or their remnants.

It is concluded that there is rather strong evidence for the majority of cosmic ray nuclei between 1 and 10 GeV having been produced within the Galaxy.

PREFACE

The work presented in this thesis was carried out between 1973 and 1976 while the author was a research student under the supervision of Professor A.W.Wolfendale in the Physics Department of the University of Durham.

In 1975 a visit was made to the Institute of Nuclear Research in Lodz, Poland, to work with Dr. J.Wdowczyk.

Some of the work reported here was carried out in collaboration with Drs A.W.Strong and J.Wdowczyk but most represents the work of the author.

The results obtained in this thesis have been reported in the following papers

Dodds, Strong, Wolfendale & Wdowczyk, Nature, 250, 716, (1974).

Dodds, Strong, Wolfendale & Wdowczyk, Proc. 9th ESLAB Symposium Frascati, Italy. ESRO SP 106. 221.

Dodds, Strong & Wolfendale, J.Phys. A., 8, 624, (1975).

Dodds, Strong & Wolfendale, Mon. Not. R.Astro. Soc., 171, 569, (1975).

Dodds, Strong & Wolfendale, Proc. 19th Int. Conf. Cosmic Rays, 1, 80, (1975).

Dodds, Wolfendale & Wdowczyk, Mon. Not. R.Astr. Soc., 176, 345, (1976).

Dodds & Wolfendale, GSFC Symposium on Gamma-ray Astronomy, June 1976.

CONTENTS   <u>PAGE</u>

CHAPTER ONE

INTRODUCTION

The question of the origin of the cosmic radiation is a fundamental problem in high energy astrophysics. This thesis is concerned with the contribution to the solution of this problem which may be gained from a study of the Galactic gamma ray emission.

There are two schools of thought regarding the origin of the cosmic rays. According to the first, the cosmic rays which are observed at Earth are Galactic in origin, possibly the result of cosmic ray acceleration in supernova explosions. One of the basic arguments in favour of this hypothesis is based on the energy injection required to maintain the present density. The observed energy density of cosmic rays with energy $>1\text{GeV}$ is about 0.5eV cm^{-3} (see for example, Wolfendale, 1973). If this density is constant throughout a disk confinement region of 15 kpc radius and 1 kpc thickness, then the total energy content is $\simeq 5 \ 10^{54}$ ergs. If now equilibrium is assumed and the observed mean path length of 5 g cm^{-2} (Shapiro et al, 1971) is interpreted as a mean lifetime of $3 \ 10^{6}$ years, this would imply an energy injection rate of $10^{40 \ - \ 41}\text{ergs s}^{-1}$. A similar value is obtained if a halo confinement region is assumed (Ginzburg and Syrovatskii, 1964). For comparison a supernova rate of 1 per 26 years and a typical supernova energy release of 10^{50-51}ergs gives an energy release rate of $10^{41-42}\text{ergs s}^{-1}$. However, there are some problems with this picture. There is no direct

evidence for the acceleration of cosmic rays in super-
novae and there are difficulties in reconciling the
observed low anisotropy of the cosmic rays with the
short lifetime, (see Osborne, 1975).

According to the second school, the cosmic rays
are extragalactic in origin. In this case the cosmic
ray density outside the Galaxy will be equal to the
density inside. While there is no doubt that there
do exist powerful extragalactic cosmic ray sources
capable of filling considerable volumes of intergalactic
space with relativistic particles (Willis et al, 1974),
the principal difficulty is one of providing enough
energy. The energy requirement to populate the entire
universe with a cosmic ray density of 0.5 eV cm^{-3}
represents about 0.5% of the total rest mass of the
visible matter. This difficulty is reduced somewhat
in the modified extragalactic model of Brecher and
Burbidge (1972). These authors suggest that at
1 GeV the confinement volume may be restricted to the
regions of space which contain galaxy clusters. In
particular they envisage confinement to the supercluster
for cosmic rays with energies of 10^9 - 10^{16} eV. In this
case the energy requirements are rather less severe.

There is general agreement between these schools
that energy losses for electrons preclude an extra-
galactic origin for these particles. Similarly there
is agreement that the high isotropy at 10^{17} eV requires
cosmic rays of this energy to be mainly extragalactic.
The area of controversy is confined to nuclei with
energy between 10^9 and 10^{17} eV.

Ginzburg (1972) has proposed a test for these models which consists of searching for gamma-ray emission from the direction of the Magellanic Clouds. The argument being, that extragalactic cosmic rays interacting with the hydrogen of the Clouds will produce π^o mesons which decay to give gamma rays. Thus observation (or non-observation) of gamma rays will indicate the presence (or absence) of cosmic rays. However, the present observational limits are not good enough to resolve this debate.

This thesis is concerned with the problem of identifying which of the above models is the more satisfactory at the cosmic ray energies responsible for gamma ray production. Secondarily it is aimed at the related problem of investigating the cosmic ray distribution in the Galaxy using the available Gamma-ray astronomical data.

With these aims in mind Chapter 2 describes the important gamma ray production mechanisms. Chapter 3 reviews the observational results of Galactic gamma-ray astronomy. Chapter 4 describes the candidates for the Galactic cosmic ray sources, their distribution and the distribution of cosmic rays which may be expected. In Chapter 5 some of the important features of the Interstellar gas are described. In Chapter 6 a model is constructed for the distribution of gamma ray intensity due to Inverse Compton Scattering. The contribution to gamma ray production from π^o decay and bremsstrahlung are calculated in Chapter 7 and used to

find the Galactic distribution of cosmic rays.   In
Chapter 8 the gamma ray emission from the Galactic
anticentre is modelled using the results from Chapter
6 and 7.   Finally Chapter 9 discusses some of the
conclusions reached.

REFERENCES

Brecher, K & Burbidge, G.R., 1972. Astrophys. J., 174, 253.

Ginzburg, V.L. & Syrovatski, S.I., 1964. In 'The Origin of Cosmic Rays', Pergamon.

Ginzburg, V.L., 1972. Nature Phys. Sci., 239, 8.

Osborne, J.L., 1975. In 'Origin of Cosmic Rays', eds J.L.Osborne and A.W.Wolfendale, Reidel, Dordrecht.

Shapiro, M.M., Silverberg, R. & Tsao, C.H., 1971. Proc. 12th. Int. Conf. on Cosmic Rays, University of Tasmania. 1, 221.

Willis, A.G., Strom, R.G. & Wilson, A.S., 1974. Nature, 250, 625.

Wolfendale, A.W., 1973. In 'Cosmic Rays at Ground Level', ed. A.W.Wolfendale, The Institute of Physics, London.

CHAPTER TWO

GAMMA-RAY PRODUCTION MECHANISMS

2.1 Introduction

Gamma ray production in the Galaxy is dominated by three processes; π^0 decay, bremsstrahlung and inverse Compton scattering. This chapter will describe some of the important features of these processes, their cross-sections and spectrum of gamma rays which results.

In the sections which follow and later chapters the following notation is used. $Q_x(E_\gamma, \bar{r})$ is the number of gamma rays of energy $> E_\gamma$ per cm^3 per second produced by process 'x' at $\bar{r}$ and is called the volume emissivity. $Q_x(E_\gamma)$ is the volume emissivity due to process 'x' at the solar system. In addition to these we will also use $q_x(E_\gamma, \bar{r})$ as the gamma production rate per hydrogen atom.

Thus, the intensity of gamma radiation at the Earth, $I(>E_\gamma)$ due to π^0 production is

$$I(>E_\gamma) = \int_0^\infty \frac{Q_{\pi^0}(E_\gamma, \bar{r})}{4\pi} \, dr$$

or

$$= \int_0^\infty \frac{q_{\pi^0}(E_\gamma, \bar{r})\,n_H(\bar{r})}{4\pi} \, dr \qquad 1.$$

2.2 Gamma-ray production from cosmic ray nucleus - interstellar gas nucleus collisions.

2.2.1 Collisions of protons with hydrogen

It will be seen later that the most prolific source of 100 MeV gamma rays is the decay of π^0 mesons produced

in inelastic collisions of cosmic ray protons with interstellar hydrogen. The main channels for meson production are
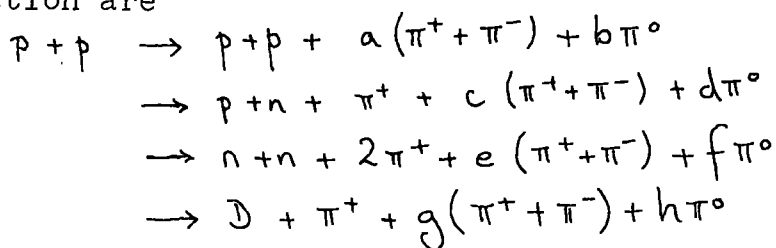
$$p + p \longrightarrow p + p + a(\pi^+ + \pi^-) + b\pi^o$$
$$\longrightarrow p + n + \pi^+ + c(\pi^+ + \pi^-) + d\pi^o$$
$$\longrightarrow n + n + 2\pi^+ + e(\pi^+ + \pi^-) + f\pi^o$$
$$\longrightarrow D + \pi^+ + g(\pi^+ + \pi^-) + h\pi^o \qquad 2.$$

where in equation 2, a to h are positive constants and p, n, D are protons, neutrons and Deuterons respectively.

The minimum kinetic energy T_{min} for production of n mesons is approximately given by the relation

$$T_{min} \simeq n(280 + 10n) \quad MeV \qquad 3.$$

Thus, for single meson production the threshold is $\simeq$ 290 MeV. At the threshold the reactions are

$$p + p \longrightarrow p + n + \pi^+ \qquad 4.$$

$$p + p \longrightarrow p + p + \pi^o \qquad 5.$$

$$p + p \longrightarrow D + \pi^+ \qquad 6.$$
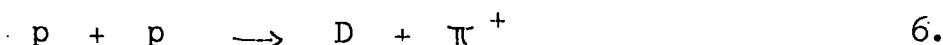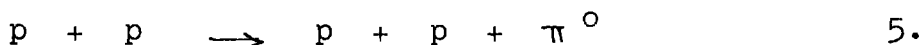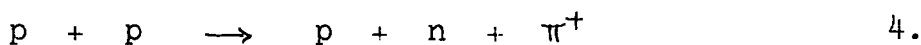
From the point of view of gamma ray production the reaction of equation 5 is the most important, since in almost 100% of cases the neutral pion decays to two gamma rays.

The total γ-ray yield, $Q_{\pi^o}(\bar{r})$, from π^o decay is given by

$$Q_{\pi^o}(\bar{r}) = 2.4\pi \int_0^\infty n_H(\bar{r}) I_p(T,\bar{r}) \sigma_{\pi^o_{pp}}(T) m_{\pi^o_{pp}}(T) dT \qquad 7.$$

where $I_p(T,\bar{r}) dT$ is the cosmic ray proton intensity at r with kinetic energy T, n_H is the density of interstellar hydrogen, $\sigma_{\pi^o_{pp}}(T)$ is the cross-section for production of π^o mesons in proton hydrogen collision and $m_{\pi^o_{pp}}(T)$ is the average multiplicity of π^o mesons in proton-hydrogen collisions.

Measurements of the product $\sigma_{\pi^\circ pp}(T) m_{\pi^\circ pp}(T)$ are now available from accelerator experiments up to kinetic energies of 1000 GeV. Figure 1 is a compilation of recent measurements from Stecker (1973). The product of cross-section and multiplicity, $\sigma_{\pi^\circ}(T)\, m_{\pi^\circ}(T)$ are shown in figure 2 for all three π mesons. Since the charged π mesons eventually decay to form secondary cosmic ray electrons it is obvious that regions of high gamma ray emmissivity will also be regions of copious secondary electron production.

The relative importance of different proton energies for π° production is illustrated in figure 3 which shows the product $I_p(T)\sigma_{\pi^\circ pp}(T)\, m_{\pi^\circ pp}(T)$.

2.2.2   The contribution from interstellar Helium

The yield from this process is given by

$$Q_{\pi^\circ}(\bar{r}) = 8\pi \int n_{He}(\bar{r}) I_p(T,\bar{r}) \sigma_{\pi^\circ p\alpha}(T) m_{\pi^\circ p\alpha}(T) dT \qquad 8.$$

The threshold kinetic energy for the production of n pions in an enelstic collision between a cosmic ray proton and a Helium nucleus is given approximately by equation 9.

$$T_{th\ p-\alpha} \simeq 170n + 2.5n^2 \quad MeV \qquad 9.$$

Where T is the proton kinetic energy in MeV. Thus for n = 1 the threshold energy is $\simeq$ 172 MeV.

There exist few experimental measurements of the cross section $\sigma_{\pi^\circ p\alpha}(T)$ and multiplicity $m_{\pi^\circ p\alpha}(T)$ for π° production in proton-alpha particle collisions. The cross-section plotted in figure 1 is based at low energies on an empirical model for the cross-section
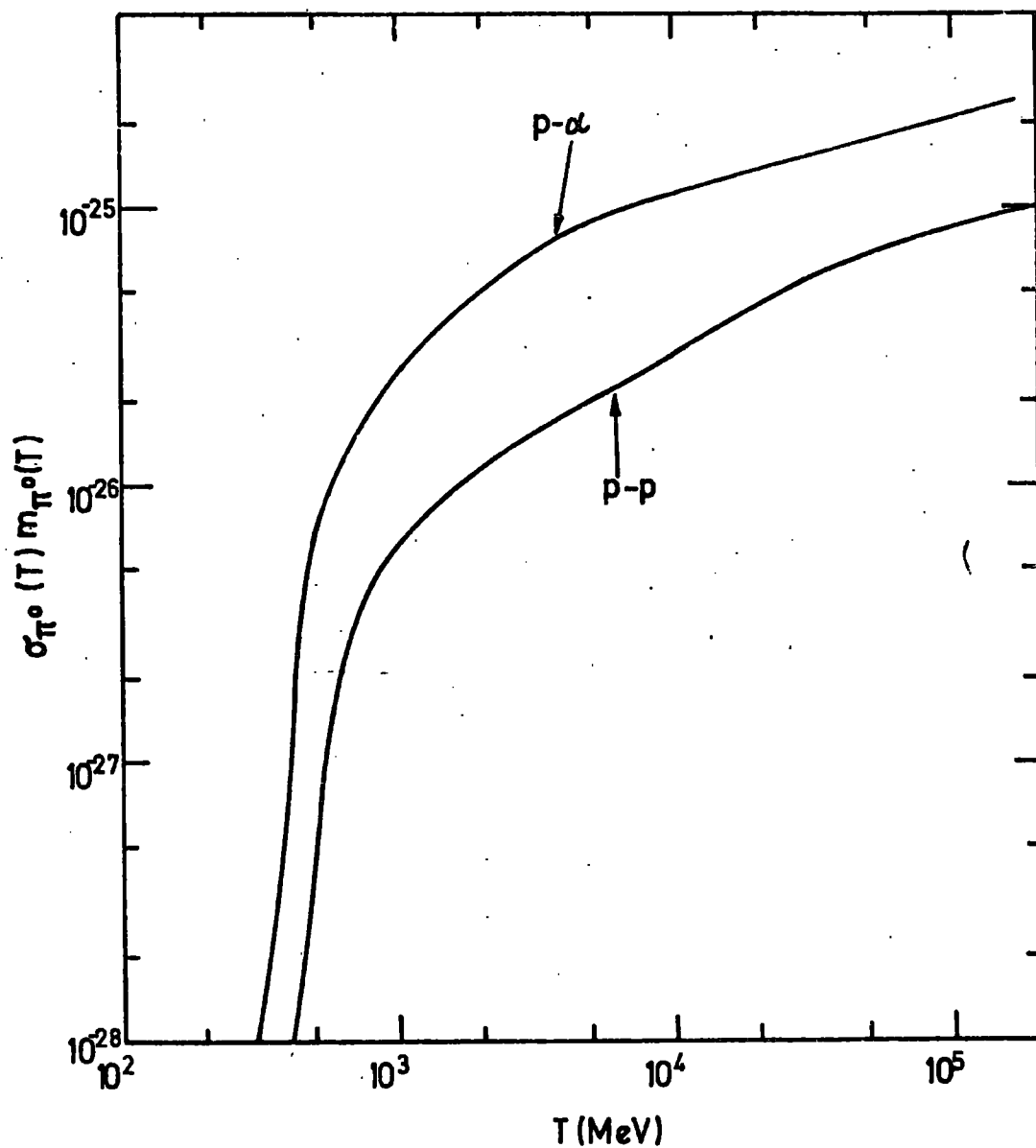
Figure 1.   The product of cross-section, σ, and multiplicity, m for π^o production in proton-proton collisions plotted against proton kinetic energy, T.
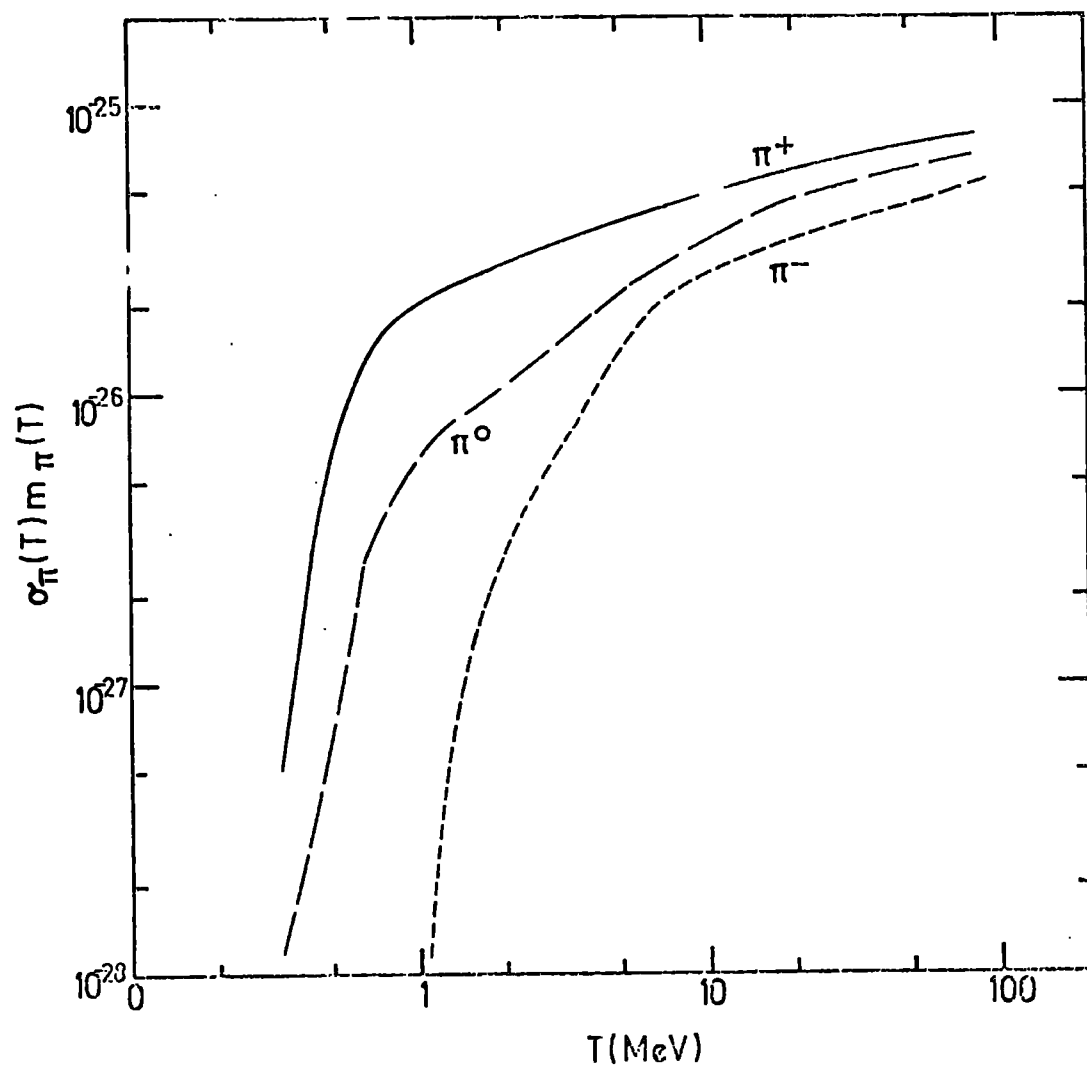
Figure 2.   The product of cross-section, σ and multiplicity, m, in proton-proton collisions for all three π mesons.
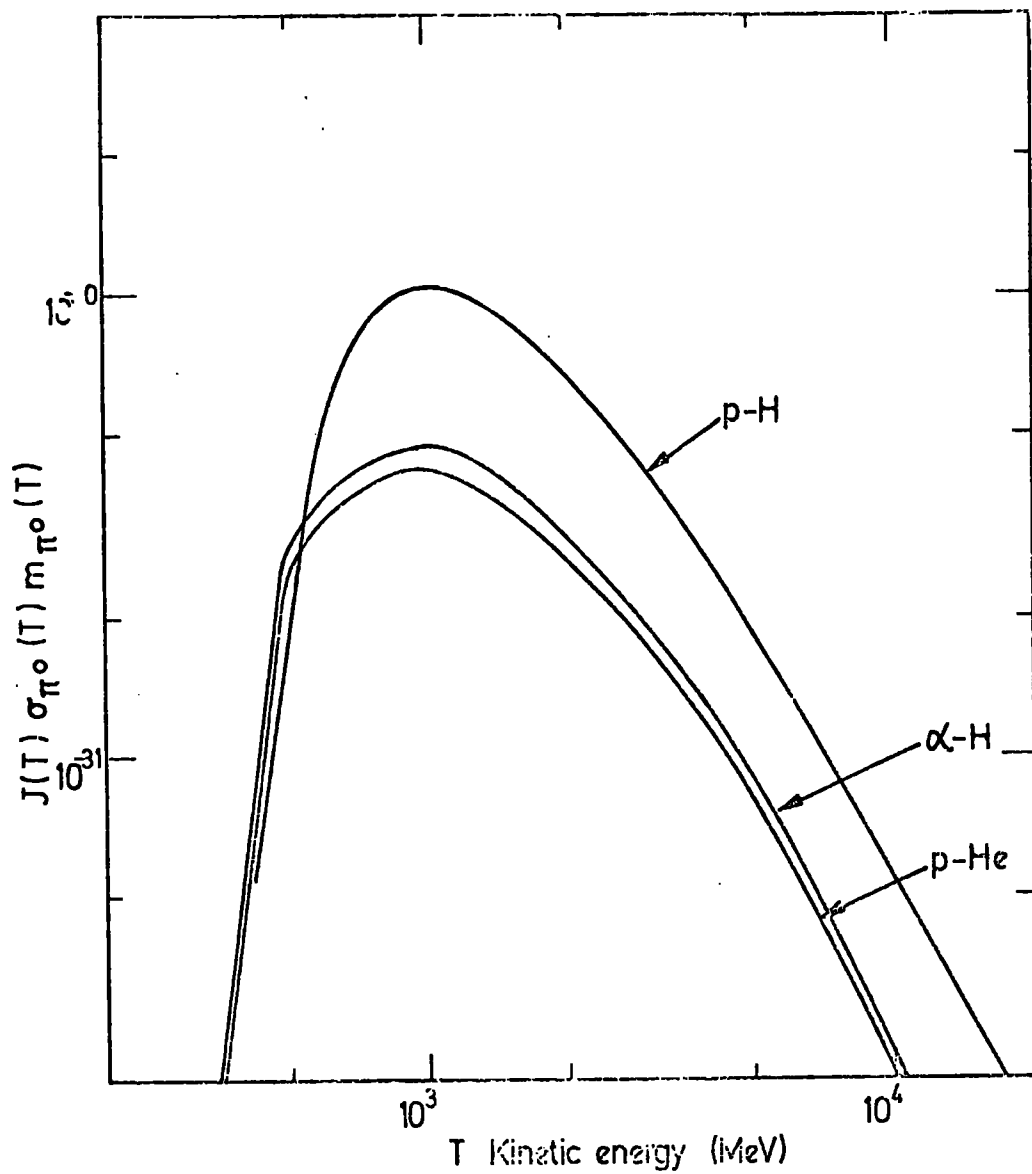
Figure 3.   The product $I_{CR}(T) \, \sigma_{\pi^o}(T) \, m_{\pi^o}(T)$ versus kinetic
energy, T, for π^o production in proton-proton, proton-
helium and alpha-hydrogen collisions.

for which the parameters are determined from experimental results on p - D and p - Li^6 collisions (Pollack and Fazio 1963). At high energies the cross-section is given by

$$\sigma_{pN} = s(Z\sigma_{pp} + Z\sigma_{pn}) \qquad 10.$$

where s is a parameter to include the effects of shadowing and is assumed to be 0.5 (Cavallo and Gould 1971). Thus, at high energies

$$\sigma_{p\alpha} \simeq 2\sigma_{pp} \qquad 11.$$

The product $(n_{He}/n_H)\ I_p(T)\sigma_{\pi^\circ p\alpha}(T)m_{\pi^\circ p\alpha}(T)$ is shown in figure 3.

2.2.3 The Contribution from cosmic ray α particle - interstellar hydrogen collisions

This process is identical with the p - He collisions discussed above. The total cross-section $\sigma_{\pi^\circ \alpha p}(T_\alpha)$ is equal to $\sigma_{\pi^\circ p\alpha}(T_p)$ at the same centre of mass (cms) energy. The relation between the laboratory kinetic energies T_p and T_α for which the cms energies are equal is given by equation 12.

$$m_\alpha T_p = m_p T_\alpha \qquad 12.$$

Since $m_\alpha \simeq 4m_p$ this gives

$$T_p \simeq \frac{T_\alpha}{4}$$

and the cross-sections $\sigma_{\pi^\circ p\alpha}$ and $\sigma_{\pi^\circ \alpha p}$ are the same for protons and alphas having the same kinetic energy per nucleon.

Figure 3 shows the product $I_\alpha(T)\sigma_{\pi^\circ \alpha p}(T)m_{\pi^\circ \alpha p}(T)$ where T is now the kinetic energy per nucleon. It can be seen from figure 3 that the total contribution from α-H and p - He collisions is approximately equal to

the contribution from p - H.

2.2.4 The Spectrum of gamma-rays from π^0 decay

This problem has been thoroughly discussed by several authors, for example Stecker (1970, 1975), Cavallo and Gould (1971) and Tkaczyk (1975). The differential spectra of π^0 gamma rays from these authors' work are in good agreement.

The most striking feature of the gamma ray spectrum from π^0 decay is its symmetry about $\log \frac{m_\pi \circ c^2}{2}$ on a logarithmic plot. This arises because the pion decays to two identical particles. A π^0 meson decaying at rest produces two gammas of identical energy $\frac{m_\pi \circ c^2}{2}$. If the pion decays in flight then the two gamma rays will have different energies. For a pion with energy $E_{\pi^0} = \gamma_{\pi^0} m_{\pi^0} c^2$ the maximum and minimum possible gamma-ray energies are

$$E_{\gamma max} = \frac{m_{\pi^0} c^2}{2} \gamma_{\pi^0} (1 + \beta_{\pi^0}) \qquad 13.$$

$$E_{\gamma min} = \frac{m_{\pi^0} c^2}{2} \gamma_{\pi^0} (1 - \beta_{\pi^0}) \qquad 14.$$

where $\beta_{\pi^0} = \upsilon_{\pi^0}/c$. The normalized distribution function for in flight decay is

$$f(E_\gamma) \, dE_\gamma = \frac{dE_\gamma}{m_{\pi^0} \gamma_{\pi^0} \beta_{\pi^0}} \qquad 15.$$

Figure 4 shows this distribution function for several different pion energies. A consequence of the symmetry seen in figure 4 is that any spectrum of pions will always give a differential spectrum of gamma rays which is symmetric about $\log \frac{m_{\pi^0} c^2}{2}$ on a logarithmic plot.

Figure 5 shows the integral gamma ray spectra calculated by Stecker (1973) and Cavallo and Gould (1971).
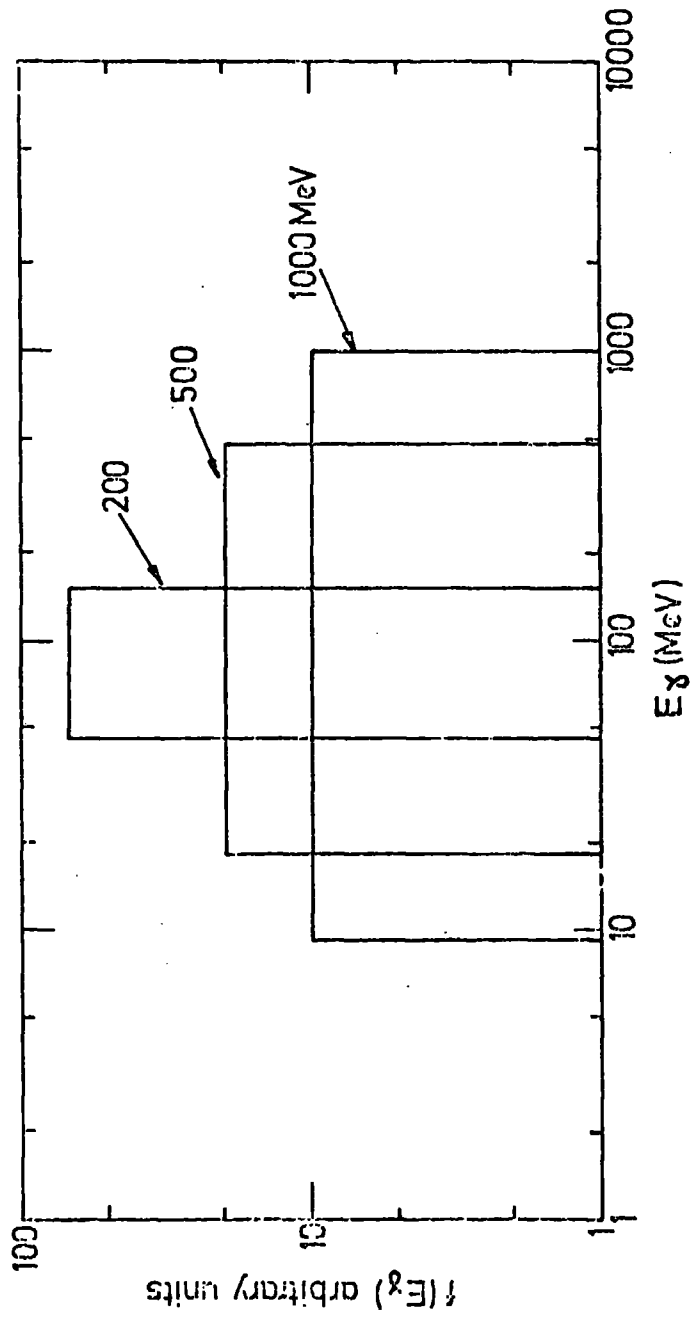
Figure 4. The distribution function of gamma rays produced by the decay of energetic π° mesons for three different energies.
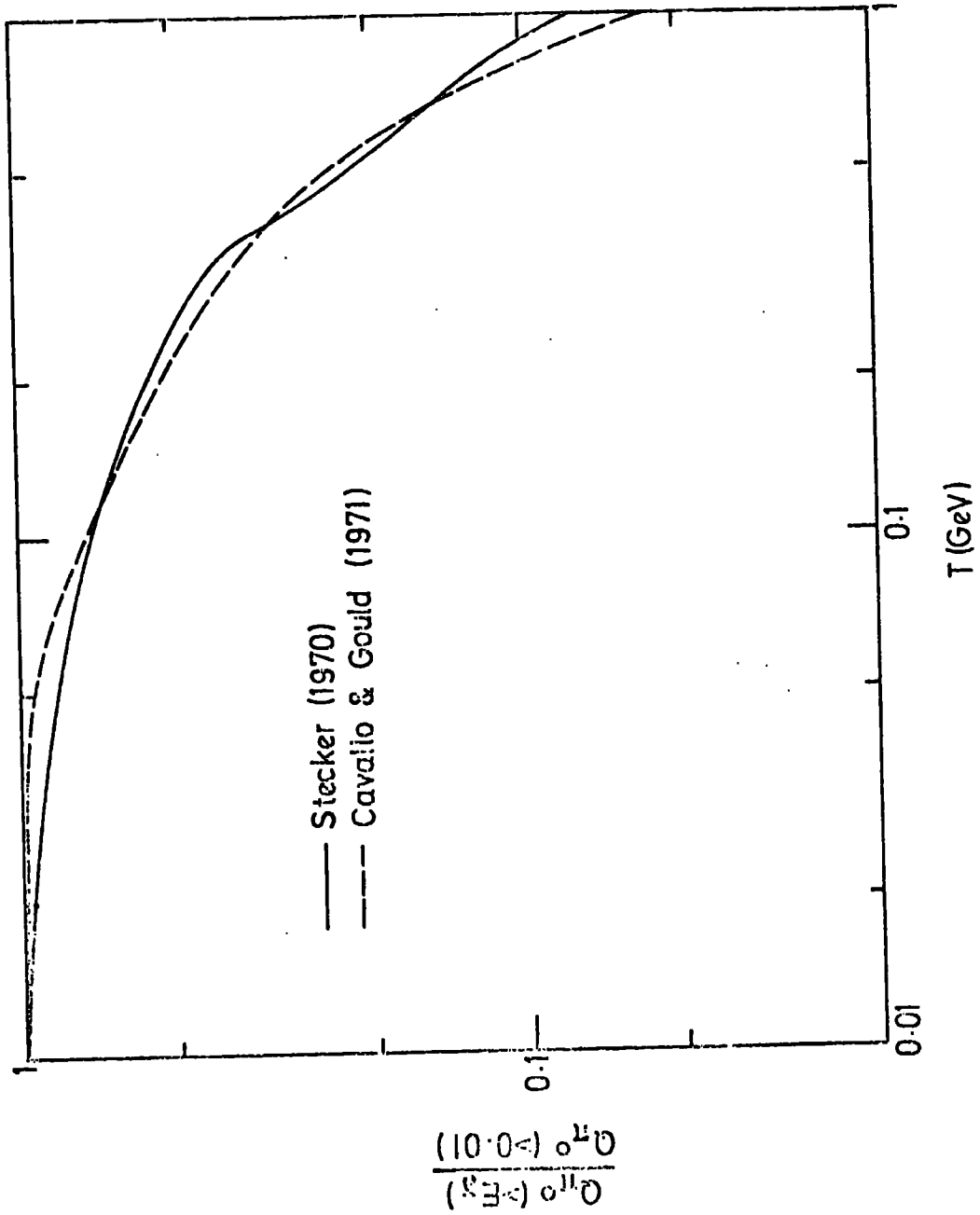
Figure 5.   The integral spectra of gamma rays from π^o decay as calculated by Stecker (1973) and Cavallo and Gould (1971).

The minor differences between the two spectra are
artefacts of the different models used by these authors.

2.3. Gamma-ray production in electron bremsstrahlung

In this process gamma-rays are produced in collisions
between cosmic ray electrons and the nuclei of interstellar
gas. In the collision the electron is deccelerated
and radiates a photon of energy $E_\gamma \leqslant E_e$ where E_e is
the electron energy. The details of the derivation
of the cross-section are given in Heitler (1954).

The cross-section $\sigma_B(E_\gamma, E_e)$ for production of a
photon of energy between E_γ and $E_\gamma + dE_\gamma$ by an extremely
relativistic electron in the field of a target nucleus of
charge Z is

$$\sigma_B(E_\gamma, E_e) \, dE_\gamma = \qquad\qquad (E_e \gg \mu)$$

$$2 \frac{Z^2 r_0^2}{137} \frac{dE_\gamma}{E_\gamma} \frac{E}{E_e} \left(\frac{E_e^2 + E^2}{2E_e E} - \frac{2}{3} \right) \left(2 \ln \left\{ \frac{2 E_e E}{\mu E_\gamma} \right\} - 1 \right) \qquad 16$$

where $E = E_e - E_\gamma$ is the energy of the electron
after the collision, r_0 is the classical electron radius
and μ is the electron rest mass. In the limit of low
energy photons (i.e. $E_\gamma \rightarrow 0$) the intensity $E_\gamma \sigma_B$
diverges logarithmically.

The cross-section given in equation 16 corresponds
to scattering by a pure Coulomb field. At the very
large impact parameters which correspond to production
of photons of very low energy the cross-section is
calculated including the screening effects of the
atomic electrons. In this case the cross-section
becomes

$$\sigma_B(E_\gamma, E_e) \, dE_\gamma = \frac{2 Z^2 r_0^2}{137} \frac{dE_\gamma}{E_\gamma} \frac{E}{E_e} \left[\left(\frac{E_e^2 + E^2}{E_e E} - \frac{2}{3} \right) 2 \ln(183 Z^{-1/3}) + \frac{2}{9} \right]$$

$$E_e \gg \mu \quad \& \quad \frac{E_e E}{\mu E_\gamma} \gg 137 \, Z^{-1/3} \qquad\qquad 17.$$

Heitler (1954).

The differential emissivity $\dfrac{\partial Q_B}{\partial L_\gamma}$ is given by equation 18.

$$\frac{\partial Q_B(E_\gamma, \bar{r})}{\partial E_\gamma} = \sum_j 4\pi \, n_j(\bar{r}) \int_{E_\gamma}^{\infty} I_e(E_e, \bar{r}) \, \sigma_{B,j}(E_\gamma, E_e) \, dE_e \qquad 18.$$

where $n_j(\bar{r})$ is the volume density of atoms of type j; $I_e(E_e, \bar{r})$ is the electron spectrum and $\sigma_{B,j}(E_\gamma, E_e)$ is the cross-section for bremsstrahlung of electrons on atoms of type j with nuclear charge z_j.

Since the screened cross-section of eq. 17 shows very little energy dependence the following approximation is often made.

$$\sigma_{B,j}(E_\gamma, E_e) \, dE_\gamma = \frac{M_j}{X_j} \frac{dE_\gamma}{E_\gamma} \qquad 19.$$

where M_j is the mass of the target atom in grammes and X_j is the radiation length in gm cm^{-2}. For hydrogen $X_H = 62.8$ gm cm^{-2} (Lang 1974).

Using the approximation given in eq. 19 in eq. 18 gives

$$\frac{\partial Q_B(E_\gamma, \bar{r})}{\partial E_\gamma} = 4\pi \, n_H(\bar{r}) \, \frac{I_e(>E_\gamma, \bar{r})}{E_\gamma} \, \frac{M_H}{X_H} \qquad 20.$$

A power-law differential electron spectrum $I_e(E_e \bar{r}) = A_e(\bar{r}) \, E_e^{-\Gamma}, (\Gamma > 2)$ yields

$$\frac{\partial Q_B(E_\gamma, \bar{r})}{\partial E_\gamma} = A_\gamma(\bar{r}) \, E_\gamma^{-\Gamma} \qquad 21.$$

Thus a differential electron spectrum of slope, Γ, gives a bremsstrahlung spectrum with the same slope.

The contribution of this process to the Galactic emission and the energy spectrum are considered in more detail in a later chapter.

2.4. Gamma Ray production in Inverse Compton Scattering

This is one of the most important energy loss mechanisms for relativistic electrons in the interstellar medium and was originally discussed from this point of view by Feenberg and Primakoff (1948). Since then the Inverse Compton (IC) process has been extensively discussed as a mechanism for creating high energy gamma rays (see, for example Felten and Morrison, 1966).

Essentially the process involves a low energy photon scattering off a relativistic electron and carrying off some of the electron's energy. Figure 6a illustrates this scattering process, for the case of an electron of energy, $E_e = \gamma M_e c^2$ moving to the right and scattering a photon of energy ϵ, creating a gamma ray of energy E_γ.

Figure 6b shows the geometry of the same process when viewed from the electron rest frame. (In this figure and below quantities measured in the rest frame frame will be denoted by a prime, thus E'). Equation 22 gives the relationship between the lab. and rest frame energies.

$$\epsilon = \gamma \epsilon' (1 - \beta \cos \alpha')$$
$$E_\gamma = \gamma E_\gamma (1 + \beta \cos \alpha_1')$$
$$\epsilon' = \gamma \epsilon (1 + \beta \cos \alpha)$$
$$E_\gamma' = \gamma E_\gamma (1 - \beta \cos \alpha_1)$$

22.

In the electron rest frame the scattering process becomes simply the ordinary Compton effect and hence the well known relation between the initial and final energies of the photons may be used. Thus

$$E_\gamma' = \frac{\epsilon'}{1 + \frac{\epsilon'}{m_e}(1 - \cos \theta')}$$

23.

LAB. FRAME

ELECTRON
REST FRAME

a)

b)
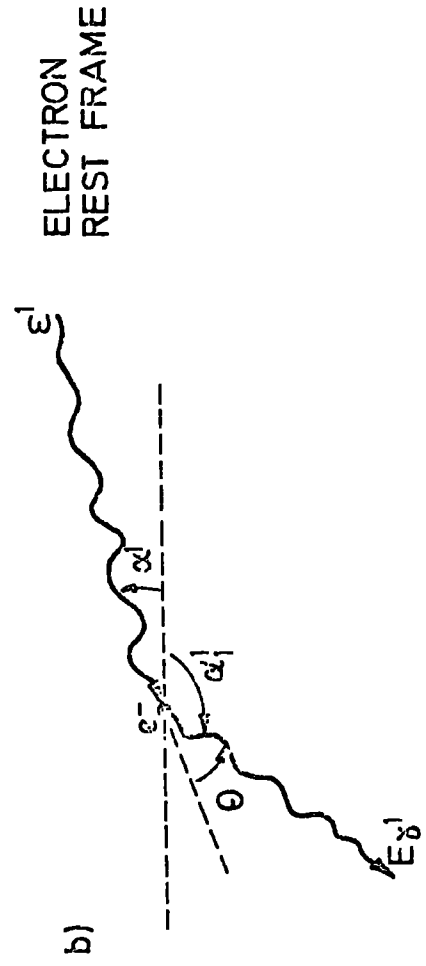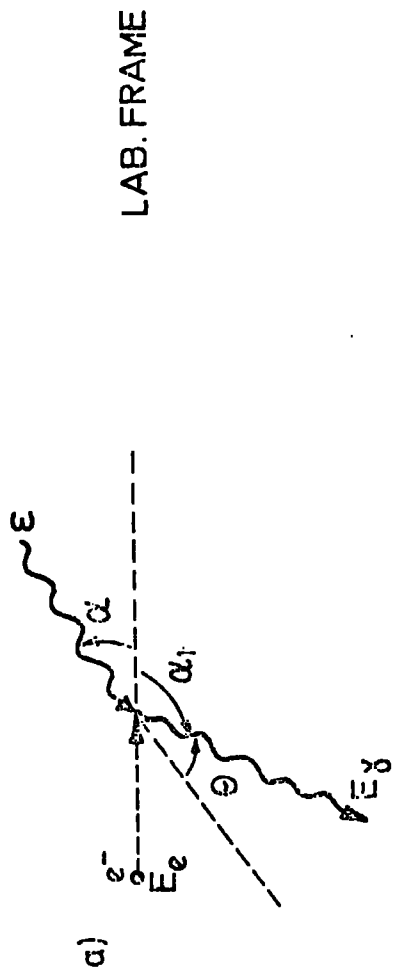
Figure 6a and 6b.   The inverse Compton scattering process,
showing the notation used above.

Substituting for E_γ and ϵ' in equation 23 using the relations in equation 22 gives

$$\frac{E_\gamma}{E_e} = \frac{\frac{\partial \epsilon}{M_e}(1 + \beta \cos \alpha')(1 + \beta \cos \alpha)}{1 + \frac{\gamma \epsilon}{m}(1 + \beta \cos \alpha)(1 - \cos \theta')} \qquad 24.$$

Examination of equation 24 shows that there are two interesting extreme cases; firstly for $\gamma \epsilon \ll M_e c^2$ then $E_\gamma \simeq \gamma^2 \epsilon$ and secondly that for $\gamma \epsilon \gg M_e c^2$ then $E_\gamma \simeq E_e$ In fact the former is simply equivalent to $\epsilon' \ll M_e c^2$ and in this limit the process in the rest frame becomes 'classical' Thomson scattering.

Now, in the interstellar medium the important photon energies lie between leV for starlight and $5 \ 10^{-4}$ eV for the 2.7° blackbody radiation. For these photons to produce 100 MeV gamma rays by this process requires electrons with γ's such that the first condition ($\gamma \epsilon \ll M_e c^2$) is satisfied. Clearly, describing this process as Inverse Compton Scattering is incorrect since strictly the process is Inverse Thomson Scattering.

The differential emissivity $\partial Q_{ic} / \partial E_\gamma$ is given by equation 25.

$$\frac{\partial Q_{ic}(E_\gamma, \bar{r})}{\partial E_\gamma} = 4\pi \int_{E_L}^{\infty} I_e(E_e, \bar{r}) \int_0^{\infty} n_{ph}(\epsilon, \bar{r}) \sigma_{ic}(E_\gamma, \epsilon, E_e) \, d\epsilon \, dE_e$$

$$25.$$

Where $I_e(E_e, \bar{r})$ is the spectrum of relativistic electrons, $n_{ph}(E, \bar{r})$ is the number density of photons with energy between ϵ and $\epsilon + d\epsilon$ and $\sigma_{ic}(E_\gamma, \epsilon, E_e)$ is the cross-section for gamma ray production by an electron of energy E_e scattering off the photon of energy ϵ.

The derivation of the cross-section $\sigma_{ic}(E_\gamma, \epsilon, E_e)$

from the Klein-Nishina cross-section is fairly simple

and is given by Ginzburg and Syrovatskii(1964). The

resulting expression for the cross-section is

$$\sigma_{IC}(E_\gamma, \epsilon, E_e) =$$

$$2\pi r_0^2 \left[\frac{m_e^2}{\epsilon E_e^2} + \frac{m_e^4 E_\gamma}{4\epsilon^2 E_e^4} - \frac{m_e^6 E_\gamma}{9\epsilon^3 E_e^5} + \frac{m_e^4 E_\gamma}{2\epsilon^2 E_e^4} \ln\left(\frac{m_e^2 E_\gamma}{4\epsilon E_e^2}\right) \right] \quad 26.$$

The cross-section may also be used to find $\langle E_\gamma \rangle$

the mean gamma ray energy which results from the collision.

This is given by

$$\langle E_\gamma \rangle = \frac{1}{\sigma_T} \int_0^{4\gamma^2\epsilon} E_\gamma \sigma_{IC}(E_\gamma, \epsilon, E_e)\, dE_\gamma \quad 27.$$

where

$$\sigma_T = \int_0^{4\gamma^2\epsilon} \sigma_{IC}(E_\gamma, \epsilon, E_e)\, dE_\gamma$$

$$= \text{Thomson cross-section}$$

Upon integration equation 27 gives

$$\langle E_\gamma \rangle = \frac{4}{3}\gamma^2\epsilon \quad 28.$$

A frequently used approximation for the cross-section

uses 28 thus

$$\sigma_{IC}(E_\gamma, \epsilon, E_e) = \sigma_T\, \delta\left(E_\gamma - \frac{4}{3}\left(\frac{E_e}{m_e}\right)^2 \epsilon\right) \quad 29.$$

For a power law electron spectrum of the type $A_e E_e^{-\Gamma}$

the spectrum of gamma rays which results from solving

equation 25 by using either 26 or the approximation 29

is also a power law, but of exponent $-(\Gamma + 1)/2$.

Thus the solution to 25 has the form

$$\frac{\partial Q}{\partial E_\gamma} = A_\gamma E_\gamma^{-\left(\frac{\Gamma + 1}{2}\right)} \quad 30.$$

The spectrum of gamma rays from this process will

be considered in detail in Chapter 6.

REFERENCES

Cavallo, G. & Gould, R.J., 1971. Nuovo Cim., 2B, 77.

Feenberg, E. & Primakoff, H., 1948.   Phys. Rev., 73, 449.

Felten, J.E., & Morrison, P., 1966. Astrophys, J. 146, 686

Ginzburg, V.L., & Syrovatskii, V.I., 1964. In 'The Origin of Cosmic Rays', Pergamon.

Heitler, W., 1954.   In 'The Quantum Theory of Radiation', Oxford.

Lang, K.R., 1974. In 'Astrophysical Formulae', Springer - Verlag, Berlin.

Pollack, J.B., & Fazio, G.G., 1963. Phys. Rev., 131, 2684.

Stecker, F.W., 1970. Astrophys. and Sp. Sci., 6, 377.

Stecker, F.W., 1973. Astrophys. J., 185, 499.

Stecker, F.W., 1975. In 'Origin of Cosmic Rays', ed. J.L. Osborne & A.W.Wolfendale, Reidel, Dordrecht.

Tkaczyk, W., 1975. Ph.D. Thesis, University of Lodz, Poland.

CHAPTER THREE

THE GALACTIC GAMMA-RAY OBSERVATIONS

3.1. Introduction

Gamma ray astronomy began with the moon-probe Ranger III which carried a scintillator sensitive to photons of about 1 MeV.   Since that first experiment many other instruments have been flown to detect cosmic gamma rays. However, the majority of these instruments were, like the first, omnidirectional detectors designed to detect the diffuse gamma ray background; only a few have been specifically designed to have the angular resolution and sensitivity necessary to be able to observe gamma rays specifically from the Galaxy.   In the sections which follow, the main observational results of these experiments are described.   Attention will be confined to observations of gamma rays with energies $>$ 1MeV.

3.2. Low Energy Gamma Rays from the Galactic Plane
    $(1 \leqslant E_\gamma \leqslant 10\text{MeV})$

The detection of gamma rays which arise in the Galaxy requires instruments with quite a high degree of directionality.   Unfortunately of the many experiments operated in this energy interval few have had sufficiently good directional sensitivity to investigate the flux from the Galactic plane.

A most important result was obtained by Schonfelder and Lichti (1974) using a double Compton telescope with an angular resolution of $30°$.   This telescope was used in drift scans across the Galactic plane and hence observed both the Galactic and diffuse gamma ray compon-

ents. These authors deduce from the angular distrib-
ution of the gamma ray intensity that at least 80%
of the flux they observed between 1 - 10 MeV belongs
to the isotropic component and hence that upper limits
only may be set for the Galactic plane.

Thus it appears that at about 10 MeV the emission
from the Galactic plane begins to disappear into the
gamma ray background. Figure 1 shows a summary of the
background from Strong et al.(1976).

3.3 High Energy Gamma rays from the Galactic Centre ($E_\gamma > 10$ MeV)

The first experiment to demonstrate the existence
of a galactic component was the telescope flown on
the satellite OSO III in 1967 - 68 (Kraushaar et al.
1972). This experiment measured a finite flux of
gammas (with energy E > 100 MeV) from the Galactic
plane and despite having only moderate ($\sim 15^\circ$) angular
resolution the telescope was able to map out most of
the main features of the Galactic plane.

This experiment was followed by a series of
balloon-borne experiments (for example, Fichtel et al.
1972, Helmken and Hoffman 1973, Frye et al. 1974, Share
et al. 1974, Sood et al. 1974). These experiments were
designed to observe the gamma ray emission from the
Galactic Centre, subsequently, a second satellite experi-
ment was launched (on SAS II, Fichtel et al 1975) and
this also has provided a map and spectrum of the Galactic
Plane.
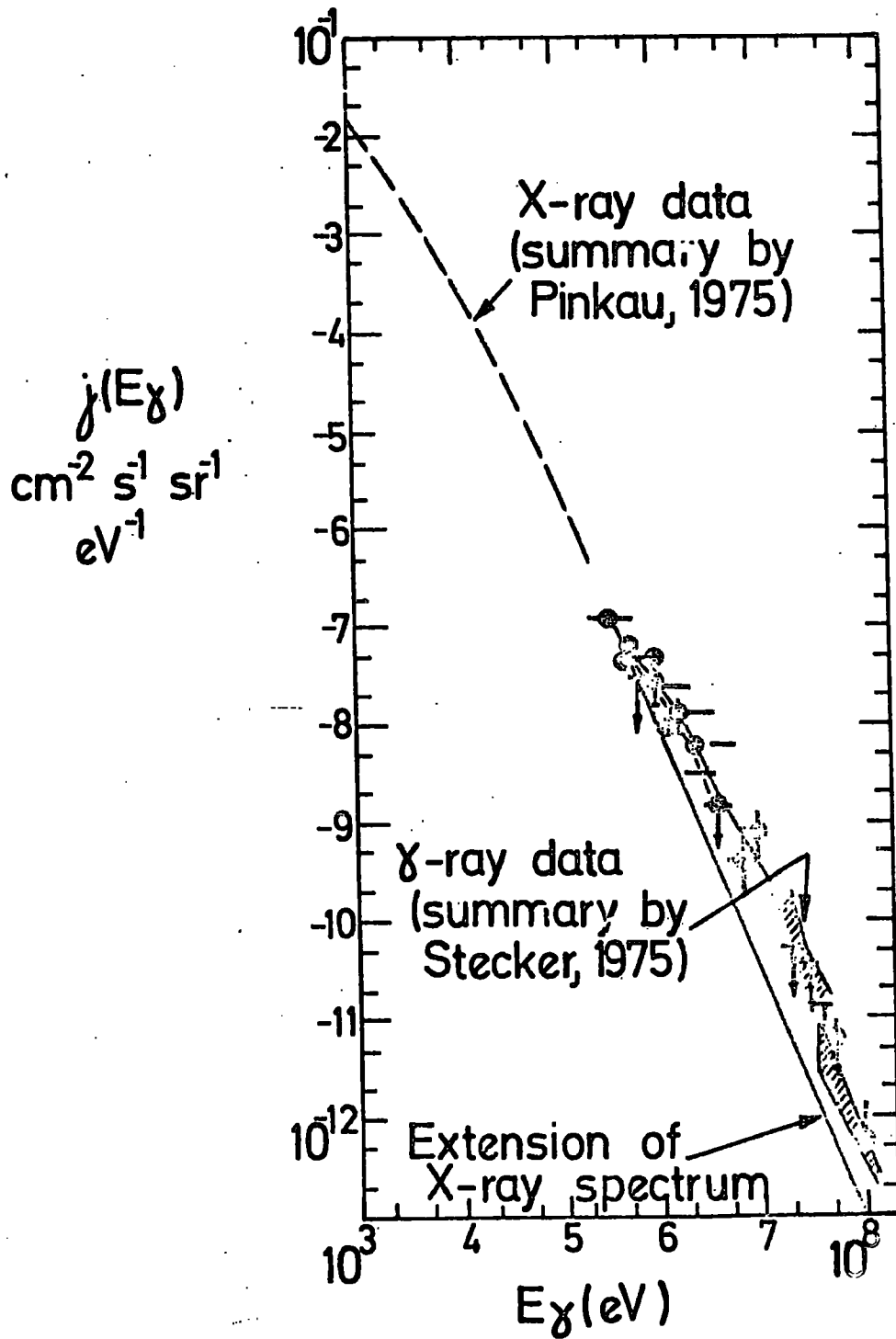
Figure 1. The diffuse gamma-ray background. A summary of
data from Strong et al (1976).

Figure 2 shows a summary of the results from these experiments for the Galactic Centre spectrum in the region between l= $330°$ and l = $30°$.

It should be noted that although in general these experiments measure the integral flux at some energy, the published results of Helmken and Hoffman and Share et al. actually refer to the differential spectrum. For this reason the integral flux calculated for these experiments and shown in figure 2 are dependent on the spectral shape assumed at higher energies. The upper and lower values shown for the Share et al. point correspond to the extreme assumptions of an entirely π^0 deca; spectrum or an E^{-2} power law respectively. The evidence of the higher energy observations in figure 2 suggests that a hard spectrum such as the π^0 spectrum dominates.

The Share et al. observations have provided evidence for a soft component of the Galactic Centre flux which may become dominant at low energies. Figure 3 shows the differential spectra for both the Galactic Centre and atmospheric albedo gamma ray fluxes. Comparison of the Galactic centre spectrum with the π^0 decay spectrum of Stecker (1973) indicates the presence of a steep component at low energies. Such an interpretation is supported by comparison with the differential spectrum of atmospheric gamma rays which shows similar structure and is known to have such a two component origin.

3.4 The Galactic Intensity vs Longitude distribution

As commented above this was first determined by the gamma ray telescope on OSO III (Kraushaar et al 1972) and
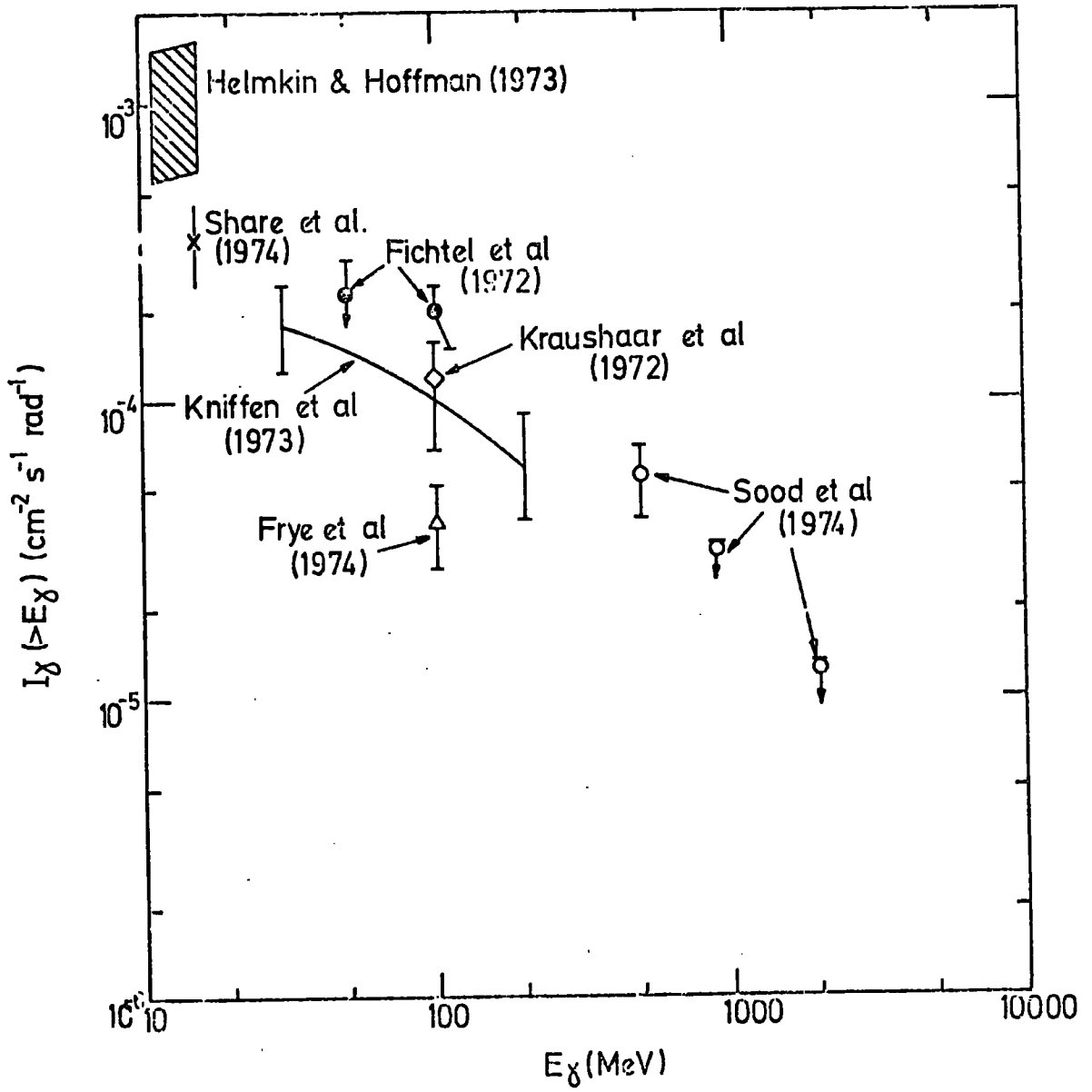
Figure 2. The spectrum of gamma-rays from the Galactic centre. Most points represent averages over a broad region around the Galactic Centre.
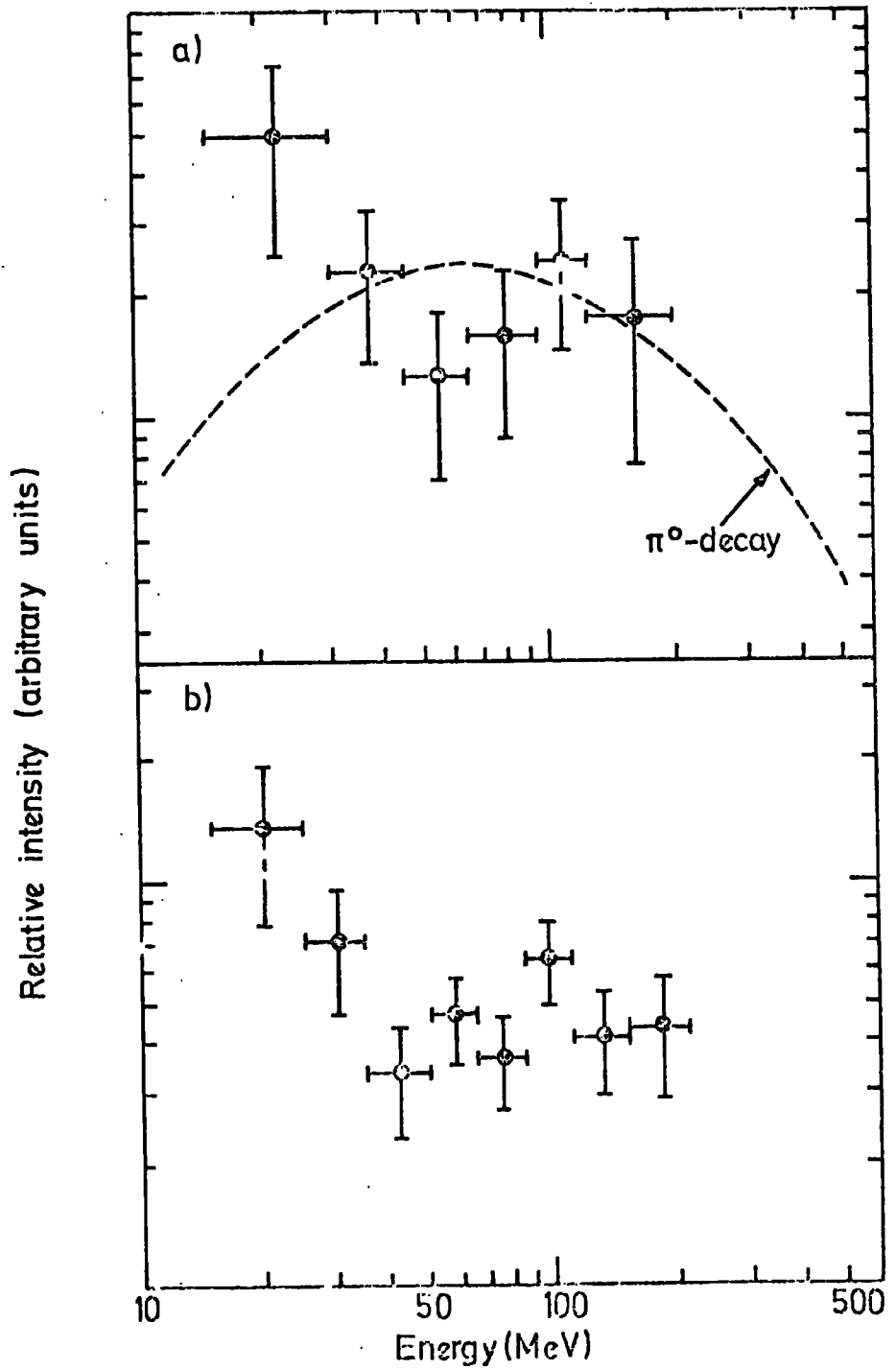
Figure 3. The differential gamma-ray spectra measured by Share et al (1974) for a) the Galactic centre and b) the atmospheric albedo gamma rays. Also included is the π^{o} decay spectrum of Stecker (1973).

later studied with greater sensitivity and angular resolution by SAS II. Their results are shown in figures 4 and 5.

There are two main reasons for the differences between figures 4 and 5. Firstly, the 15° angular resolution of the OSO III telescope was very much wider than the 3° angular resolution of the SAS II instrument. Secondly, the sensitivity of the latter was such that about three times the number of photons were detected by the SAS II experiment than were detected by OSO III.

There is however, good general agreement between the results from the two satellite. In particular, SAS II confirms the existence of a broad region of enhanced intensity near the Galactic centre. Away from the Galactic centre a recent balloon telescope experiment (McKechnie et al, 1976) has measured a line strength from the Cygnus region in good agreement with SAS II results.

Four point sources have been identified by SAS II group, three associated with the pulsars, 0833 - 45, 0531 + 21, 1747 - 46 (Thompson et al 1974b,1975, 1976) and a fourth unidentified source at $1 = 193^{\circ}$ $b = + 3^{\circ}$. (Kniffen et al 1975). Browning et al (1972) previously detected a number of point sources in the Galactic centre with a balloon-borne telescope and suggested that the excess from this region arises from the superposition of a number of faint sources. However, Thompson et al (1974a) reports that the SAS II data does not indicate any point sources in this region and
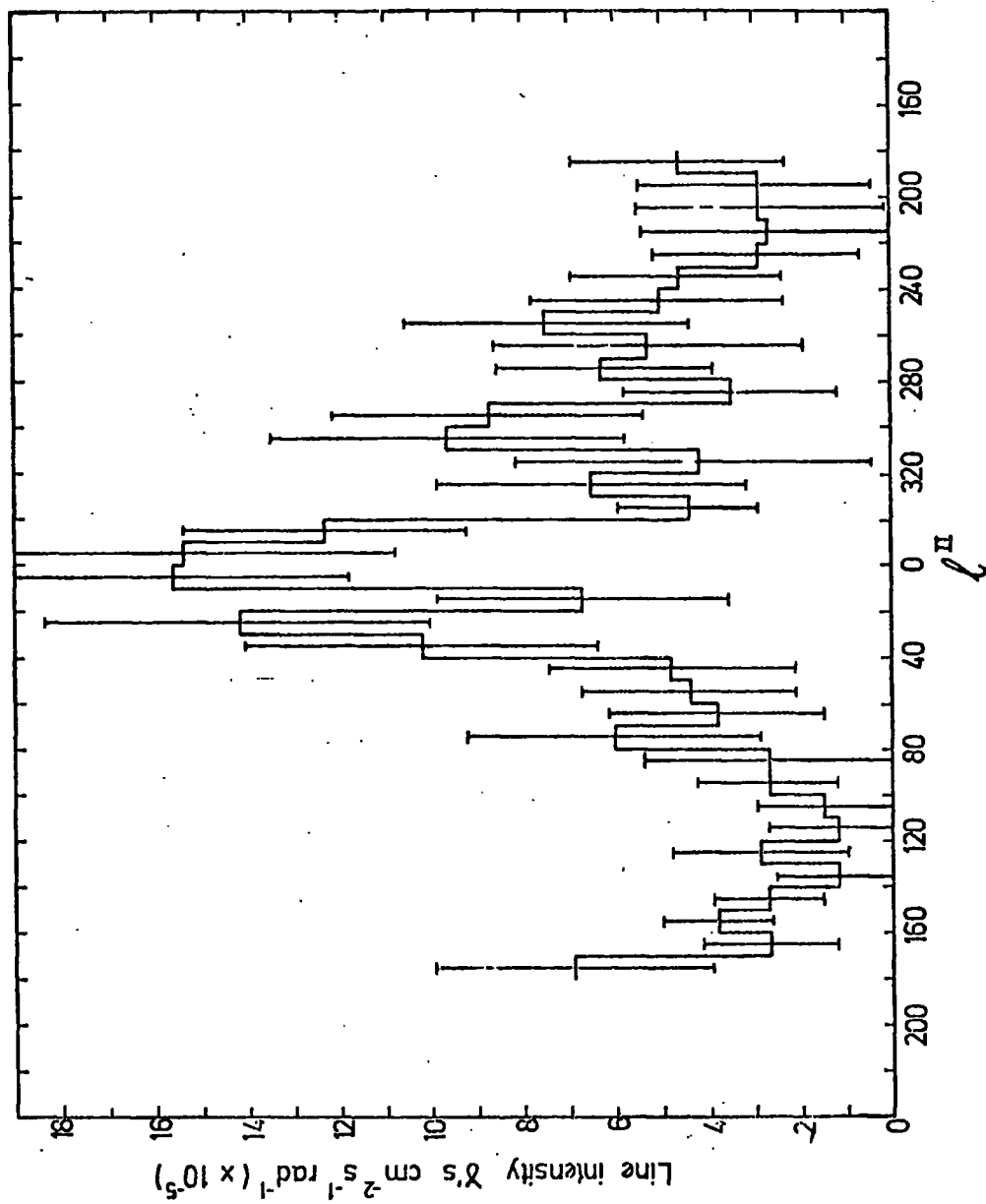
Figure 4. The distribution of gamma-ray intensity with Galactic longitude as measured by Kraushaaur et al (1972) using the OSO III satellite.
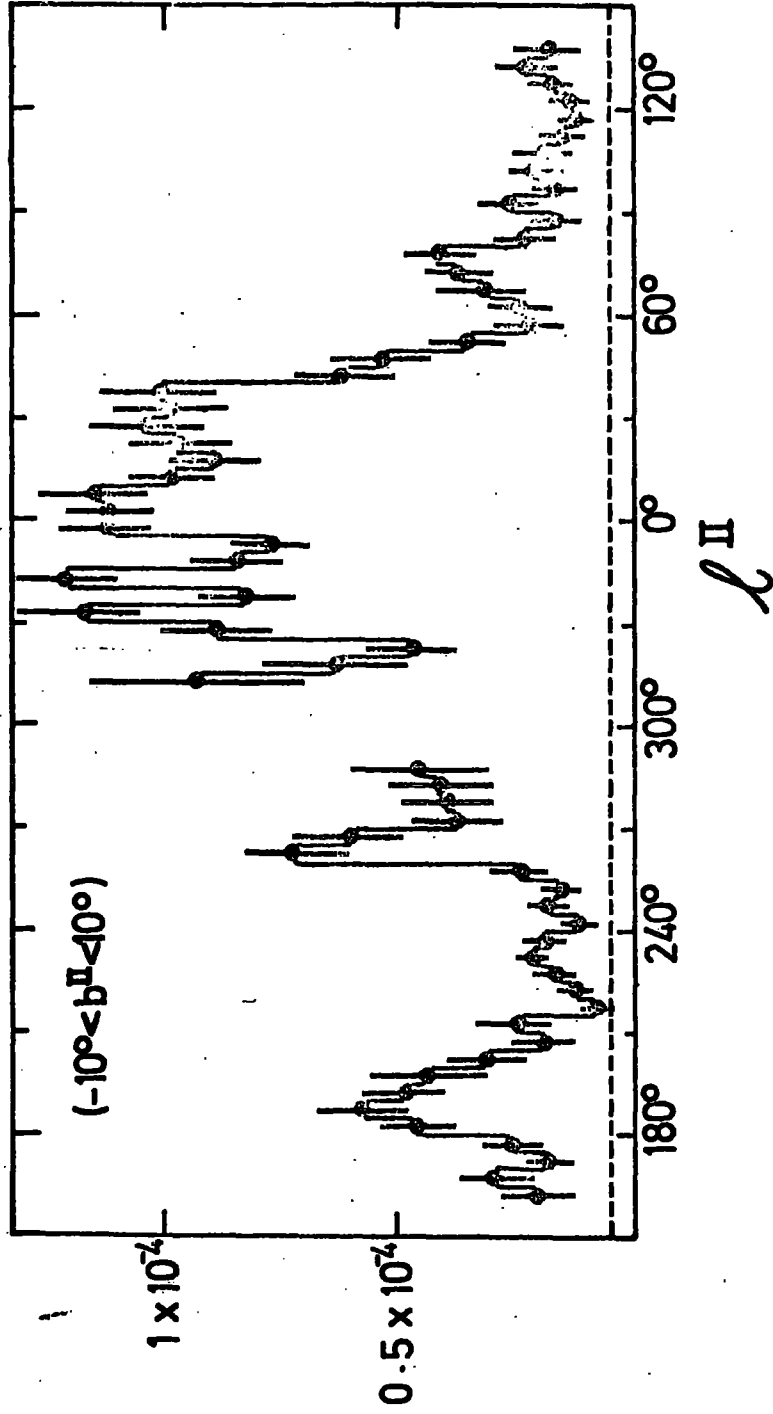
Figure 5. The distribution of gamma ray intensity with Galactic Longitude as measured by Fichtel et al using the SAS II satellite.

that there is no change in the spectral shape with position in the Galactic plane. This is very suggestive of a single process responsible for gamma ray production at all longitudes.

3.5. The Distribution of Gamma-ray Intensity with Latitude

The intensity vš latitude distribution obtained by the OSO III telescope had an angular width of about 15°; however, as this was the angular resolution of the telescope the true width was obviously considerably less than this value.

This result was considerably improved upon by the balloon-borne telescope of Share et al. (1974). Their telescope had an angular resolution of $1\frac{1}{2}^{\circ}$ at 15 MeV and recorded a width of 3° in latitude for the Galactic plane towards the Galactic centre. This result highlights one distinct advantage that balloon borne telescopes possess over satellites, namely that the telescope is recoverable. As a result nuclear emulsions may be used and this gives a very remarkable improvement in the angular resolution over the resolution of, say, a spark chamber at the same energy.

The angular width of the Galactic centre source may be used to give a mean distance to the emitting region, when the width of the emitting layer is known. If the main process is π° decay, then the width of the emitting layer will be the width of the gas layer which is $\sim 200\,pc$. Using this value, then the Share et al. result implies a distance to the source region of 3 to 4 kpc.

The more comprehensive data from the SAS II
telescope confirms the existence of a narrow emitting
region.   Their results are shown in figure 6.   In
this figure the distributions are shown for two regions;
the Galactic centre (from $l = 330^{\circ}$ to $l = 30^{\circ}$) and
for a broad region around the Galactic anticentre
comprising $l = 90^{\circ} - 150^{\circ}$, $160^{\circ} - 170^{\circ}$ and $200^{\circ} - 260^{\circ}$.

In figure 6 the width in latitude of the Galactic
Centre emission is very close to that expected for
pure instrumental broadening.   At these energies
(> 100 MeV) the SAS II telescope angular resolution is
$\lesssim 2^{\circ}$.

At higher latitudes, the slight enhancement at $+20^{\circ}$
towards the Galactic Centre and -20° towards the anti-
centre has been tentatively identified (Fichtel et al
1975) as being due to the local hydrogen feature
associated with Gould's belt (Davies 1960).

The broadness of the anticentre distribution is
particularly interesting, it reflects the rapid increase
of the gas layer thickness which occurs at the edge of
the Galaxy.   However, this will be discussed in more
detail in chapter 9.
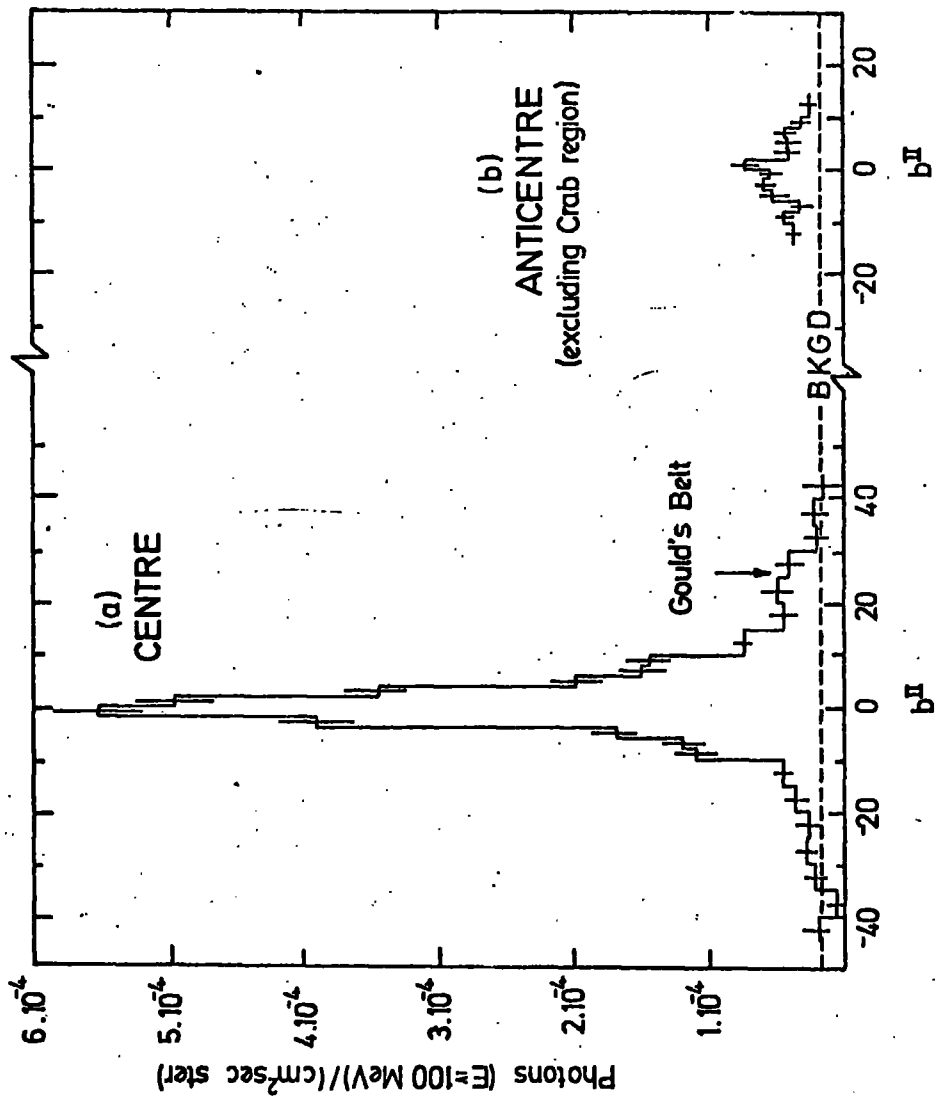
Figure 6.   The distribution of gamma ray intensity with Galactic latitude, within $\pm 30°$ of the Galactic centre and for a broad region around the anticentre comprising $l = 90°$ to $150°$, $160°$ to $170°$ and $200°$ to $260°$.

REFERENCES

Browning, R., Ramsden, D. & Wright, P.J., 1972. Nature, 238, 138.

Davies, R.D., 1960. Mon. Not. R. astr. Soc., 120, 483.

Fichtel, C.E., Hartman, R.C., Kniffen, D.A., & Sommer, M., 1972. Astrophys. J., 171, 31.

Fichtel, C.E., Hartman, R.C., Kniffen, D.A., Thompson, D.J., Bignamie, G.F., Ogelman, H., Ozel, M.F., Tumer, T., 1975. Astrophys. J., 198, 163.

Frye, G.M., Albats, P., Thomson, G.B., Hopper, V.D., Mace, O.B., Thomas, J.A., & Staib, J.A., 1974. Proc. Ninth ESLAB Symposium, ESRO SP - 106, p. 265.

Helmken, H. & Hoffman, J., 1973. Nature Phys. Sci., 243, 6.

Kniffen, D.A., Bignami, G.F., Fichtel, C.E., Hartman, R.C., Ogelman, H., Thompson, D.J., Ozel, M.F. & Tumer, T., 1975. Proc. 14th Int. Conf. on Cosmic Rays, Munich, 1, 100.

Krauschaar, W.L., Clark, G.W., Garmire, G.P., Borken, R., Higbie, P., Leong, C. & Thorsos, T., 1972. Astrophys J. 177, 341.

McKechnie, S.P., Mount, K.E. & Ramsden. D., 1976. Astrophys J. 207, L157.

Schonfelder, V. & Lichti, G., 1974. Astrophys J. 192, L1.

Share, G.H., Kinzer, R.L. & Seeman, N., 1974. Astrophys. J. 187, 45.

Sood, R.K., Bennett, K., Clayton, P.G., & Rochester, G.K., 1974. Proc. Ninth ESLAB Synposium, ESRO SP- 106, p. 217.

Stecker, F.W., 1973. Astrophys. & Sp. Sci., 20, 47.

Strong, A.W. , Wolfendale. A.W., & Worrall, D.M., 1976.
J.Phys. A. In the press.

Thompson, D.J., Bignami, G.F., Fichtel, C E., Hartman, R.C.,
& Kniffen, D.A., 1974a. Proc Ninth ESLAB Symposium, ESRO
SP- 106, p. 201.

Thompson, D.J., Fichtel, C.E., Kniffen D.A. & Ogelman, H.,
1975. Astrophys. J., 200, L.79.

Thompson. D.J., Fichtel, C.E., Kniffen, D.A., Lamb, R.C.
& Ogelman, H. 1976. GSFC preprint X-662 - 76 - 94.

CHAPTER FOUR

ON THE ORIGINS AND DISTRIBUTION OF COSMIC RAYS

IN THE GALAXY

4.1. Introduction

If the main source of cosmic rays do in fact lie within our galaxy there are three important questions which naturally arise:-

1. What are these sources?

2. How are they distributed?

3. What is the distribution of cosmic rays which results?

In this chapter the aim is to describe the main candidates for the sources of cosmic rays and their distribution in the Galaxy. Having thus answered (1) and (2) above, the answer to (3) is approached through a discussion of present ideas on cosmic ray propagation.

4.2. The nature of the CR sources

The total energy injection rate to maintain the present energy density in cosmic rays severely limits the possible candidates. If the local cosmic ray energy density of 0.5 eV/cm^3 is assumed constant over the whole galaxy, then for a disk of radius 15 kpc and thickness 1 kpc the total energy content in cosmic rays is 5 10^{54} ergs. There is evidence (Lal 1974) that the cosmic ray flux has remained constant for at least the last 10^9 yr. Equilibrium between the energy input from the sources and the energy loss by escape

must therefore have been achieved and this enables
an estimate of the total power of the sources to be made.
The measured escape time of $3 \cdot 10^6$ yr implies a total
power for the sources of 10^{40-41} ergs. sec^{-1}.

The observation of synchrotron radiation from
cosmic ray electrons in the shells of supernova remnants
make supernovae strong candidates.   An often quoted
figure for the mean rate of supernovae in our galaxy
is 1 per 26 yr.   In order to supply all the cosmic rays
in the Galaxy each supernova must therefore release 3
10^{50} ergs in cosmic rays out of a total energy release
of 10^{50} to 10^{52} ergs.   Thus the energy available in
SNe explosions is quite adequate to provide the whole
of the cosmic ray flux observed.

The mechanism by which the energy release of a super-
nova may be channelled into cosmic rays remains uncertain.
The acceleration may occur during the supernova explosion
itself, or at some later stage, either in the shell of
ejecta and swept up interstellar matter, or near the
surface of a pulsar which forms from the supernova.

The first of these alternatives, namely that cosmic
rays are accelerated   hydrodynamically during the super-
nova explosion has been described in detail by Colgate
(1975).   In this model the cosmic rays are accelerated
by a shock wave which in propagating through the outer
layers of the star becomes relativistic as it reaches
the atmosphere of the star.   For a $1.4 \, M_\odot$ star Colgate
calculates that $\sim 10^{-6} \, M_\odot$ of relativistic ejecta will
be produced taking $3 \cdot 10^{50}$ ergs out of a total available

energy of $7 \ 10^{51}$ ergs.   The spectrum of relativistic

particles produced is in good agreement with the

observed cosmic ray spectrum.   However, the Galactic

cosmic ray composition does not appear to be consistent

with the expected composition of supernovae ejecta.

Reeves (1975) has summarized recent work on the cosmic

ray source composition and concludes that there is

strong evidence for an acceleration mechanism which

becomes operative after the ejected matter has mixed

with a few times its own mass in interstellar matter and

hence by implication that acceleration occurs some time

after the supernova.

Mechanisms for the acceleration of cosmic rays in

supernova remnants have been discussed by Gull (1973)

and Scott and Chevalier (1975).   The first author

envisages the acceleration taking place at the boundary

between the ejecta and the interstellar matter when

the amount of interstellar gas swept up becomes equal

to the ejected mass.   In this situation a Rayleigh-

Taylor instability occurs and the dense matter of

the shell penetrates the interstellar gas, the resulting

turbulence generated amplifies the magnetic field and

thereby accelerates the cosmic rays.   Scott and

Chevalier propose a similar mechanism in their model

of cosmic ray acceleration in the Supernova remnant

Cas A.   These authors suggest that the fast moving

knots in Cas A are responsible for generating magnetic

turbulence with a typical scale size like that of the

knots themselves.   Acceleration is due to the Fermi

process, the particles gain energy as they are reflected from the fast moving turbulent eddies. Both models easily satisfy the restrictions on the source composition imposed by observations.

An alternative source of cosmic ray particles and yet another possible way of transferring the energy release of a supernova explosion could be pulsars. In the Crab nebula the observed Xray spectrum is radiated by electrons whose lifetime is much less than the known age of the remnant, implying that within the nebula particle acceleration still takes place. The Crab nebula pulsar could well be the source of these electrons but the mechanism is uncertain. Gunn and Ostriker (1969) have proposed a model in which the acceleration is due to the low frequency electromagnetic waves produced by a magnetized neutron star with the axis of rotation and magnetic axis non parallel. They have investigated the history of a charged test particle in these waves and showed that energies up to 10^{21} eV were possible by this mechanism. In this model the composition of the cosmic rays which result will depend on where the particle originates. If the nuclei come from the surface of the neutron star mainly iron nuclei are to be expected, alternatively, if the pulsar accelerates material in a supernova remnant shell it is quite easy to obtain the composition required by experiment, provided acceleration takes place after the ejecta has thoroughly mixed with matter from the ISM.

4.3 The Galactic Distribution of Supernovae and Pulsars

4.3.1 The distribution of supernovae

The low rate of occurence of supernovae and the presence of obscuring dust in the Galactic disk makes the task of determining the time averaged distribution of supernovae in our own Galaxy impossible. Studies of extra-galactic supernovae in spiral galaxies have been used to give the general features of the supernovae distribution. Barbon et al. (1975) have recently published a study of the radial distribution of supernovae within their parent galaxies. These authors derive the surface density distribution shown in figure 1. In figure 1, θ = r/R where r is the distance of the supernova from the centre of the galaxy and R is the galactic radius. The straight line represents an exponential fitted to the data and, adopting a mean Galactic radius of 8 kpc as suggested by Barbon et al. gives a radial surface density distribution of the form ρ/ρ_0 = exp (-αr) where α^{-1} = 3.66 kpc. This distribution is very similar to the distribution of surface brightness in spiral galaxies for which α^{-1} = 1 to 5kpc (Freeman 1970). If the average Mass to luminosity ratio is assumed constant over the galaxies, then in the absence of significant amounts of absorption the distribution of surface brightness is also the distribution of stellar surface mass density. Figure 1 must therefore imply a proportionality between the supernova rate and mass density and hence that in our Galaxy the distribution of the stellar mass density will give
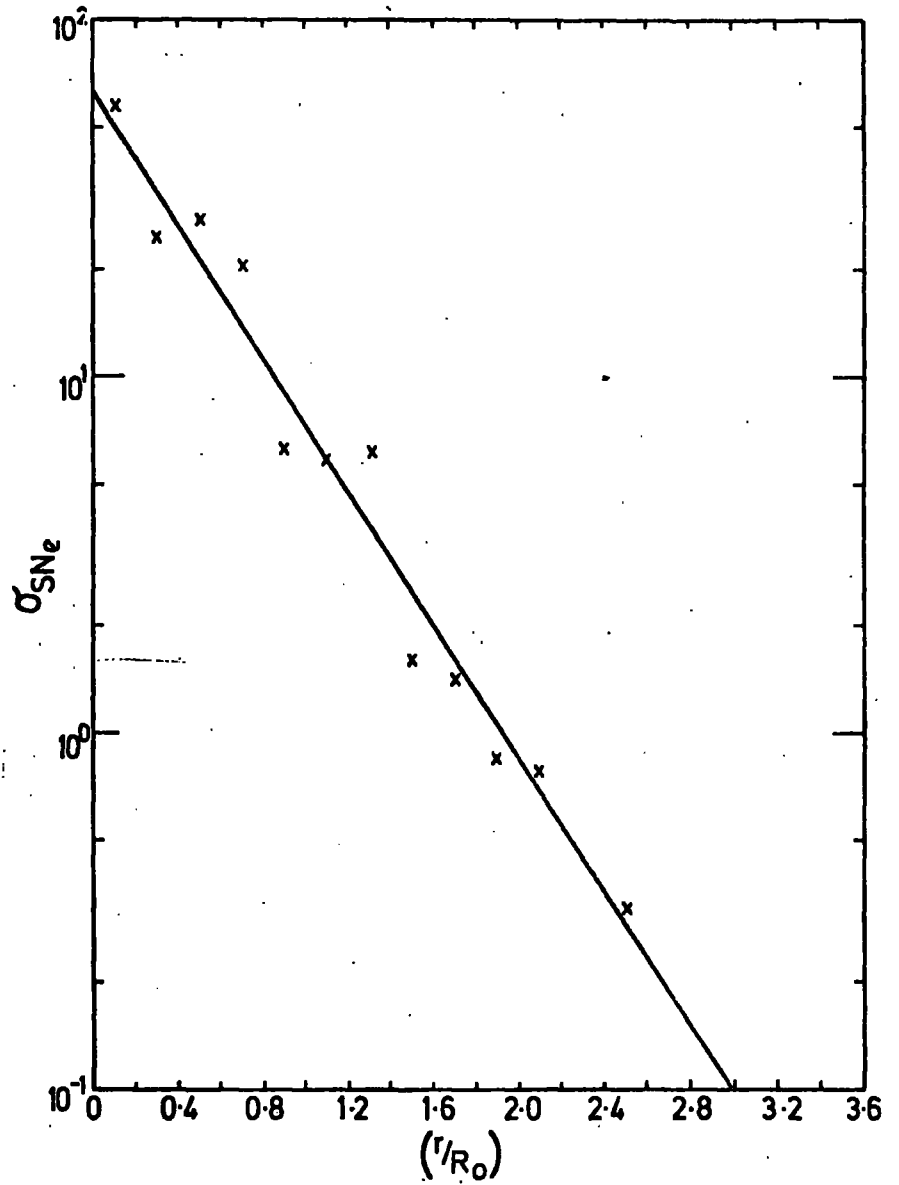
Figure 1.   The surface density distribution of supernovae as a
             function of galactic radius as deduced by Barbon
             et al (1975) from extragalactic supernovae.

the time averaged radial distribution of supernovae.

The problem of the Galactic supernova rate has been examined by Tammann (1973) using the statistics of extra-galactic supernovae.   He has analysed the data for the various galaxy types and deduces a rate for supernovae in our galaxy of 1 per 31^{+40}_{-11} yr. if the Galaxy is a type Sb.

4.3.2 The Distribution of Galactic Supernova Remnants

The remnant of a supernova expands into the surrounding interstellar gas at a rate which depends on the total energy released and the density of inter-stellar gas (see for example Shklovsky, 1968).   It remains intact for up to 10^5 years after the original explosion.   Since every known supernova remnant radiates a non-thermal radio spectrum these remnants are observable by radio telescopes over the whole of the Galaxy.   A number of catalogues of supernova remnants have been compiled which give the positions of these objects (for example Ilovaisky and Lequeux, 1972, Downes 1971).

However, there are various selection effects which limit the number of detectable supernova remnants and this means that the Galactic distribution of remnants cannot be derived from the catalogues in any simple manner, (see Ilovaisky and Lequeux 1972).   A number of authors have attacked this problem and deduced the radial distribution of supernova remnants from the catalogues after corrections for the various selection effects have been included.   Figure 2 shows the

radial distribution of supernova remnants from Kodaira (1974) and Pimley (1975) and, for comparison, the surface density of stars is included.   It is interesting to compare the distribution of supernova remnants with the time averaged supernova distribution which is predicted in 4.3.1a to follow the stellar mass density. Good agreement is obtained except in the innermost regions of the Galaxy where there is a deficit of SNR's and it is possible that remnants are being missed in radio surveys due to the high background flux.   Vettolani and Zamorani (1976) have investigated the apparent distribution of SNR's which would result from a time-averaged supernova distribution which follows the stellar mass denisty.   They find a distribution of remnants in good agreement with the observed distribution of remnants and argue that the distribution of supernovae in the Galaxy has the same form as is deduced for other galaxies. Ilovaisky and Lequeux (1972) have deduced the SNe rate for our galaxy based on the statistics of supernova remnants.   They deduce a rate 1 per 50 ± 25 yr which agrees well with the estimate above.

4.3.3 The Galactic Distribution of Pulsars

As with supernova remnants the deduction of the pulsar distribution from the catalogues of known pulsars requires inclusion of various corrections to cancel out the selection effects.   In this particular case this is best achieved by using the results of a pulsar search made by a single instrument to provide a complete sample.
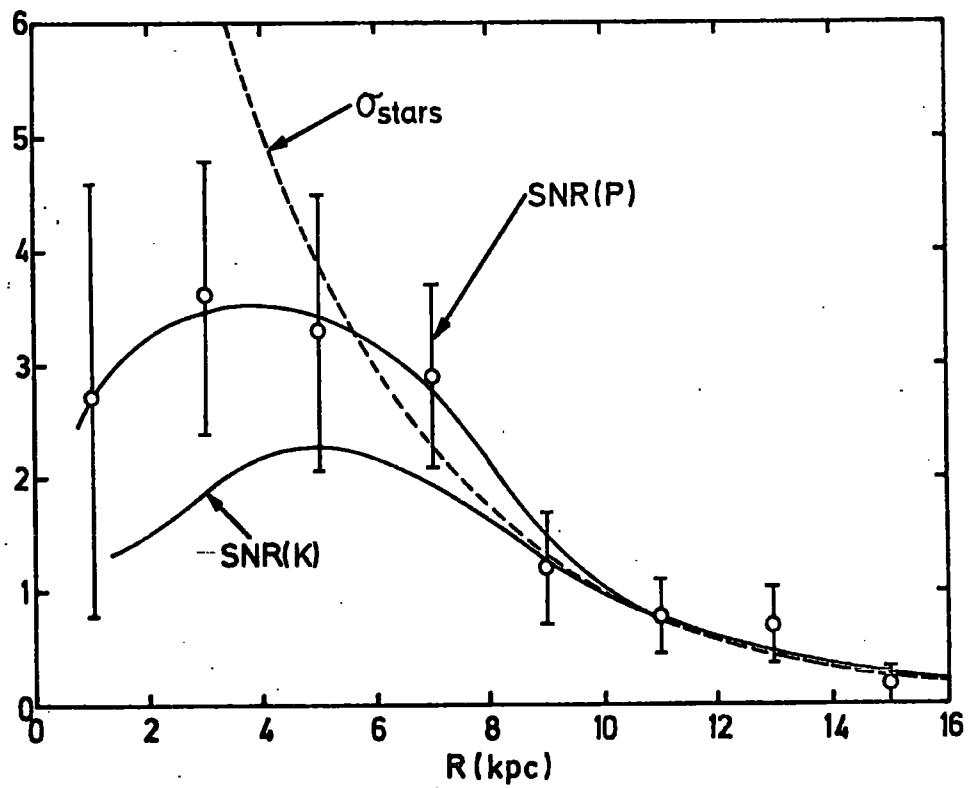
Figure 2.   The radial distribution of supernova remnants in the Galaxy as deduced by Kodaira (1974) and Pimley (1975).

Two sky surveys have now been carried out,by the
Jodrell Bank (Lyne, 1974) and the Arecibo groups
(Hulse and Taylor 1975). Figure 3 shows the radial
distribution obtained using the Jodrell Bank data (Lyne,
Private Communication). Comparison with the SNR distrib-
ution of Kodaira indicates that the pulsars are peaked
somewhat higher at 6 kpc than the SNR's. Once again
there is a suggestion of a deficit of pulsars near the
Galactic centre although the uncertainty becomes large.
Hulse and Taylor find evidence for a cut off in the
radial distribution of pulsars at radii 10 kpc, a
result which is in general agreement with the radial
distribution of figure 3.

The pulsar birth rate has been estimated using
the data of figure 3 Seiradakis (1976) gives a rate of
1 per 25 years which is in good agreement with the SNe
rate deduced by Ilovaisky and Lequeux and is therefore
quite consistent with the hypothesis of a supernova
birth for all pulsars.

4.4 Cosmic ray Propagation

The propagation of cosmic rays in the Galaxy is
a very difficult problem. The aim of a propagation
model is to reconcile the observational properties of
the cosmic rays with the hypothesis of origin in discrete
sources. In the section which follows some of the
important features of the cosmic ray propagation models
will be outlined with the object of predicting the
distribution of Cosmic rays which may result from a
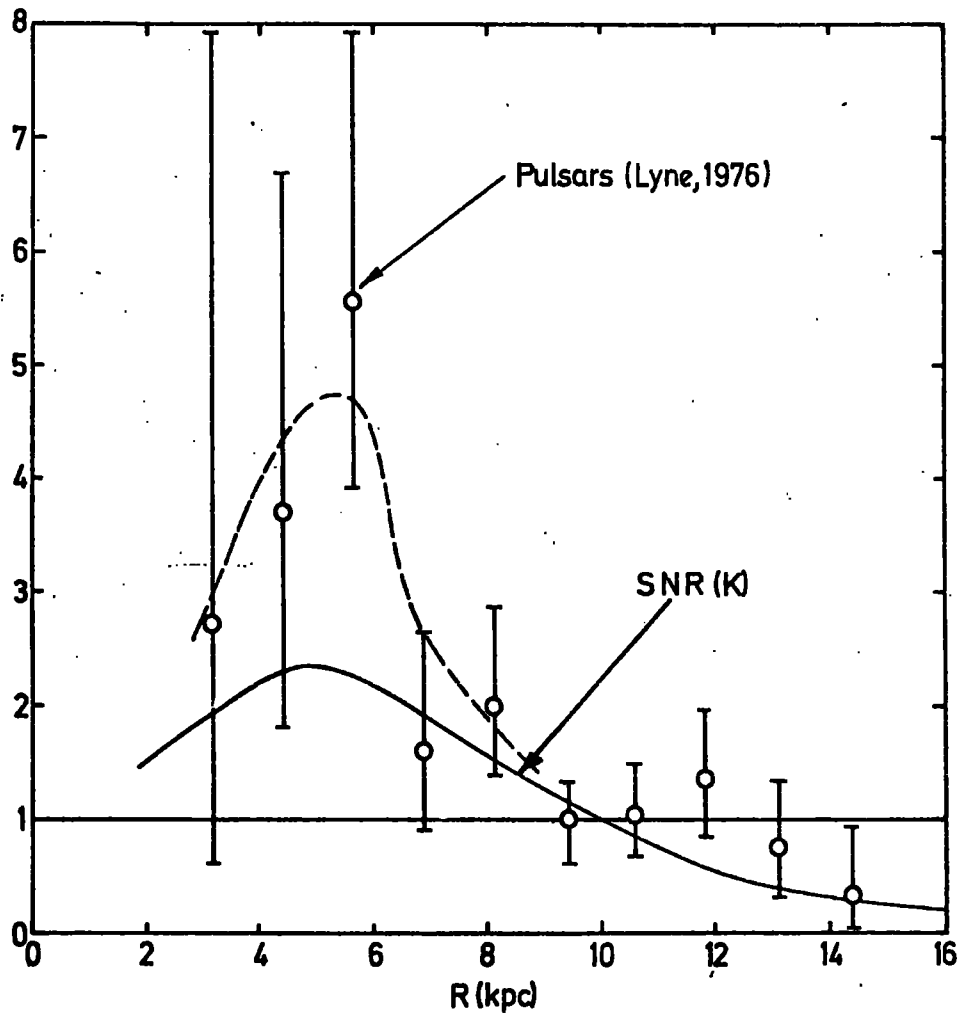source distribution such as those described above.

Figure 3.   The radial distribution of pulsars in the Galaxy
derived from the Jodrell Bank survey.

4.4.1 Diffusion Models

The simplest approach is to assume that the cosmic ray motion is random and that the density satisfies a diffusion equation. For the case of 3 dimensional diffusion one obtains a general equation for the density of cosmic rays $N(\bar{r}, t, E)$ as a function of space time and energy of the form

$$\frac{\partial N}{\partial t} - \nabla \cdot (D \nabla N) + \frac{\partial}{\partial E}\left(\frac{\partial E}{\partial t}N\right) + \frac{N}{T_c} = Q(\bar{r}, t, E) \qquad 1$$

where D is the diffusion coefficient, $\frac{\partial E}{\partial t}$ is the energy loss rate, T_c is the life time of the particles due to catastrophic processes and $Q(\bar{r}, t, E)$ is the source per unit time and per unit energy at $\bar{r}$ and t. The diffusion coefficient for isotropic diffusion is $D = \lambda c/3$ where λ is the mean free path and may be a function of energy. For protons the energy loss term is ignored but for electrons this is important. The catastrophic life-time T_c is ∞ for both electrons and protons and is important only for nuclei.

Consider the case of a disk confinement region 280 pc thick and 15 kpc in radius with a source function $Q(\bar{r}, E)$. Since the escape time of the particles is $\ll$ the loss time by collisions, the equilibrium density of cosmic rays is governed only by the local value of the source function and the escape time. Thus by assuming an escape time T_e independent of position the equilibrium density $N(\bar{r}, E)$ is given by

$$N(\bar{r}, E) = Q(\bar{r}, E) T_e$$

This equilibrium solution may be derived from equation 1 by setting $\frac{\partial N}{\partial t}$, $\frac{\partial}{\partial E}\left(\frac{\partial E}{\partial t}N\right)$ and $\frac{N}{T_c} = 0$

and by replaing the diffusion term by N/T_e which

corresponds to postulating an energy independent escape

probability (Ramaty 1974).

The general solution to equation 1 has been

discussed in detail by Ginzburg and Syrovatskii(1964).

In the solution the choice of parameters are governed

by the observables of the cosmic radiation i.e. the

anisotropy, mean age and constancy.

The natural choice for the diffusion mean free

path, λ is the observed scale length of irregularities

in the magnetic field which is 10 to 30 pc. Unfortun-

ately, however, for the disk confinement region described

above the choice of λ = 10 pc leads to an escape time

in clear disagreement with observation. Even more

severe difficulties are encountered with the anisotropy.

The probability of obtaining an anisotropy in the observed

range for a supernova rate such as that discussed above

is extremely low for this choice of λ .

The assumption of isotropic 3-dimensional diffusion

may not be valid. The protons in the cosmic radiation

with $E < 10^{14}$ eV the gyroradius is <10pc. Hence the

cosmic rays will behave as though bound to the field

lines and experiments at the Earth sample only those

cosmic rays bound to field lines passing within one

gyroradius of the Earth. The problem thus becomes one-

dimensional diffusion and even greater difficulties are

encountered in trying to reconcile the observed anisotropy

with a set of discrete sources randomly distributed in space

and time (Dickinson and Osborne 1974).

4.4.2 Self Confinement of Cosmic Rays

One type of model frequently discussed can achieve consistency with observation. This is the 'leaky-box' model, in which cosmic rays are pictured as propagating almost freely inside a box with partially reflecting walls. A version of this model has been proposed by Skilling (1971) and Holmes (1974) in which the partially reflecting boundaries are formed by the scattering of cosmic rays on Alfven waves.

Resonant scattering of cosmic rays by Alfven waves occurs when the wavelength is a few times the gyroradius (Wentzel 1974). In this process the mean free path for reversing the cosmic ray direction is approximately the gyroradius multiplied by the ratio of the energy densities in the galactic magnetic field and the Alfven waves. These waves are set up whenever cosmic rays stream down a density gradient with a streaming velocity $V_s >$ V_A, where V_A is the Alfven velocity. Such a situation would arise at, say, the surface of a disk confinement region or near a cosmic ray producing supernova. Thus on this model the cosmic rays are self-confined i.e. the Alfven waves which scatter the cosmic rays are generated by the cosmic rays themselves.

In passing it is interesting to note that when this model is applied to the propagation of cosmic rays away from a source such as a supernova the predicted adiabatic energy losses for the cosmic rays become prohibitively large. (Kulsrud 1975). The problem then becomes one of understanding how a source

can inject enough energy to overcome this problem.

In the Skilling-Holmes model the region close to the Galactic plane is labelled the 'free' zone and the region of strong scattering by Alfven waves is the 'wave' zone. The boundary between these zones is the z height from the Galactic plane at which the growth rate Γ_G and damping rate Γ_D of the Alfven waves are equal and for any particular energy and spectrum of cosmic ray particles is specified by the z distributions of the ionized and neutral gas. Thus, for a 3GeV particle and a cosmic ray spectrum of exponent 2.5 the boundary occurs at 286 pc.

The basic version of this model pictures cosmic rays propagating at almost the velocity of light within the free zone being frequently reflected in collisions with the wave zone.

Dickinson (1975) has modified this basic model to include a realistic model of the propagation of the particles in the free zone and examines in detail the consequences for the Galactic distribution of cosmic rays. His models E and F are of particular interest here since he uses a source distribution proportional to the stellar mass density which is the same source distribution as is implied by the observations of extragalactic supernovae. His results are surprising. Despite having a source distribution which peaks at the Galactic centre at 60x the local value he finds variations in cosmic ray concentration across the Galactic disk which are very much smaller than this. At 1GeV he finds in model E an increase of only 30% at

the Galactic Centre and in model F, which includes the effects of propagation in spiral arms, he finds an increase of 15% at 5 kpc and a decrease of 15% at 14 kpc relative to the concentration at 10 kpc. For source distributions which are constant in R he finds variations in concentration between 0 and 10 kpc of < 1%.

-38-

REFERENCES

Barbon, R., Capaccioli, M. and Ciatti, F., 1975.
Astron.Astrophys., 44, 267.

Caswell, J.L., Clark, D.H., Crawford, D.F. and Green, A.J.,
1975. Aust. J. Phys. Astrophysical Supplement No. 37.

Colgate, S.A., 1975. Origin of Cosmic Rays, Ed. J.L.
Osborne and A.W.Wolfendale. D.Reidel, Dordrecht.

Dickinson, G.J. and Osborne,J.L., 1974. J.Phys. A., 7, 728.

Dickinson, G.J., 1975. Ph.D. Thesis, University of Durham.

Freeman, K.C., 1970. Astrophys. J., 160, 811.

Ginzburg, V.L. and Syrovatskii, S.I., 1964. The Origin
of Cosmic Rays, Pergamon, Oxford.

Gull, S.F., 1973. Mon. Not. R.A.S., 161, 47.

Gunn, J.E. and Ostriker, J.P., 1969. Phys. Rev. Lett.,
22, 728.

Holmes, J.A., 1974, Mon. Not. R. Astr. Soc., 166, 155.

Hulse, R.A. and Taylor, J.H., 1975. Astrophys. J. Lett,
201, L55.

Ilovaisky, S.A. and Lequeux, J., 1972. Ast. Astrophys.,
20, 347.

Kodaira, K., 1974. Publ. Astron. Soc. Japan, 26, 255.

Kulsrud, R, & Zweibel, E., 1975. Proc. 14th Int. Conf.
Cosmic Rays, Munich. 2, 465.

Lal, D., 1974, Phil Trans. Roy. Soc., 277, 395.

Lyne, A.G., 1974.   Galactic Radio Astronomy, IAU
Symposium 60, D.Reidel, Dordrecht.

Pimley, K., 1975.   M.Sc. Thesis, University of Durham.

Ramaty, R., 1974.   High Energy Particles and Quanta in
Astrophysics.   Eds. F.B.McDonald and C.E.Fichtel,
MIT Press.

Reeves, H., 1975.   Origin of Cosmic Rays.   Ed. J.L.
Osborne and A.W.Wolfendale.   D.Reidel, Dordrecht.

Scott, J.S. and Chevalier, R.A., 1975. Astrophys. J.,
197, L5.

Seiradakis, J., 1976. Goddard Space Flight Centre Symposium
on Gamma Ray Astronomy, to be published.

Shklovsky, I.S., 1968.   Supernovae, Wiley-Interscience.

Skilling, J., 1971 Astrophys. J. 170, 265.

Tammann, G.A., 1974. Supernovae and Supernova Remnants.
Ed. C.B. Cosmovici, D.Reidel, Dordrecht.

Vettolani. G. and Zamorani, G., 1976. Reprint.

Wentzel, D., 1974. Ann. Rev. Astron. and Strophys. Vol.12.

CHAPTER FIVE

THE INTERSTELLAR GAS

5.1 Introduction

This chapter reviews the main observational results

on the interstellar medium (ISM) which are relevant to

the problem discussed later.   In particular interest

is concentrated on the observed distribution of the

interstellar gas on a galactic scale.   Since the

dominant component of the ISM is hydrogen, studies of

this atom are obviously of paramount importance.

5.2 The Galactic Distribution of Neutral Atomic Hydrogen

5.2.1 21cm Observations

The hyperfine transition of neutral hydrogen

produces a spectral line of wavelength 21 cm which has

been observed in emission in every direction on the

sky.   As a result, emission studies in this line have

become one of the major tools in the study of the large

scale structure of our Galaxy.   This importance is

enhanced by the fact that the 21 cm emission regions are

completely resolvable in both velocity structure and

angle by the typical radio telescope.

A typical profile in this line gives the intensity

as a function of frequency, I_ν, Doppler shifted from the

line's natural frequency of 1420.406 MHz.   In radio

astronomy it is common practice to express intensity

in terms of a brightness temperature, T_b, where

$$T_b = \frac{c^2}{2\nu^2 k} I_\nu \quad \text{(Rayleigh-Jeans approximation)}$$

The condition for this approximation is that $h\nu/kT \ll 1$. Since for the 21 cm line $h\nu/k = 0.07K$, this condition is always satisfied in 21 cm studies.

In studies of the Galactic plane the measured frequencies are converted to radial velocities relative to the local standard of rest which has been determined from the motions of the nearby stars. The Galactic rotation curve may then be obtained from profiles in the Galactic longitude interval $270 < l < 90$. This involves the measurement of the terminal velocities contributed by material on the locus of subcentral points for which the Galactocentric radius is $R = R_0 |\sin l|$. The rotation curve so determined for $R < R_0$ can be extended to $R = 13$ kpc by observations of Cepheid variables and is extrapolated beyond this distance by using a model of the Galactic mass distribution which is constructed to fit the galactic rotation curve for $R < R_0$. Figure 1 shows the rotation curve and surface density of matter on the Mass model which is derived from the rotation curve (Innanen 1973).

The primary goal of 21 cm astronomy has always been the transformation of the observed intensity-velocity profiles into a map of the spatial distribution of hydrogen. In particular it was hoped that the spiral structure would become evident in the HI maps. Burton (1976) has discussed in detail the major problems encountered in achieving this goal. He stresses that a grand design of a spiral structure in the overall HI distribution is not established and there is little
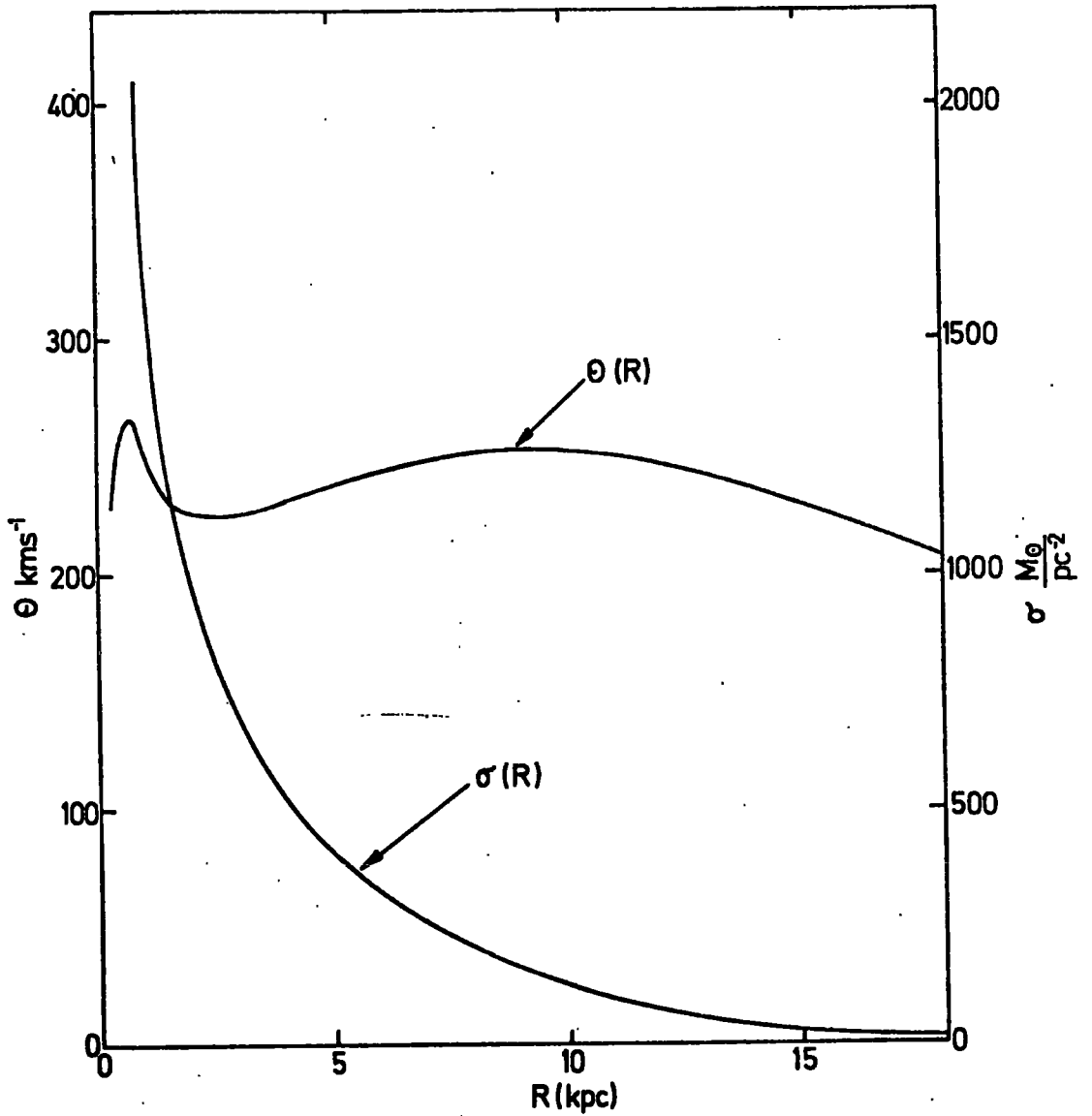
Figure 1.   The Galactic rotation curve and surface mass
density distribution from the mass-model of
Innanen (1973).

evidence at all for spiral structure features in the
radial distribution of atomic neutral hydrogen from
these studies.

5.2.2.1 The R and Z distributions of atomic hydrogen

The column density of atomic hydrogen in a
particular direction is given by

$$N_{HI} = 1.823 \times 10^{18} \int T_k \tau(v)\, dv$$

cm^{-2} v is the velocity

where T_k is the excitation temperature of the line,
and τ is the optical depth.   As mentioned above, the
observations give $T_B(v)$ where

$$T_B(v) = T_k \left[1 - \exp(-\tau(v)) \right]$$

If the line is optically thin i.e. $\tau \ll 1$ then $T_B(v) =$
$T_k \tau(v)$ and the column density is given by

$$N_{HI} = 1.823 \times 10^{18} \int T_B(v)\, dv$$

which is easily obtained by integration of the observed
profile.

In the galactic plane $T_k \simeq 120$ K and the line
is usually optically thick; if the line is completely
saturated, $T_B(v) = T_k$.

Figure 2 shows the radial variation of atomic
hydrogen density in the galactic plane from Gordon and
Burton (1976).   The average hydrogen density along a
line of length Δr is calculated from

$$n_H = \int_{v(r)}^{v(r+\Delta r)} \frac{T_b(v)\, dv}{\Delta r}$$

when the line is optically thin.   Figure 2 includes
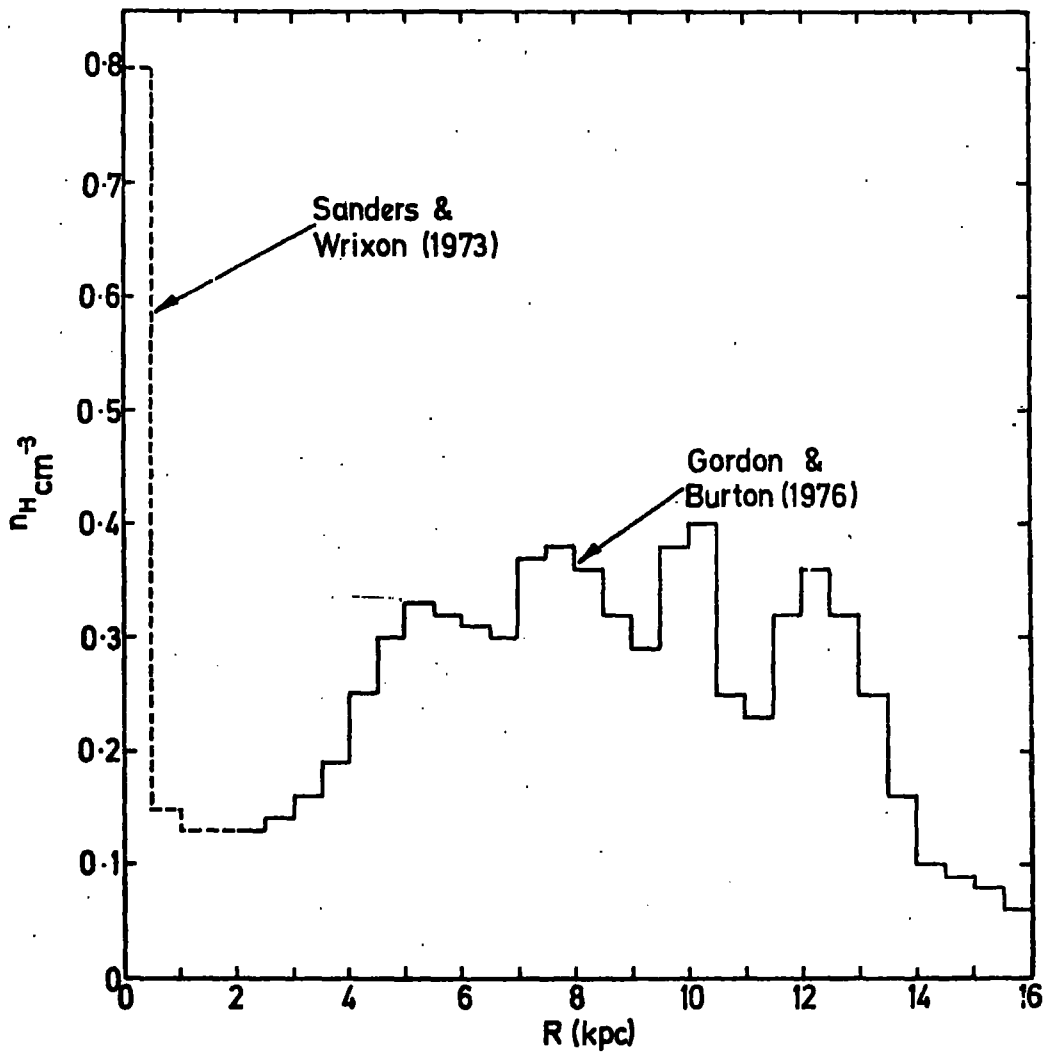corrections for the partial saturation of the line.

Figure 2. The radial variation of atomic hydrogen density
in the Galactic plane. The densities for R > 2 kpc
come from Gordon and Burton (1976), for R < 2 kpc
the model of Sanders and Wrixon has been used.

The densities near the galactic centre were taken from the model of Sanders and Wrixon (1973).

A further important observation in 21 cm astronomy is the thickness of the atomic hydrogen layer. This has been determined for a range of positions in the Galaxy by Jackson and Kellman (1974) from the portions of profiles corresponding to the locus of subcentral points, where the distance is unambiguous. Figure 3 shows that their results for the variation of $Z_{\frac{1}{2}}$ with R.Burton (1976)has also determined the variation of $Z_{\frac{1}{2}}$ with R, he gives the expressions

$$Z_{\frac{1}{2}} = 200 \text{ pc} \quad , \quad R < 9.5 \text{ kpc}$$
$$Z_{\frac{1}{2}} = 200 + 38 \ (R - 9.5) \text{ pc}; \quad R > 9.5 \text{ kpc}$$

This is plotted in figure 3 for comparison with the results of Jackson and Kellman.

Gordon and Burton (1976) utilize these data on the scale height to calculate the surface density of atomic hydrogen which is shown in figure 4. Once again the model of Sanders and Wrixon is used to calculate the surface density of gas in the nucleus.

5.2.2.2 <u>The fine scale structure of the atomic hydrogen</u>

Although 21 cm emission in the galactic plane can provide an accurate description of the large scale distribution of atomic hydrogen in the Galaxy, for details of the fine scale structure observations of the emission profiles at high latitude are used. An alternative technique in this kind of study is to observe the absorption profile of the 21 cm line in front of bright radio continuum sources. Comparison with a nearby emission profile enables

Figure 3. The variation of $Z_{\frac{1}{2}}$ with Galactocentric radius R.
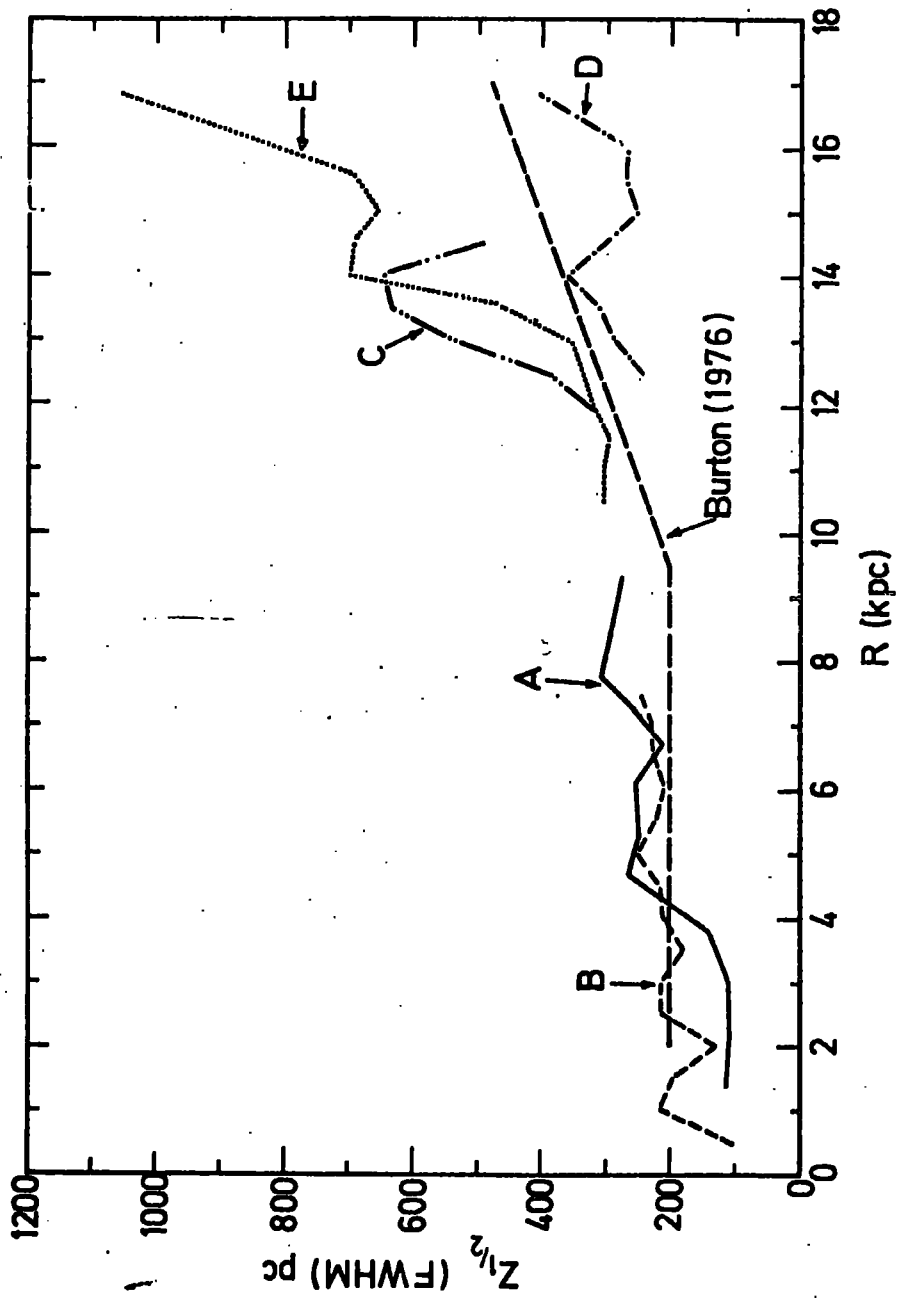Curves A-E are from Jackson and Kellman (1974) and
refer to the longitude intervals; A, $0 < 1 < 90$;
B, $270 < 1 < 360$; C, $160 < 1 < 205$; D, $110 < 1 < 160$;
E, $200 < 1 < 300$. For comparison the results of
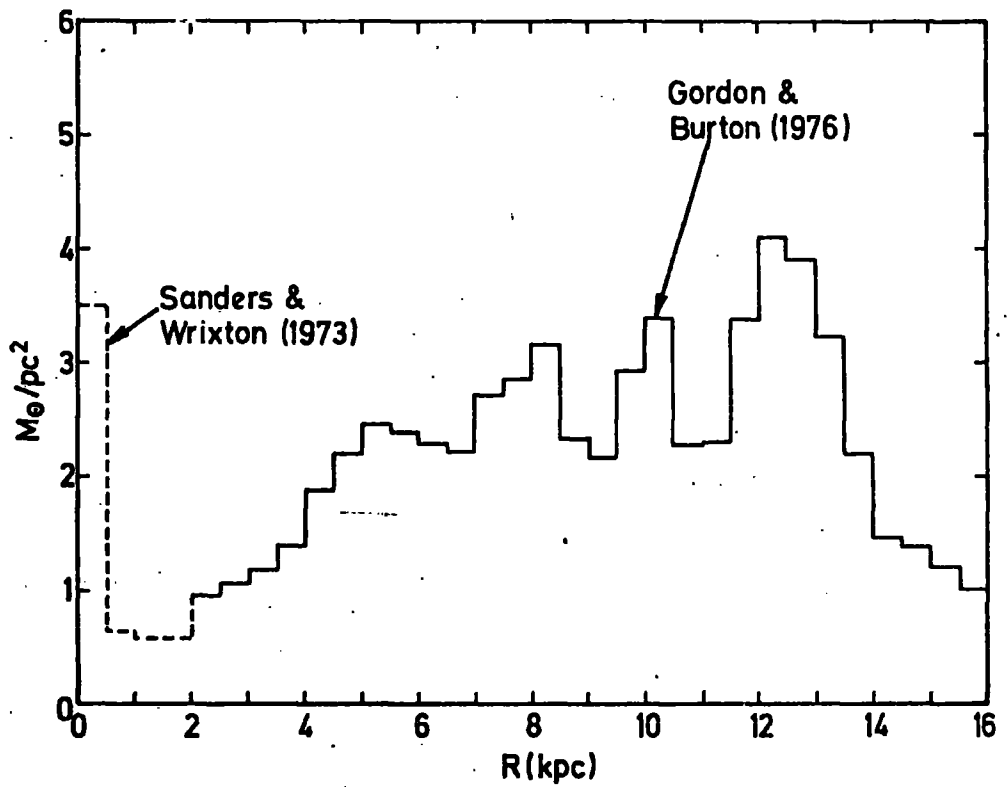Burton (1976) are also shown.

Figure 4.   The Distribution of the surface density of atomic
            hydrogen with Galactocentric Radius, R.

the column density, spin temperature and velocity structure of the emitting gas to be determined unambiguously.

A general picture which emerges from these studies is of a 'raisin pudding' interstellar medium consisting of cold, dense clouds in a hot tenuous intercloud medium. The properties of the cold clouds have been investigated in absorption studies (Radhakrishnan and Goss 1972, Hughes et al. 1971) and an average HI cloud is found to have a column density of $3 \ 10^{20}$ cm^{-2} and a temperature of 60 K, which is significantly less than the 120 K quoted above.   If this lower temperature is correct the use of 120 K would lead to the under-estimation of column densities.   This may be important for the work of section 9 where the γ-ray flux in the anticentre is calculated from the measured hydrogen column densities in this region.

5.2.3 Far UV Observations

This involves the observation of the resonance absorption lines (e.g. Lyman α at 1216Å) in the line of sight to hot stars which are used to provide continuum background light sources.

Since the technique relies upon rocket or satellite borne instruments this is an even younger branch of astronomy than 21 cm radio astronomy.   It is, however, a very powerful method of investigating the spatial distribution of atomic hydrogen out to 1 kpc from the Sun.

Jenkins and Savage (1974) use data from rocket flights and OAO-2 observations to determine the local distribution of gas.   They find an average density of 0.6 atoms cm^{-3} with a large range in the observations (from < 0.1 to > 1.0 atoms

cm^{-3}). Near to the sun they suggest a density of $n_H = 0.25$ atoms cm^{-3} may be representative. More recently Bohlin (1975) has reanalysed the available data on Ly - α absorption and attempts to correct for the observational bias. This author finds a mean atomic hydrogen density near the sun of 0.9 atoms cm^{-3}. In addition these authors find a correlation between the hydrogen column density to a star and the stellar colour excess E(B-V), yielding

$$\frac{N_H}{E(B-V)} = 5 \quad 10^{21} \text{ atoms } cm^{-2} \text{ mag}^{-1}$$

This correlation has important implications for gamma ray astronomy. Adopting an $A_V/E(B-V)$ ratio of 3 it is found that in dense dust clouds for which A_V may be > 6 this suggests column densities $> 10^{22}$ atoms cm^{-2}. However, 21 cm studies of dark clouds give much lower column densities (Heiles, 1969). The implication of this result, which is that the atoms have been converted to molecules is examined in the next section.

5.3 The Galactic Distribution of Molecular Hydrogen

In the last section it was mentioned that the correlation of hydrogen column density with inter-stellar extinction appears to break down when applied to regions in which the interstellar absorption is large, such as in large dust clouds. The interpretation of this result is that in the centre of these clouds the atomic hydrogen is converted to molecular hydrogen with almost 100% efficiency. In the general

interstellar medium hydrogen molecules are rapidly
dissociated by UV photons in starlight; however, in
dust clouds molecular hydrogen is shielded from UV
photons and hydrogen atoms rapidly combine to form
molecules.   The next two subsections will describe
the distribution of molecular hydrogen as deduced
from observations.

5.3.1 Direct Observations

Unfortunately, molecular hydrogen has no observable
transition in the optical and radio wavebands.   In
fact, under interstellar conditions it is observable
only via the absorption lines in the far ultraviolet
and is thus accessible to direct observation only from
rockets and satellites.

The richest source of data came from the studies
using the Copernicus satellite (Spitzer et al. 1973)
which has been used to measure the column density of
molecular hydrogen in the line of sight to nearby hot
stars.   They find that for stars for which the line
of sight intersects an interstellar gas cloud (i.e.
those for which E(B-V) > 0.1) the fraction of hydrogen
in molecular form exceeds 0.1.   On the other hand, for
stars with E(B-V) < 0.05 there is no trace of the absorp-
tion implying < 10^{-7} of the hydrogen in molecular form.
Thus, they confirm the hypothesis that H will form at
the centre of clouds for which the extinction is large
enough to shield the molecules.   Their results imply
that some 50% of the local interstellar hydrogen is in

molecular form.

In a recent review paper Jenkins (1976) gives
an average molecular hydrogen density near to the
solar syste of 0.2 atoms cm^{-3} which together with the
atomic hydrogen density gives a total density of 1.1
atoms cm^{-3}.

Unfortunately these techniques are limited to the
space within 1 kpc of the sun. The unravelling of the
Galactic distribution of molecular hydrogen requires
recourse to indirect methods.

5.3.2 <u>Indirect Observations of the distribution of Galactic</u> <u>H_2</u>.

After molecular hydrogen, carbon monoxide is expected
to be the most abundant molecule in the interstellar
medium. This is due, not only to the relative
abundance of its constituents and the ease by which
it can form, but mainly to the fact that it is the
most stable diatomic molecule known, with a dissociation
energy of > 11 eV. The far UV observations by Jenkins
et al. (1973) have confirmed its abundance especially
in the spectra of reddened stars which also show H_2
lines. Jenkins et al. find a $N(CO)/N(H_2)$ ratio of
$\sim 10^{-8}$ for the four stars they observed.

Large column densities of CO have also been
detected in dense dust clouds by observing the $J(1 \rightarrow 0)$
rotational transitiion of ^{12}CO at 2.6 mm, (Penzias et al
1972). Since it is the same dust clouds which have a
dense core of molecular hydrogen the 2.6 line presents

itself as a powerful tool for the examination of the Galactic Distribution of molecular clouds.

The actual brightness temperature-velocity profiles in this line have provided further confirmation of the existence of high densities of neutral molecules alongside the CO. The typical excitation temperature in this line is 20 K, it can be shown, (Robinson 1973), that to achieve this sort of temperature excitation must be due to collisions with neutrals and that the density of neutrals must be of order 10^3 - 10^4 cm^{-3}. Thus implying the existence of molecular hydrogen in high densities.

Several surveys of the galactic plane have now been made in this line (Scoville and Soloman 1975, Burton et al. 1975, Gordon and Burton 1976) and there is now some concensus on the general features of the Galactic distribution of CO and hence by inference the distribution of molecular Hydrogen. Figure 5 shows the distribution of CO in R as determined by Gordon and Burton. In obtaining figure 5 the average density of CO molecules along a line of sight distance Δr is calculated from

$$n(CO) = \frac{N(CO)}{r} = 3.43 \times 10^{14} \frac{[^{12}C]}{[^{13}C]} \int \frac{T_B(^{12}CO)dv}{\Delta r}$$

(Gordon and Burton 1976). In this expression $[^{12}C]/[^{13}C]$ is the relative abundance of the ^{12}C and ^{13}C isotopes. In calculating N(CO) Gordon and Burton assume a $[^{12}C]/[^{13}C]$ ratio of 40 for the ISM compared to a terrestial abundance ratio of 89.

Figure 5 also shows the surface density of CO

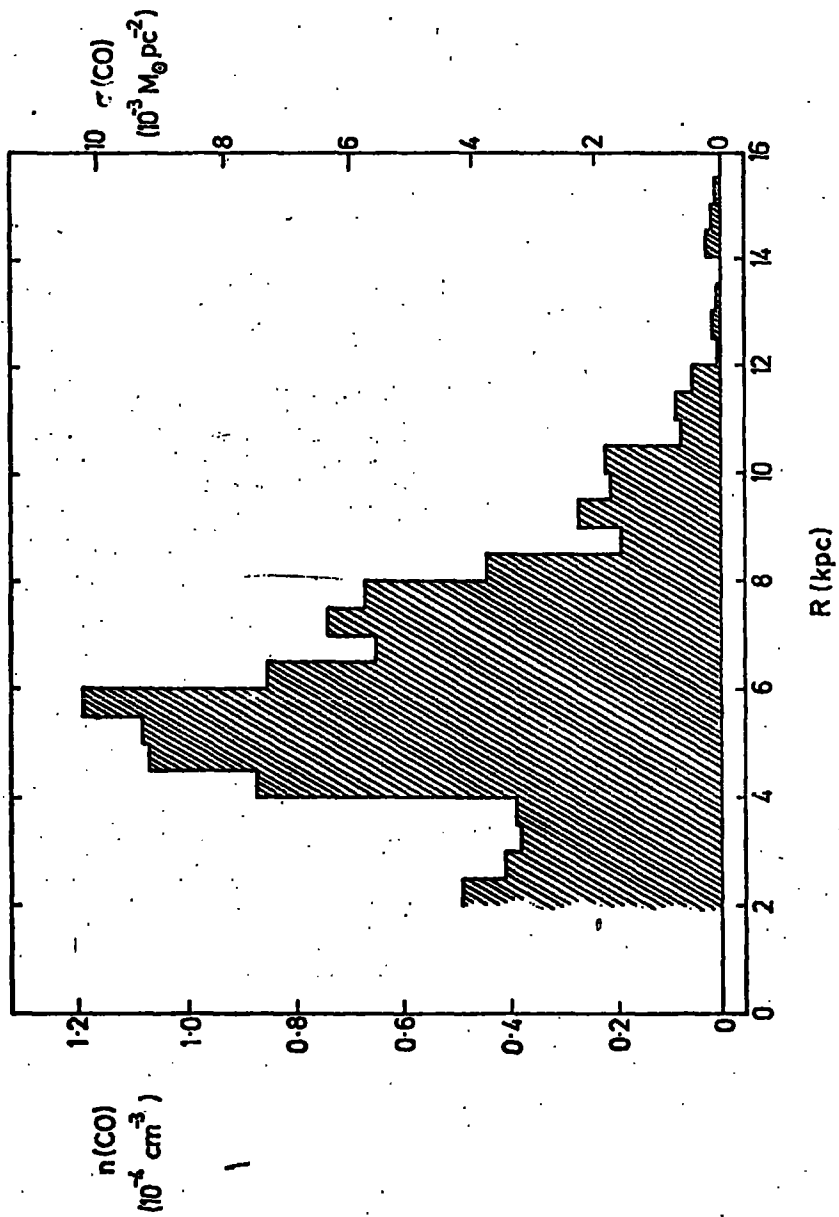Figure 5. The distribution of the carbon-monoxide density n(CO), and surface density, N(CO), with Galacto-centric radius, R. The data is from Gordon and Burton (1976).

which is calculated from n(CO) and the total layer
thickness, which was measured by Burton and Gordon
(1976) at $1 = 21°$ and found to be 117pc. Scoville
and Solomon also quote a layer thickness, which at
100pc is in quite good agreement with the Burton and
Gordon figure.

The volume and surface density of molecular
hydrogen can be calculated using the data in figure 5
from the relative abundance of carbon and hydrogen in
the ISM if the fraction of carbon in CO is known.
Gordon and Burton quote a figure of 10% for the latter
quantity leading to an $n(CO)/n(H_2)$ ratio of $6 \ 10^{-5}$.
Figure 6 shows the distribution of molecular hydrogen
in the galactic plane calculated from the data in
figure 5 and using this ratio. In addition, to the
molecular hydrogen $n(H_2)$ figure 6 also shows the
distribution of atomic hydrogen, $n(HI)$ and the total
hydrogen density $2n(H_2) + n(HI)$. Essentially the same
distribution was found by Scoville and Solomon except
that these authors quote a density of 5.0 molecules
cm^{-3} at the peak near 5.5 kpc., compared to Gordon
and Burton's peak value of 1.9 molecules/cm^3.

Figure 7 shows the surface density of molecules,
atoms and the total hydrogen. The molecular surface
density is calculated from the data in figure 6
using the layer thickness quoted above. The data
presented in figure 7 strongly implies that the
picture of the inner galaxy derived from 21 cm
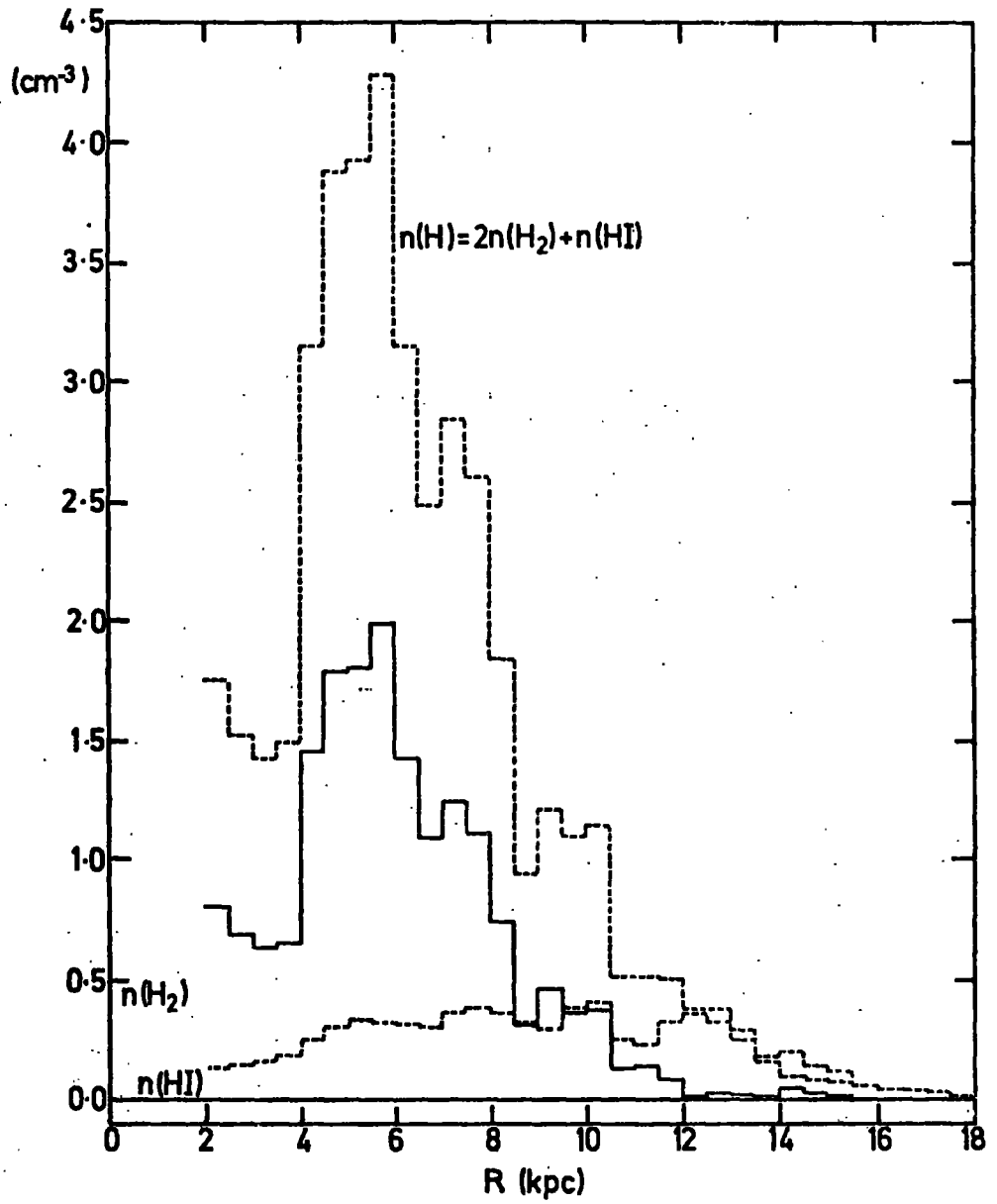astronomy greatly underestimates the total gas content.

Figure 6.   The radial distribution of the total hydrogen density,
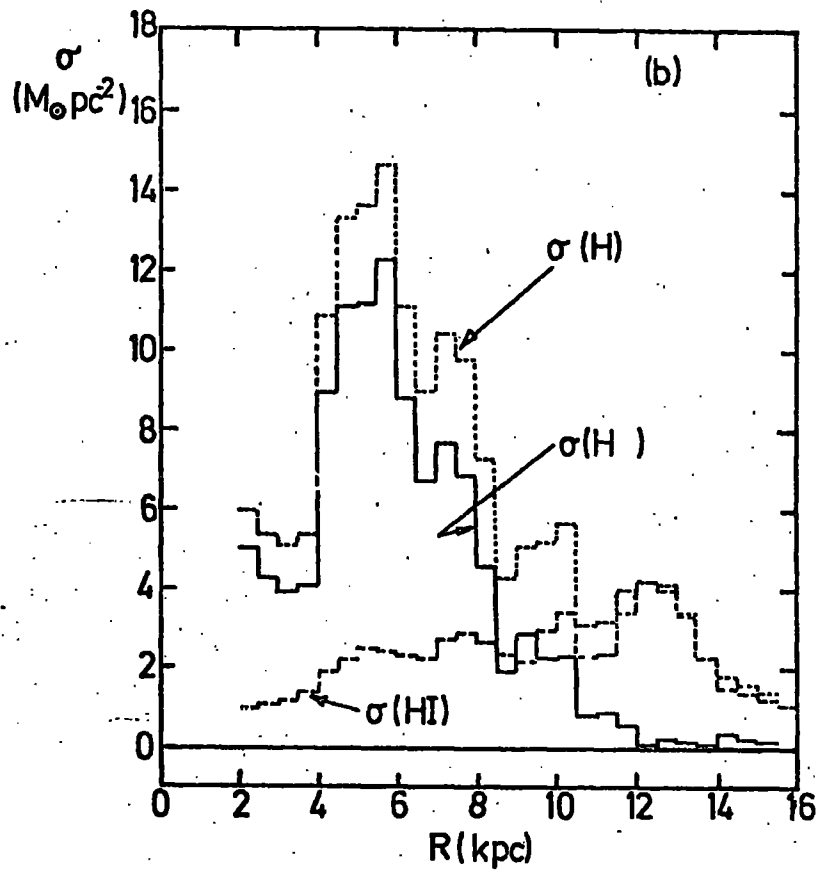 $n(H) = 2n(H_2) + n(HI)$.

Figure 7.   The radial distribution of the surface density of hydrogen according to Gordon and Burton (1976).

In fact Burton (1976) estimates that as much as 93% of the hydrogen gas in the inner galaxy may be in molecular form. However, the difficulties in calculating the molecular hydrogen density from the CO observations mean that there must remain considerable uncertainty in this estimate. In addition there remains an uncertainty in the density of molecular hydrogen in lower density clouds. The Gordon and Burton results pertain only to the distribution of dense clouds, the large fraction of H_2 discovered by Spitzer et al. 1973 is simply not included in their results. Clearly, the possible uncertainty in the published figures is large.

5.4 The Density and Distribution of other Atoms

In later chapters the interstellar gas will be regarded mainly as a target material for interactions of the interstellar cosmic ray flux. Thus, in addition to the hydrogen it is important to include the material in the interstellar medium with atomic number above 1. This is best achieved through a multiplying factor $\overline{M}$ such that

$$\overline{M} = \sum_A \frac{M_A f(M_A)}{M_H}$$

where M_A is the mass of the atom of atomic number A and $f(M_A)$ is the relative abundance of this atom compared to hydrogen.

Trimble (1975) in a recent survey gives abundances for three regions: the solar atmosphere, the Orion nebula and for planetary nebulae. Using these abundances $\overline{M}$ is found to be 1.34, 1.46 and 1.71. Allen (1973) quotes 1.36 but both

Pagel (private communication 1976) and Trimble (private communication 1976) propose higher values, 1.42 and 1.46 respectively. Therefore for the best estimate for $\bar{M}$ pertaining to the locality of the sun a value $\bar{M} = 1.42$ is adopted.

However, it is likely that the composition of the interstellar gas will vary with position in the galaxy. Measurements on other galaxies support this view and there is evidence from our own galaxy too (see D'Odorico et al. 1976). Peimbert (Private Communication 1976) considers that $\bar{M}$ may increase from 1.42 near the sun to 1.8 or 1.9 near the Galactic centre.

In the region near 5-6 kpc where the peak of the hydrogen density occurs $\bar{M}$ might only be larger by 10% than the solar value. A 10% variation in the C/H ratio between 10 and 5 kpc might have to be taken into account in deriving the molecular hydrogen densities when better data are available.

Robinson,B.J.,1974. The Interstellar Medium, Ed. K.Pinkau, D.Reidel, Dordrecht.

Sanders, R.H. and Wrixon, G.T., 1973. Astron Astrophys, 26, 365.

Scoville, N.Z. and Solomon, P.M., 1975. Astrophys. J., 199, L105.

Spitzer, L., Drake, J.F., Jenkins, E.B., Morton, D.C., Rogerson, J.B. and York, D.G., 1973. Astrophys. J., 181, L116.

Trimble, V., 1975. Rev. Mod. Phys., 47, 877.

CHAPTER SIX

THE CONTRIBUTION TO GALACTIC GAMMA-RAYS FROM INTER-
ACTIONS BETWEEN COSMIC RAYS AND THE INTERSTELLAR
RADIATION

6.1. Introduction

The aim of this chapter is to calculate the contribution to the gamma radiation which arises from the Inverse Compton Effect (ICE) and to investigate the longitude distribution of gamma radiation which arise from this process.

This problem has received the attention of several authors (Cowsik and Hutcheon 1971, Dodds et al. 1974, Beuermann 1974) but the actual fraction of the observable gamma flux which is produced in this process remains the subject of debate. Cowsik and Voges (1975) argue that the contribution from the Galactic centre is at least 60% ICE, whereas in earlier work we obtained a maximum of 10%. (Dodds et al. 1974). Needless to say it is important for our understanding of the origin and distribution of CRs that narrower limits be set.

6.2 A Model for the Gamma-ray emission due to ICE.

6.2.1 The ICE Mechanism and Cross-section

The kinematics of this process were described in chapter 2. In the calculation the cross-section used is that given in equation 1

$$\sigma(E_\gamma,\epsilon,E_e)dE = 2\pi r_o^2 \left[\frac{m_e^2}{\epsilon E_e^2} + \frac{m_e^4 E_\gamma}{4\epsilon^2 E_e^4} - \frac{m_e^6 E_\gamma^2}{8\epsilon^3 E_e^6} + \frac{m_e^4 E_\gamma}{2\epsilon^2 E_e^4} \ln\left(\frac{m_e^2 E_\gamma}{4\epsilon E_e^2}\right) \right] dE_\gamma$$

1.

6.2.2 The intensity of the interstellar radiation field.

This is an important problem for several areas of
Astrophysics and as a result has received the attention
of a number of authors (Zimmermann 1964, Witt and
Johnson 1975, Habing 1968, Gondhalekar and Wilson 1976)
In particular interest has been focussed on the wave-
length region between 912 and 3000 Å which is of importance
in understanding the ionization equilibrium of the inter-
stellar medium. Figure 1 shows the radiation intensity
as a function of frequency from the results of several
different calculations.

It is immediately obvious from an examination of
the luminosity function of stars as a function of their
spectral type that the intensity of starlight is dominated
by the radiation from G-type stars with surface tempera-
ture of 6000 K (for example see Mihalas 1968). To a
good approximation the interstellar radiation can be
represented by a 'greybody' spectrum (i.e. a diluted
black-body spectrum) with temperature 6000 K. Figure
1 shows the spectrum adopted here, the dilution factor
was obtained by adopting a total energy density for
starlight of 0.45 eV cm^{-3}(Allen 1973). This spectrum
is in good agreement with results of the other calcula-
tions.

In addition to the local energy density and spectrum
of starlight the spatial variation of energy density
with position is required. In these calculations it
is assumed that the energy density of starlight follows
the total mass density in the galaxy and the Innanen
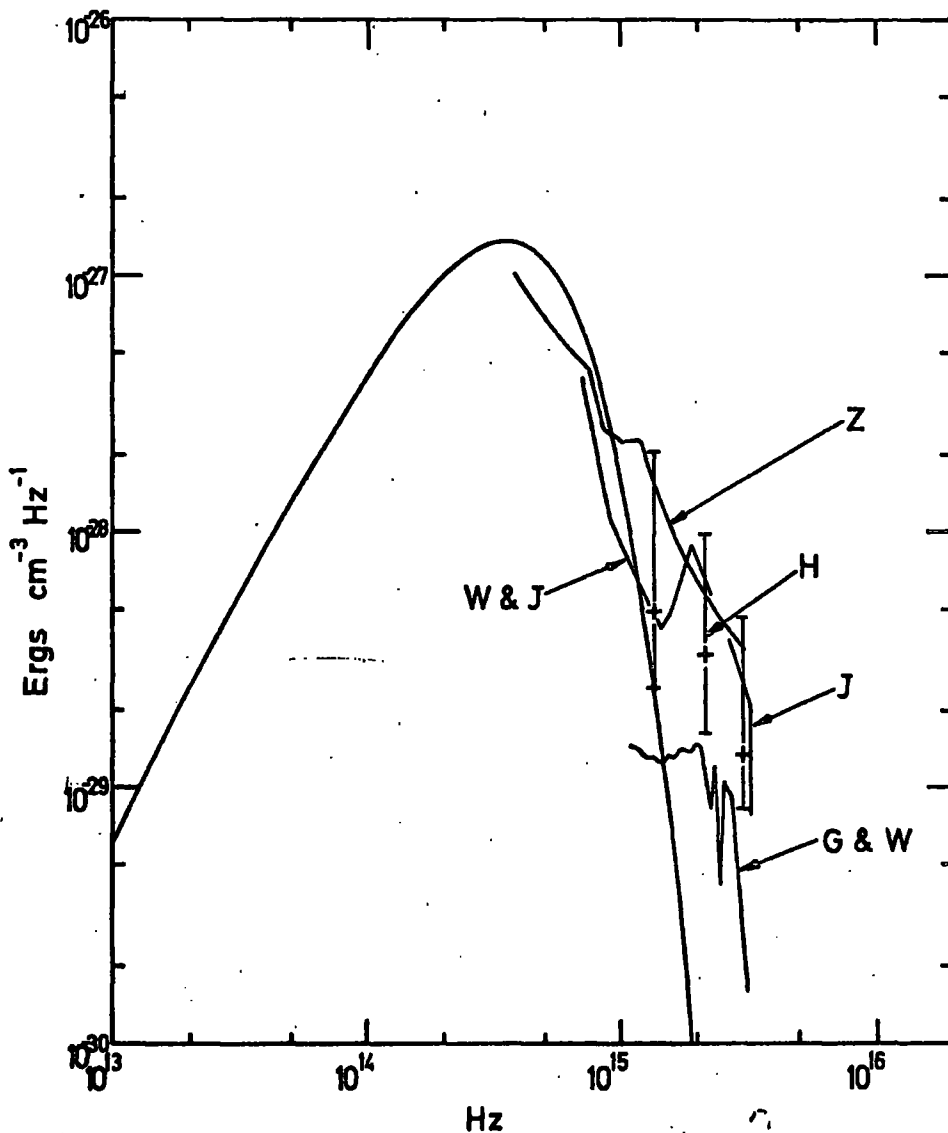
Figure 1.   The distribution of starlight energy density with
             frequency for a 6000 K diluted black body spectrum
             with total energy density 0.45 eV cm^{-3}.   Also included
             for comparison are the results of the calculations
             mentioned in the text;

                    Z - Zimmerman (1964)
                    H - Habing (1968)
                  W&J - Witt and Johnson (1973)
                    J - Jura (1975)
                  G&W - Gondhalekar and Wilson (1976).

(1973) mass model has been adopted.   Confirmation
of the validity of this approach comes from studies
of other spiral galaxies (de Vaucouleur 1959, Freeman
1970, Simkin 1975) which show that the surface bright-
ness distribution of spiral galaxies have the general
form $I(R) = I_0 exp(-\alpha R)$.   This is also the form of
the distribution of the surface density of matter as
obtained by Innanen.   Furthermore it is assumed
that there is no change in the spectral distribution of
the light as a function of position, in agreement with
the recent observations by Simkin (1975).

The other component of the interstellar radiation
field which is included in the calculations is the
universal blackbody radiation.   The thermal nature
and (near perfect) isotropy of this radiation is well
established, in these calculations a temperature of
2.7 K is adopted.

6.2.3 The Electron Spectrum

Figure 2 shows a compilation of observations of
the cosmic ray electron spectrum from Meyer (1975).   Above
10GeV the experimental points probably represent
accurately the local interstellar electron spectrum,
however, below this energy the spectrum is modulated
by interaction with the solar wind and the correct
interstellar spectrum is somewhat uncertain.

The energies of the electrons required to produce
Compton gamma rays may be estimated from equation 28
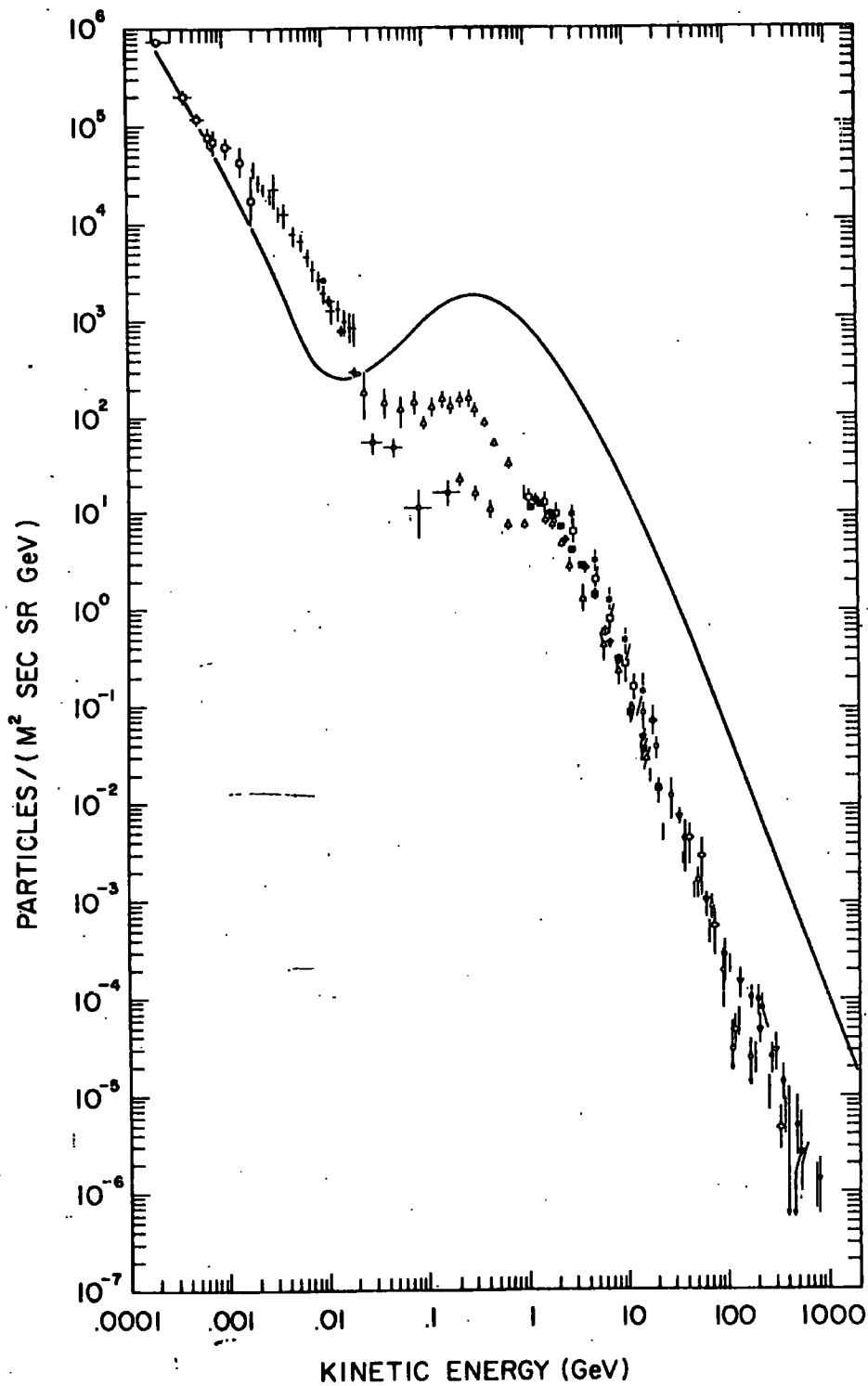of chapter 2.   The mean photon energies of the two

Figure 2. A compilation of measurements of the interstellar
electron spectrum from Meyer (1975). The contin-
uous line gives the proton spectrum for comparison.

radiation fields described above are 1.39 and 6.3 10^{-4} eV respectively. Upon using equation 28 it is found that the electron energies required to produce γ-rays with a mean energy of 100 MeV are 3.5 10^9 eV and 1.8 10^{-11} eV respectively. Referring again to figure 2 it is noted that the former energy lies in the region where the spectrum is modulated by the solar wind. In addition it is to be noted that this implies that for

$\epsilon = 1.4$ eV and $E_\gamma = 100$ MeV the minimum electron energy required is 2 10^9 eV.

Although the interstellar electron spectrum in this energy region is not directly observable because of solar modulation the main features of the spectrum can be identified from an examination of the galactic non-thermal radio emission; for example, Cummings et al. (1973) have used the available observations of the galactic radio spectrum to derive an interstellar electron spectrum under the assumption that the radiation process is synchroton radiation in an interstellar magnetic field. Figure 3 shows the derived electron spectra which are compatible with the radio observations. The large range in the spectra which they deduce is due to the uncertainty in the important astrophysical parameters; nevertheless, the medial spectrum is in very good agreement with the demodulated spectrum of Bedijn et al. (1973).

The most important point about the electrum spectrum to emerge from studies of the radio emission is that the radio spectrum requires an electron spectrum which is flatter below about 2 GeV than the high energy electron
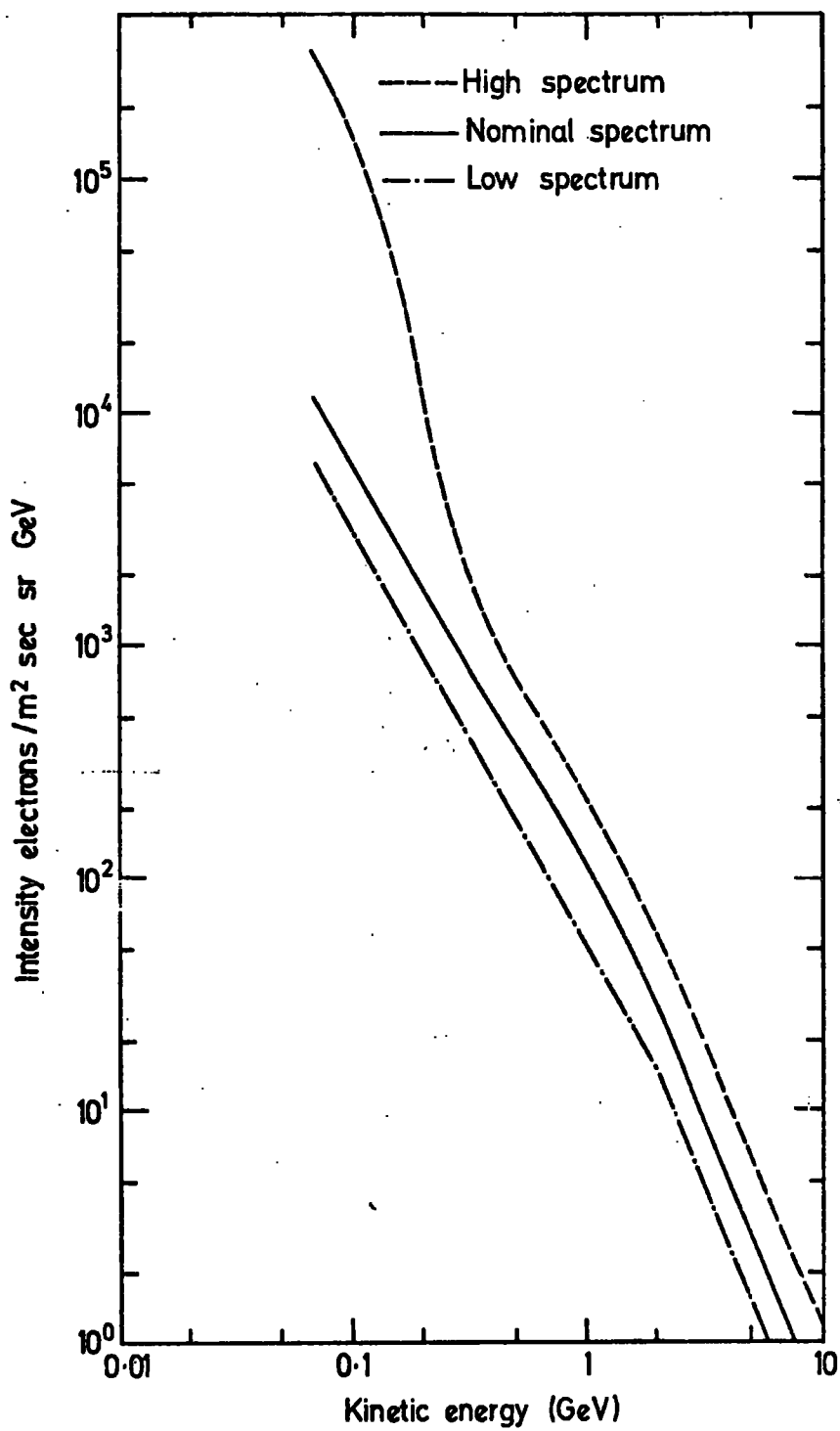
Figure 3.   The interstellar electron spectrum at low energies
            as derived by Cummings et al (1973) from the observed
            Galactic non-thermal radio emission.

spectrum. Meyer (1975) points out that this flattening is confirmed by the measurements of the electron positron ratio. This increases with decreasing energy below about 1 GeV, implying that the slope of the spectrum of positrons is steeper than that of the electrons. The former can be calculated from the kinematics of π^+ decay and turns out to be of order 2.0. Therefore the slope of the low energy ($\leqslant 2$ GeV) electron spectrum must be considerably less than the slope of the high energy spectrum which is $\simeq 3.0$.

The nominal spectrum of figure 3 adopted in the calculations is:-

$$I_1(E_e) = 1.34 \ 10^5 \ E_e^{-1.8} \qquad\qquad 7.0 \ 10^7 \leqslant E_e \leqslant 2 \ 10^9 \ eV$$

$$cm^{-2} \ s^{-1} \ sr^{-1} \ eV^{-1} \qquad\qquad\qquad\qquad\qquad\qquad 2.$$

$$I_2(E_e) = 4.35 \ 10^{11} \ E_e^{-2.5} \qquad\qquad 2 \quad 10^9 \leqslant E_e$$

At high energies the spectrum adopted is that proposed by Webber (1973) as the best fit to the measurements above 10 GeV; $I(E) = 2 \ 10^{16} \ E_e^{-3}$.

6.2.4 The Spatial Variation of the Electrons

In the calculation the spectral shape and composition of the cosmic ray electrons are assumed constant over the whole galaxy. These simplifying assumptions are in agreement with the results of a study of the Galactic non-thermal radio spectrum by Stephens (1969) who found that the spectrum of radio emission was independent of position. However, these assumptions are probably not true for the high energy electrons which interact with the microwave radiation. The reason is straightforward

It is well known that at the very highest energies
the equilibrium electron spectrum is steeper than the
injection spectrum by one power, due to the electrons
losing energy by synchroton radiation and Inverse Compton
Scattering.   Approximately, the energy at which the
steepening begins is the energy at which the escape and
energy loss lifetimes are equal.   Thus:

$$E_{cr} = \frac{1}{b \, T_e \, (\Gamma - 1)} \qquad\qquad 3$$

where T_e is the escape lifetime, Γ is the exponent
of the injected energy spectrum and b is defined by
the energy loss rate $\frac{dE}{dt}$:-

$$\frac{dE}{dt} = -bE^2 = -(4 \times 10^{-6} B^2 + 10^{-16} w_{ph})E^2 \qquad 4.$$

Near the sun the break energy, E_{cr} is expected to
be   200 GeV.   If the escape lifetime is constant over
the whole galaxy then in the Galactic Centre where the
starlight energy density is some 60x higher, the value
of E_{cr} becomes   6 - 10 GeV.   Clearly the assumption
of the same high energy spectrum over the whole galaxy
is not valid.   However, it will be seen later that
the emission from the Galactic Centre is so completely
dominated by the scattering off starlight that the
effects of this assumption will be minor.

For the spatial variation of the cosmic ray density
the two most extreme cases are the most interesting.
These are a) the cosmic ray density constant over the
whole galaxy, and b) the cosmic ray density varying
as the stellar mass distribution.   In chapter 4 some
of the current ideas on cosmic ray propagation were

discussed and the cosmic ray density distribution which
would result were described.   Thus case a) would be
the result of the cosmic ray propagation model of
Holmes (1975) were correct and case b) would be the
result, if the cosmic ray escape time, T_e, were
constant over the galactic disk and the cosmic ray
sources were distributed as the stars.   Case b
probably represents the most extreme large scale
variation of the cosmic ray density which is consistent
with the radio observations of the synchroton radiation.
French and Osborne (1976) have modelled the observed
longitude distribution of brightness temperature at
150 MHz in terms of emission by electrons in the random
and ordered magnetic fields of the Galactic spiral arms.
These authors find the ratio of emissivities between 5
kpc and 10 kpc to be about 3:1.

The z distribution of cosmic ray electrons is also
studied via their radio emission.   Figure 4 shows the
observed brightness temperature versus latitude distribution
at 150 MHz at a galactic longitude of 60 .   The data for
figure 4 were taken from the compilation of Landecker
and Weilebinski (1970).   Ilovaisky and Lequeux (1972)
used this same data with the observed longitude distrib-
ution to derive the z distribution of the radio emission
which is shown in figure 5.   Baldwin (1976) has used
a similar approach with the 400 MHz observations and
obtains a z distribution in good agreement with that
of figure 5.   In both cases the z distribution implies
the existence of cosmic rays and magnetic fields at

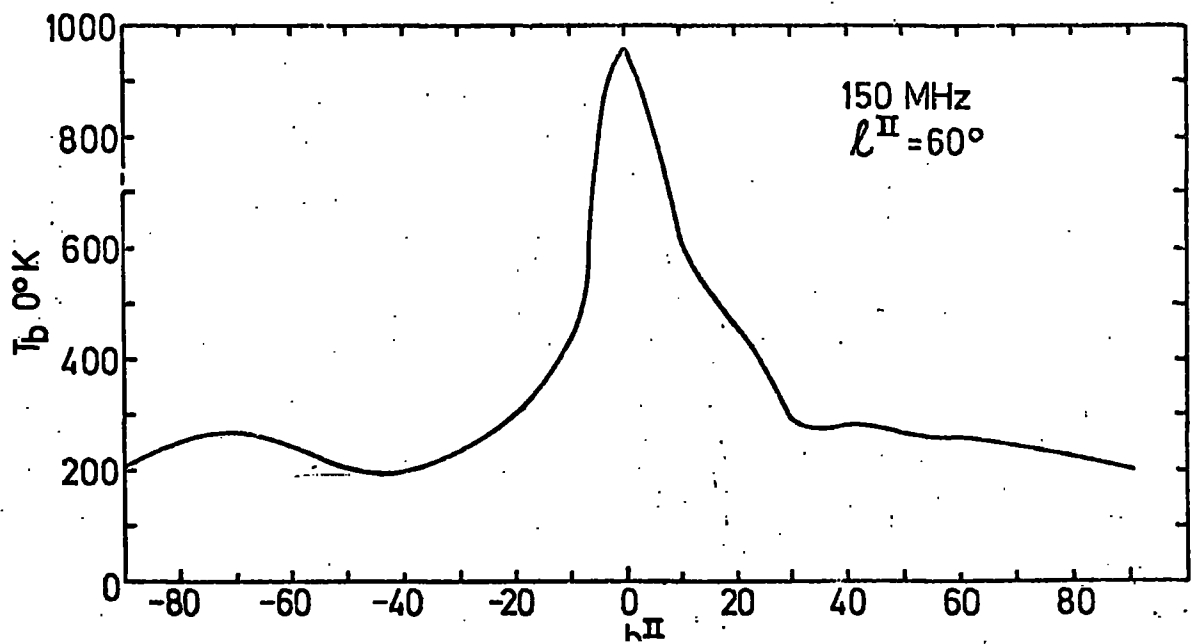Figure 4.   The distribution of the radio brightness temperature
             with Galactic latitude at a longitude of 60°.   The
             data for this figure comes from the compilation of
             Landecker and Wielebinski (1970).

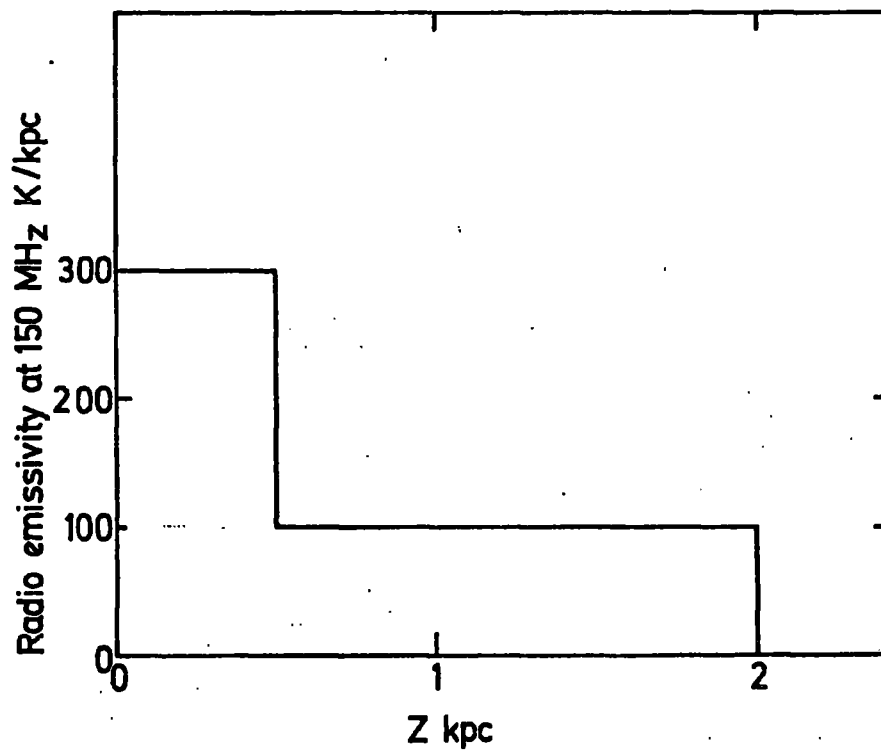Figure 5.   The distribution of radio emissivity with height, z,
            above the Galactic plane as derived by Ilovaisky and
            Lequeux (1972).

large distances from the Galactic plane.

In the calculations the z distribution of figure 5 was used to represent the electrons. The results are not sensitive to the form of the z-distribution but to the equivalent width which is 1 kpc. For comparison calculations were performed using a Gaussion with the same equivalent width. These gave results in good agreement with those described above.

The starlight density has a very broad distribution in z (Shukla and Paul 1976) since the scale height of the most important stellar component, the G stars, is 700 pc. Here the starlight density is assumed to be constant in z at least over the region occupied by the electrons. Thus the z-distribution used for the electrons is used to represent that of the gamma-ray emissivity.

As described in chapter 3 the intensity versus longitude data of Fichtel et al. (1975) is presented as the strength of a line source i.e. as γ's $cm^{-2}s^{-1}rad^{-1}$. In the calculation, the flux, $F_\gamma(l)$, from a bin of width 5° in 1 extending to $\pm 10^{\circ}$ in b is first calculated, where

$$F_\gamma(1) = \int_{1-2.5}^{1+2.5}\int_{-10}^{+10}\int_{0}^{\infty} q^{IC}(r,z)\ dr\ db\ dl \qquad 5$$

and the line strength $I_\gamma(l)$ averaged over 5° in 1 is given by

$$I_\gamma(\ell) = \frac{36}{\pi} F_\gamma(\ell) \qquad 6$$

The integrations in equation 5 were performed numerically using the R, and z dependences of the gamma ray emission function which were described above. The

resulting intensity v.s longitude plots are described below

6.3. Results

Near the solar system the calculated emissivities for interactions with a) starlight and b) the 2.7K blackbody are

a) q^{IC} (> 100 MeV) = 2.75 10^{-27} γ's cm^{-3} s^{-1}

b) q^{IC} (> 100 MeV) = 8.5 10^{-28} γ's cm^{-3} s^{-1}

The integral spectra from these two processes are shown in figure 6 with the upper and lower limits to both spectra calculated using the upper and lower limits on the electron spectra in the relevant energy intervals.

Figure 7 shows the longitude distribution of the gamma-ray intensities from the calculations described above compared with the 100 MeV data of Fichtel et al. (1975). In figure 8 these data are combined to give the predicted galactic centre spectra from both the starlight and 2.7 K for each of the cosmic ray distributions described above. Figure 8 also shows the observed spectra of Fichtel et al.

6.4. Discussion

Comparison of the observed intensity longitude distribution with the predictions of the model (figure 7) indicates that the maximum contribution which results from the IC process for the case in which the cosmic ray density is constant is a few percent. This is
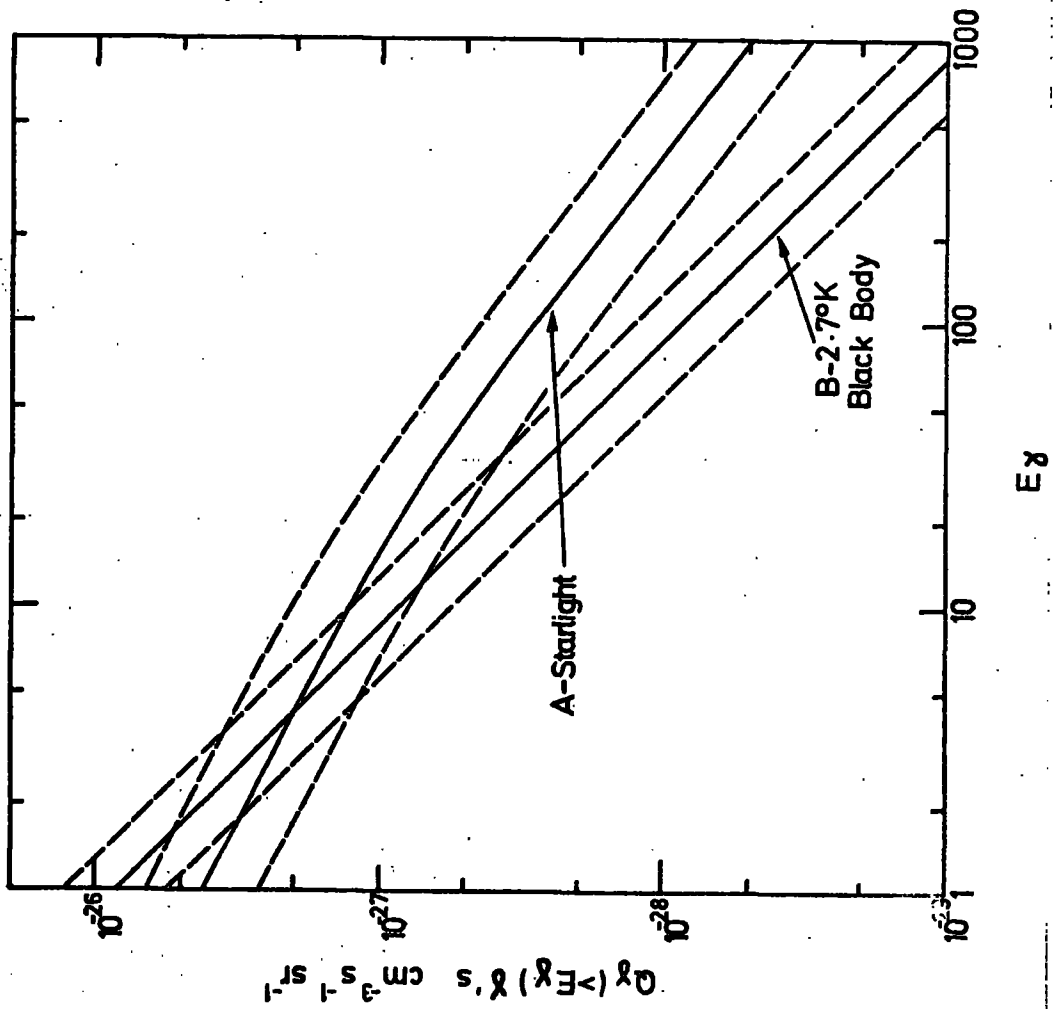
Figure 6. The integral spectra of inverse Compton gamma-rays near the solar system. The dashed lines give the upper and lower limits to the spectra which are obtained using the upper and lower limits to the spectra in figure 3.
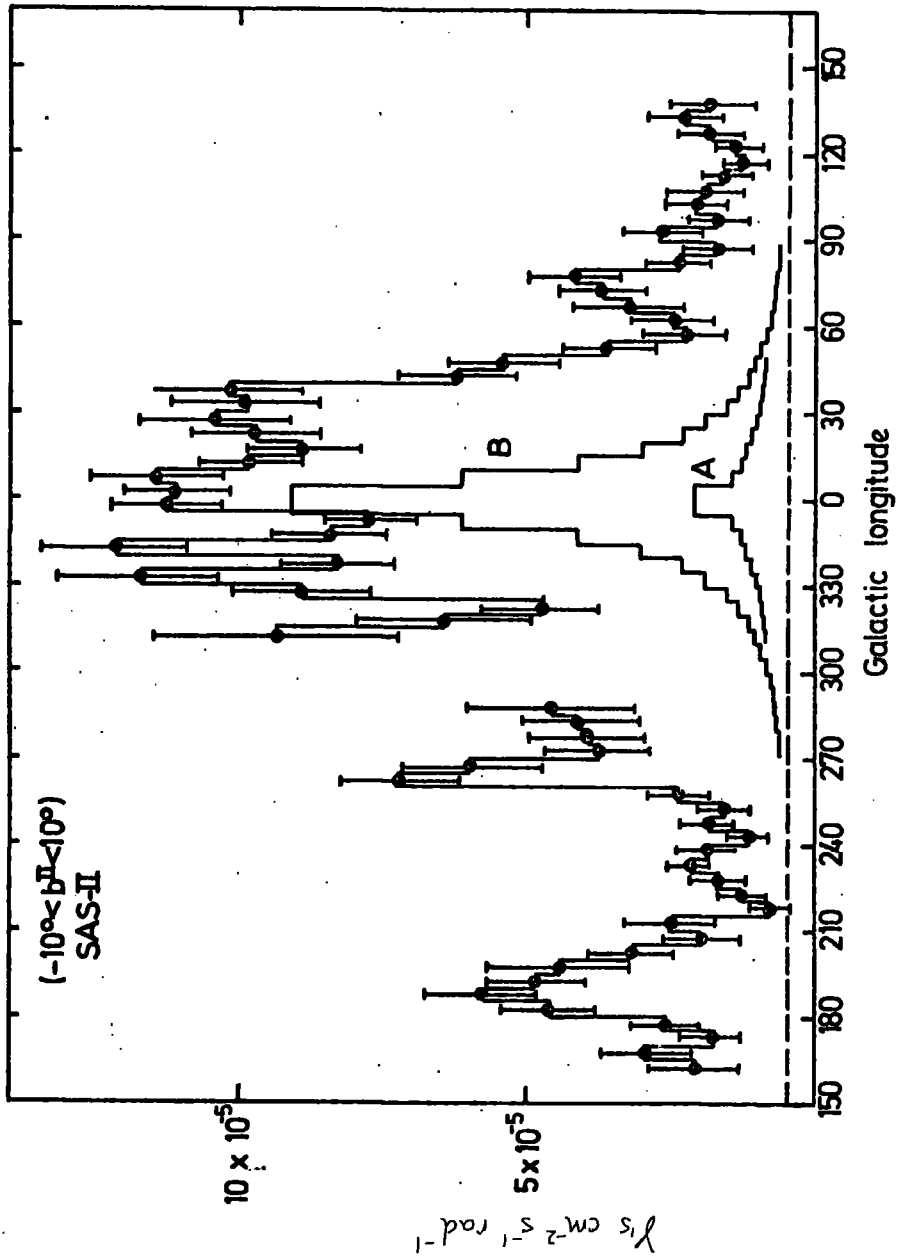
Figure 7. The predicted longitude distribution of gammas from inverse Compton scattering for: A, the density of cosmic rays constant throughout the Galaxy and B, the density of cosmic rays proportional to the density of matter. Also included is the observed distribution from Fichtel et al (1975.
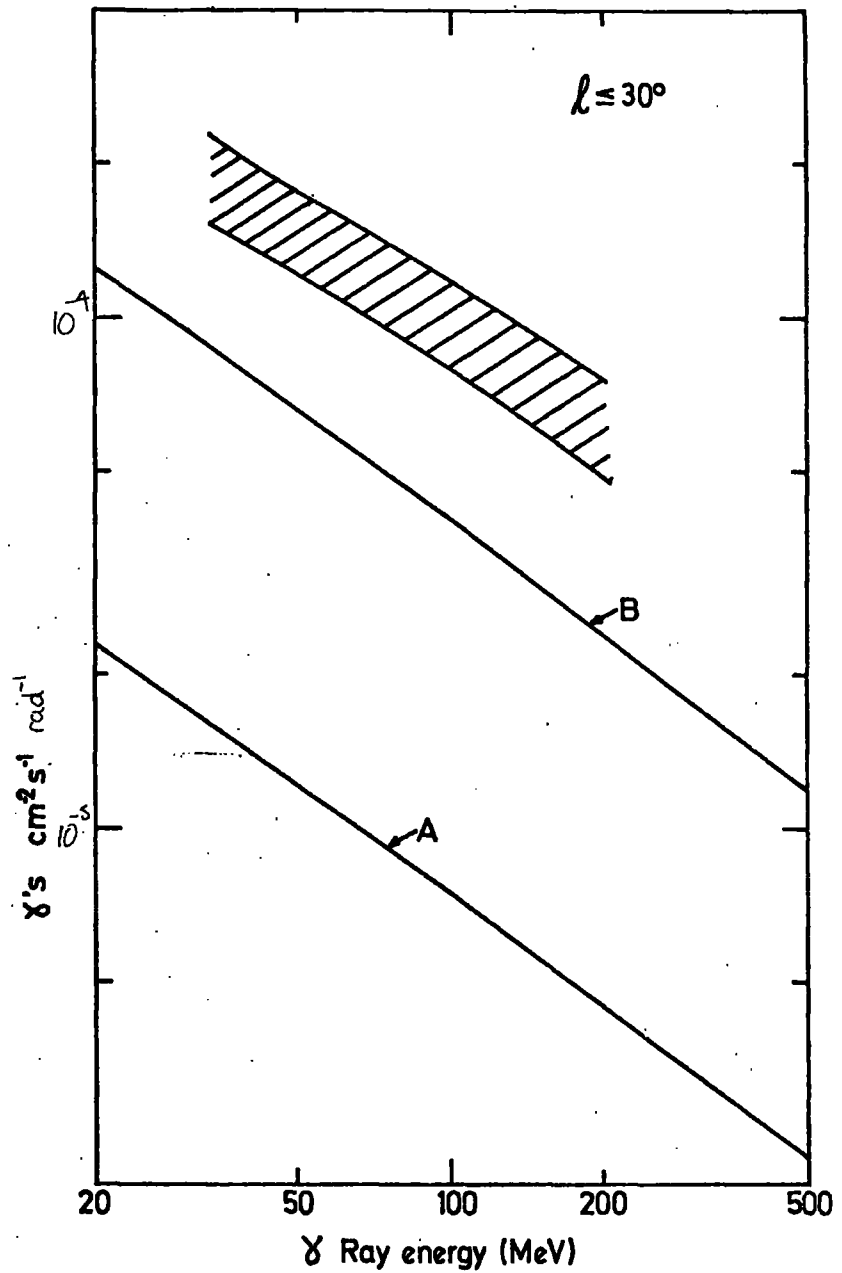
Figure 8. The predicted gamma ray spectrum from the Galactic
          centre for cases A and B as in figure 7. The
          hatched region is the Galactic centre spectrum
          from Fichtel et al (1975).

in clear disagreement with the work of Cowsik and
Voges (1974) who predict a 60% contribution.   The
reasons for the disagreement are threefold.

Firstly, Cowsik and Voges have used a starlight
spectrum with a temperature of 10^4K and a mean photon
density near the sun of 0.8 photons cm^{-3}.   Together,
these assumptions imply an energy density which is
1.86 eV/cm^3 or approximately 4X the energy density used
in the calculations here.   The observational evidence
is strongly in favour of a smaller value, say, 0.4 - 0.5
eV/cm^3 as quoted by Allen (1973) or perhaps an even
lower value (Stecher and Milligan, 1962).

Secondly, these authors have used a thickness of
2 kpc for the electron disk which will give an increase
of a factor of two over the intensities calculated above.

Finally, over a large part of the Galaxy ($2 \leqslant R \leqslant 8$)
the stellar mass distribution used by Cowsik and Voges
is   4X the density given by the model of Innanen (1973)
which probably represents the best available work on
the distribution of mass in the Galaxy.

One method of checking the above calculations is
to compare the results with the Compton gamma ray flux
calculated from the observed radio intensities (see for
example Felten and Morrison 1966).   This method
used the fact that the same electrons which produce
inverse Compton gamma rays will also produce radio
frequency synchrotron radiation with the same spectral
slope.

Using the 150 MHz data from Landecker and Wielebinski

(1970) and assuming a uniform magnetic field of $3 \ 10^{-6}$ gauss, this method predicts a flux of 1.0×10^{-8} photons $cm^{-2} \ s^{-1} \ ster^{-1} \ MeV^{-1}$ from the Galactic pole. The above model gives a value of 8.6×10^{-9} photons $cm^{-2} \ s^{-1} \ ster^{-1} \ MeV^{-1}$. This excellent agreement supports the choice of parameters above and suggests that the results of Cowsik and Voges represents an overestimate of the contribution from this process.

It is noticeable from figure 7 that the most important features of the observed intensity vs longitude plot, viz the broad flat central maximum, cannot be reproduced by having a cosmic ray distribution in which the density is proportional to the density of sources. The models considered here clearly predicts that the greatest contribution to the Galactic flux will occur in narrow region around the Galactic centre. The magnitude of the observed peak at the Galactic Centre may be used to set limits on the Galactic centre cosmic ray flux (Wolfendale and Worrall, 1976).

Finally, it must be remarked that in these calculations it has been assumed that the ratio of primary to secondary electrons is constant over the whole disk. The effect of this varying will be small since the ratio is 10 to 1 in the Solar System. It will however be considered in the calculations of the next Chapter.

REFERENCES

Allen, C.W., 1973. Astrophysical Quantities. Athlone
Press, London.

Baldwin, J.E., 1976. GSFC Symposium on Gamma-Ray Astronomy,
to be published.

Beuermann, K.P., 1974. Proc. Ninth ESLAB Symposium, ESRO
SP-106, p. 259.

Cowsik,R.& Hutcheon   I.D., 1971. Proc. 12th Int. Conf.
on Cosmic Rays, $\underline{1}$, 102.

Cowsik, R. & Voges, W., 1974. Proc. Ninth ESLAB Symposium,
ESRO SP-106, p. 229.

Cummings, A.C., Stone, E.C. & Vogt, R.E., 1973. Proc.
13th Int. Conf. on Cosmic Rays., Denver, $\underline{1}$, 355.

Dodds, D., Strong, A.W., Wolfendale, A.W., Wdowczyk, J.,
1974. Proc. Ninth ESLAB Symposium, ESRO SP-106, p.221.

Fichtel, C.E., Hartman, R.C., Kniffen, D.A., Thompson, D.J.,
Bignami, G.F., Ögelman, H., Ozel, M.F., & Tumer, T., 1975.
Astrophys. J., $\underline{198}$, 163.

Freeman, K.C., 1970. Astrophys. J., $\underline{160}$, 811.

French, D.K. & Osborne, J.L., 1976. Mon. Not.R.astr. Soc.,
to be published.

Gondhalekar, P.M. & Wilson, R., 1975. Astr.Astrophys.,
$\underline{38}$, 329.

Habing, H.J., 1968. Bull.astr. Inst. Netherlands, $\underline{19}$, 421.

Holmes, J.A., 1979. Mon. Not. R. astr. Soc., $\underline{166}$, 155.

Ilovaisky, S.A..& Lequeux, J., 1972. Astr. Astrophys., 20, 347.

Innanen, K.A., 1973. Astrophys. Sp. Sci., 22, 393.

Jura, M., 1975. Astrophys. J., 191, 375.

Landecker, T.L. & Weilebinski, R., 1970. Aust. J. Phys. Astrophys. Suppl., 16, 1.

Meyer, P., 1975. In 'Origin of Cosmic Rays", Eds. J.L. Osborne & A.W.Wolfendale, D.Reidel, Dordrecht.

Mihalas, D., 1968. Galactic Astronomy, Freeman & Co., San Francisco.

Shakla, P.G. & Paul, J., 1975. Preprint.

Simkin, S.M., 1975. Astr. J., 80, 415.

Stecher, T.P. & Milligan, J.E., 1962. Ann.d'Astrophys., 25, 268.

Stephens, S.A., 1969. Ph.D. Thesis, University of Bombay.

Vancouleurs, G.de., 1959., Hdb. d. Phys., 53, 311.

Webber, W.R., 1973. Proc. 13th Int. Conf. on Cosmic Rays, Denver. 5, 3568.

Witt, A.N. & Johnson, 1973. M.W., Astrophys. J., 181, 363.

Wolfendale, A.W. & Worrall, D.M., 1976. Nature, to be published.

Zimmermann, H., 1964. Ast. Nachr., 288, 99.

CHAPTER SEVEN

THE GALACTIC DISTRIBUTION OF GAMMA RAY EMISSION FROM
COSMIC RAY-MATTER INTERACTIONS

7.1 Emissivity near the Solar System due to π^o Production

The details of this mechnism were discussed in Chapter 2. In this section the aim is to determine the emissivity of gamma radiation in nearby interstellar space using the observed spectrum of cosmic rays.

The threshold for π^o production in p-H, p-He reactions is a few hundred MeV. Unfortunately the cosmic ray spectrum above this energy and up to a few GeV is not accurately known, the measured energy spectrum at the top of the atmosphere varies over the solar cycle due to the time dependent modulation of the solar wind. Thus the local interstellar spectrum near 1 GeV has to be deduced from the observed modulated spectrum using a theory for the interaction of the solar wind and cosmic rays.

Comstock et al. (1972) have performed a demodulation of the energy spectra measured at solar minimum in 1965. These authors find that the best fit to the data is obtained for an interstellar spectrum which is a power law in total energy, W, with a constant exponent $\Gamma = 2.6$. Their spectra of protons and α particles are shown in figure 1. The actual form of these spectra are for protons $J(T_p) = 5.9 \ 10^8 \ (T + E_o)^{-2.6} \ m^{-2} \ sr^{-1} \ s^{-1}$ (MeV/nucleon)$^{-1}$ and for α-particles $J(T_\alpha) = 6.5 \ 10^7 \ (T + E_o)^{-2.6} \ m^{-2} \ sr^{-1} \ s^{-1}$ (MeV/nucleon)$^{-1}$ where T is the kinetic energy
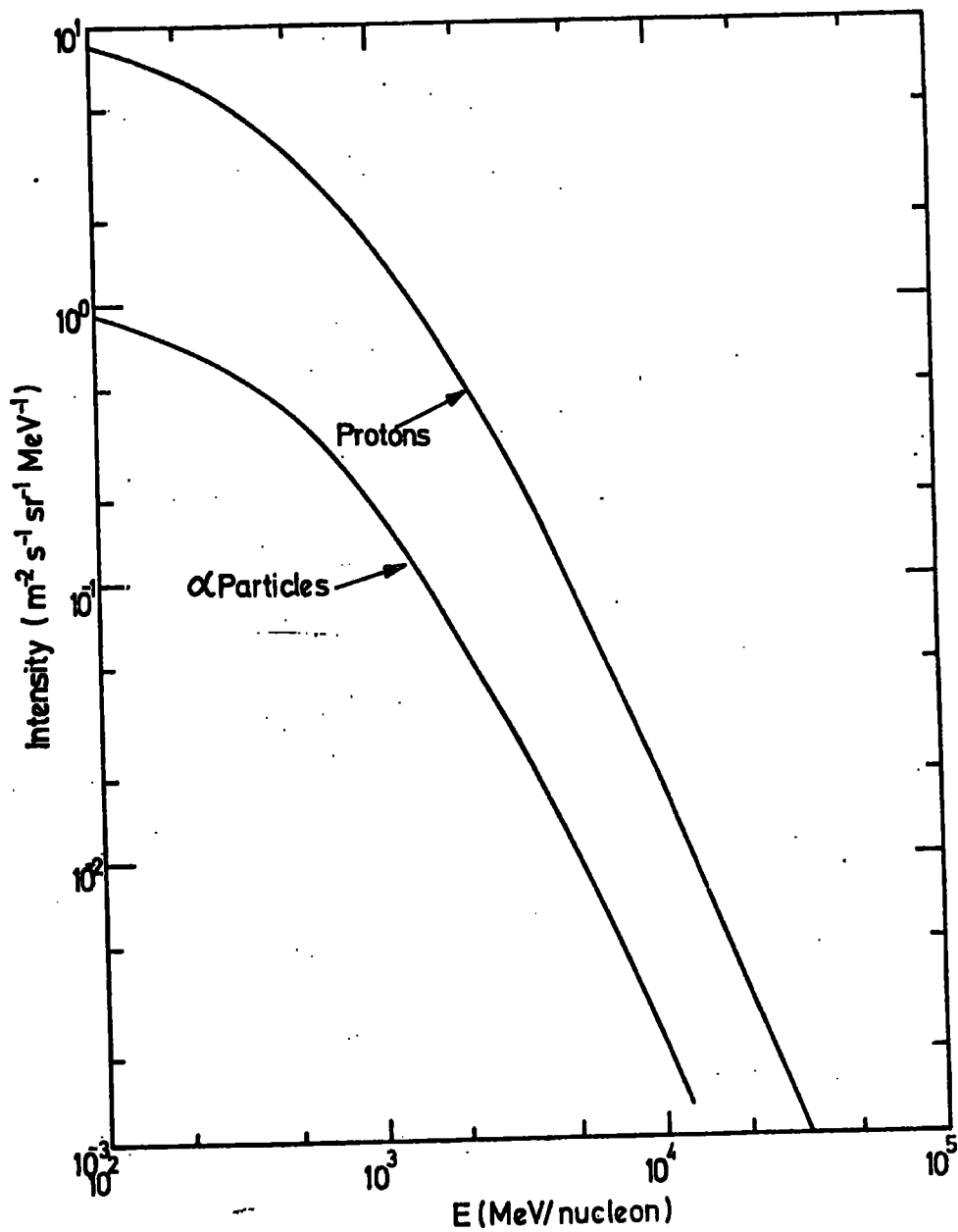
Figure 1.   The interstellar spectra of protons and alpha
particles according to Comstock et al (1972.

and E_0 is the rest energy per nucleon.

Figure 2 shows the product of $J_{CR}(T)$ and $q(T) \, m_{\pi^0}(T)$ for both p - H and α - H collisions. The total yield of gamma rays from π^0 decay is given by the equation

$$Q_{\pi^0} = \sum_{\ell} \sum_{k} 8\pi \int_0^\infty J_k(T) \sigma_{\pi^0 k\ell}(T) \, m_{\pi^0 k\ell}(T) \, dT$$

where the summations extend over the gas nuclei, l; and the cosmic ray nuclei, k.

Considering p - H collisions only, the yield is given by integration under the distribution in figure 2. Figure 3 is a plot of the cumulative distribution given by

$$\frac{Q_{\pi^0}(<T)}{Q_{\pi^0}} = \frac{\int_0^T J_p(T) \, \sigma_{\pi^0 pH}(T) \, m_{\pi^0 pH}(T) \, dT}{\int_0^\infty J_p(T) \, \sigma_{\pi^0 pH}(T) \, m_{\pi^0 pH}(T) \, dT} \qquad 1.$$

From an examination of figure 3 the median energy for gamma ray production can be determined. For protons on hydrogen this is 2.7 GeV. In addition, it can be seen from figure 3 that 80% of the emission arises from protons between 900 MeV and 15 GeV. Table I lists the median energies for the three most important processes viz. p - H, p - He and α - H collisions.

Now, although the dominant contribution to π^0 production will arise from the collision processes already described and listed in Table I, it is important to consider the possible contribution from cosmic ray nuclei with Z>2, which in practice involves mainly the nuclei C, O, Ne, Mg and Si. The observational results on the relative abundances of these elements in cosmic ray has recently been reviewed by Waddington (1974). This author gives the ratio of the number of the nuclei to the total C + O nuclei as 25:1, with approximately equal fluxes of each nucleus.

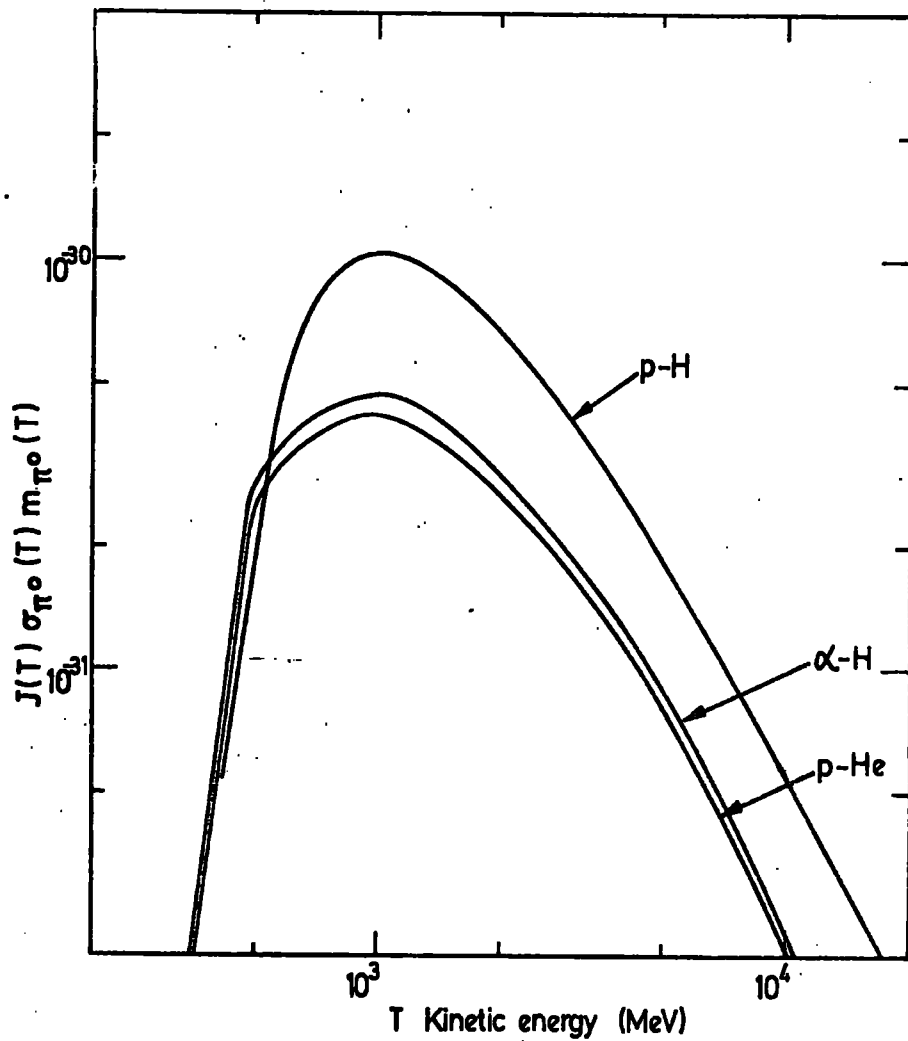Unfortunately, there are no measurements of the cross-

Figure 2. The product of $J_p(T)$ with $\sigma_{\pi^0}(T)\, m_{\pi^0}(T)$ for collisions between: protons and hydrogen (p-H), protons and helium, (p-He); alpha particles and hydrogen, (α - H). The spectra of protons and alpha's in figure 1 was used.
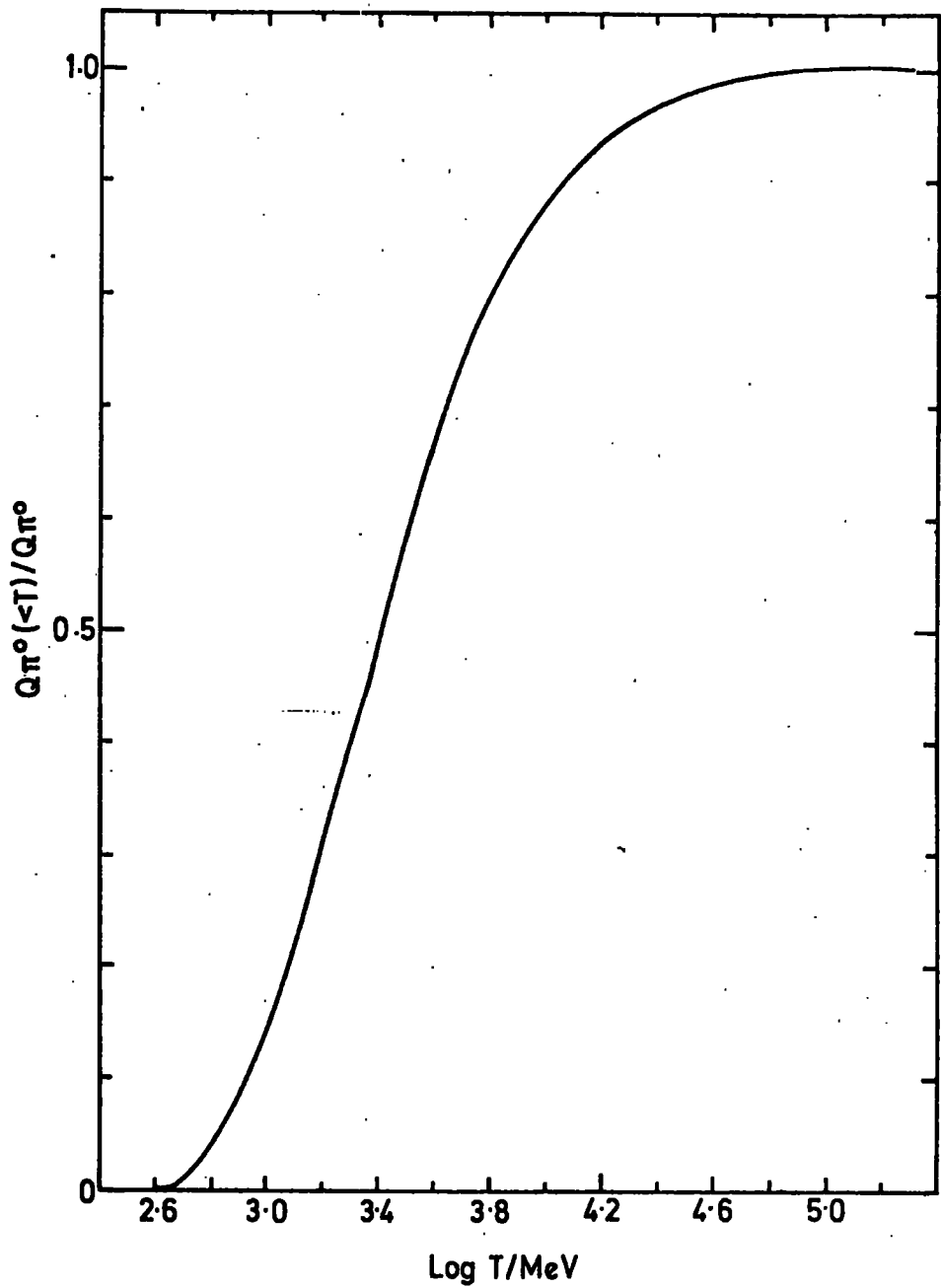
Figure 3.   The cumulative distribution of the gamma-ray emissivity
in p-H collisions.

sections $\sigma_{\pi^\circ p\text{-}c}$, $\sigma_{\pi^\circ p\text{-}o}$ etc.. Following Pollack and Fazio

(1963) the ratio of the cross-sections $\sigma_{\pi^\circ p\text{-}N}$: $\sigma_{\pi^\circ p\text{-}\alpha}$ are

assumed to be in the ratio of their atomic numbers. Using

this assumption the total contribution was estimated from

the data on the abundance relative to Helium and this comes to

25% of the contribution from cosmic ray alpha particle-

hydrogen collisions.

Table II summarises the results of these calculations

and gives both the total yield and the integral flux at 100

MeV (see Chapter 2).

TABLE I

Contributing Collision Process	Median Energy (GeV)
proton - hydrogen	2.7
alpha - hydrogen	2.6
proton - helium	2.5

TABLE II

	Contributing Collision Processes	Emissivity in gamma's (hydrogen atom)$^{-1}$s^{-1}
Total Yield	protons on hydrogen	0.84 $\times 10^{-25}$
	alphas on hydrogen	0.38 $\times 10^{-25}$
	Z $>$ 2 nuclei on hydrogen	0.09 $\times 10^{-25}$
	All CR on hydrogen	1.31 $\times 10^{-25}$
	All CR on ISM	1.84 $\times 10^{-25}$
Above 100 MeV	All CR on ISM	1.25 $\times 10^{-25}$

The final input parameter for this calculation is
the hydrogen density in nearly interstellar space.
This was discussed in chapter 4. Here, it is important
to stress that there is apparent disagreement between
the local hydrogen density from the UV absorption measure-
ments and the results of the radio astronomical observations.
Thus, Jenkins (1976) gives a total density of 1.1 atoms
cm^{-3}, comprising 0.9 atoms cm^{-3} of atomic hydrogen and
0.2 atoms cm^{-3} of molecular hydrogen, whereas Gordon and
Burton (1976) give a total density of 0.8 atoms cm^{-3}
made up equally of atomic and molecular hydrogen. How-
ever, the disagreement may not be real because the UV
observations are restricted to space within 1 kpc of the
sun whereas the Gordon and Burton result refers to the
average density in an annulus of 10 kpc radius and hence
the two values may not be directly comparable.

The gamma rate production rate for a hydrogen
density of 0.8 atoms cm^{-3} is $1\ 10^{-25}$ photons $cm^{-3}s^{-1}$.
Thus the IC contribution calculated in the last chapter
is only 3% of the π^{o} contribution. Clearly the
majority of the Galactic emission will arise from the
π^{o} mechanism. In the later part of this chapter these
calculations will be used in conjunction with the
observations of Gordon and Burton and the calculations
of the next section, to determine the distribution of
cosmic rays.

7.2 Gamma Rays from Electron Bremsstrahlung

As described in chapter 2 cosmic ray electron of
energy E_e involved in a collision with a nucleus of

the interstellar gas radiate a spectrum of gamma rays with energy between 0 and E_e, the total kinetic energy of the electron. Thus, in order to determine the integral spectrum of gamma rays $I_\gamma(E_\gamma)$ produced by Bremsstrahlung of a cosmic ray electron spectrum $I_e(E_e)dE_e$ it is necessary to know the form of the electron spectrum down to the electron energy $E_{e_{min}} = E_\gamma$. As a consequence the important energy region of the cosmic ray spectrum for producing bremsstrahlung gamma rays of 100 MeV is poorly known because of the effects of the solar modulation. Figure 4 shows the differential electron spectrum of Cummings et al. (1973) which was used in the last chapter for the calculation of the inverse Compton gamma ray production rate and which extends down to 70 MeV. It is this electron spectrum which is adopted in the following calculation.

The emissivity of bremsstrahlung gamma rays is given by

$$Q_B(E_\gamma) = \sum_j 4\pi n_j \int_{E_\gamma}^{\infty} dE_b' \int_{E_\gamma'}^{\infty} dE_e I_e(E_e) \, \sigma_{B,j}(E_\gamma' , E_e) \qquad 2$$

where n_j is the volume density of atoms of type j, $I_e(E_e)$ dE_e is the local interstellar electron spectrum and $\sigma_{B,j}(E_\gamma' , E_e)$ is the cross-section.

In this calculation the uncertainty in the electron spectrum at 100 MeV justifies the adoption of the extreme relativistic, screened, cross-section even at 50-100 MeV. Thus the cross-section used was that given by equation 17 Chapter 2.

Figure 5 shows the integral energy spectrum (expressed as the yield per hydrogen atom) for the above assumptions
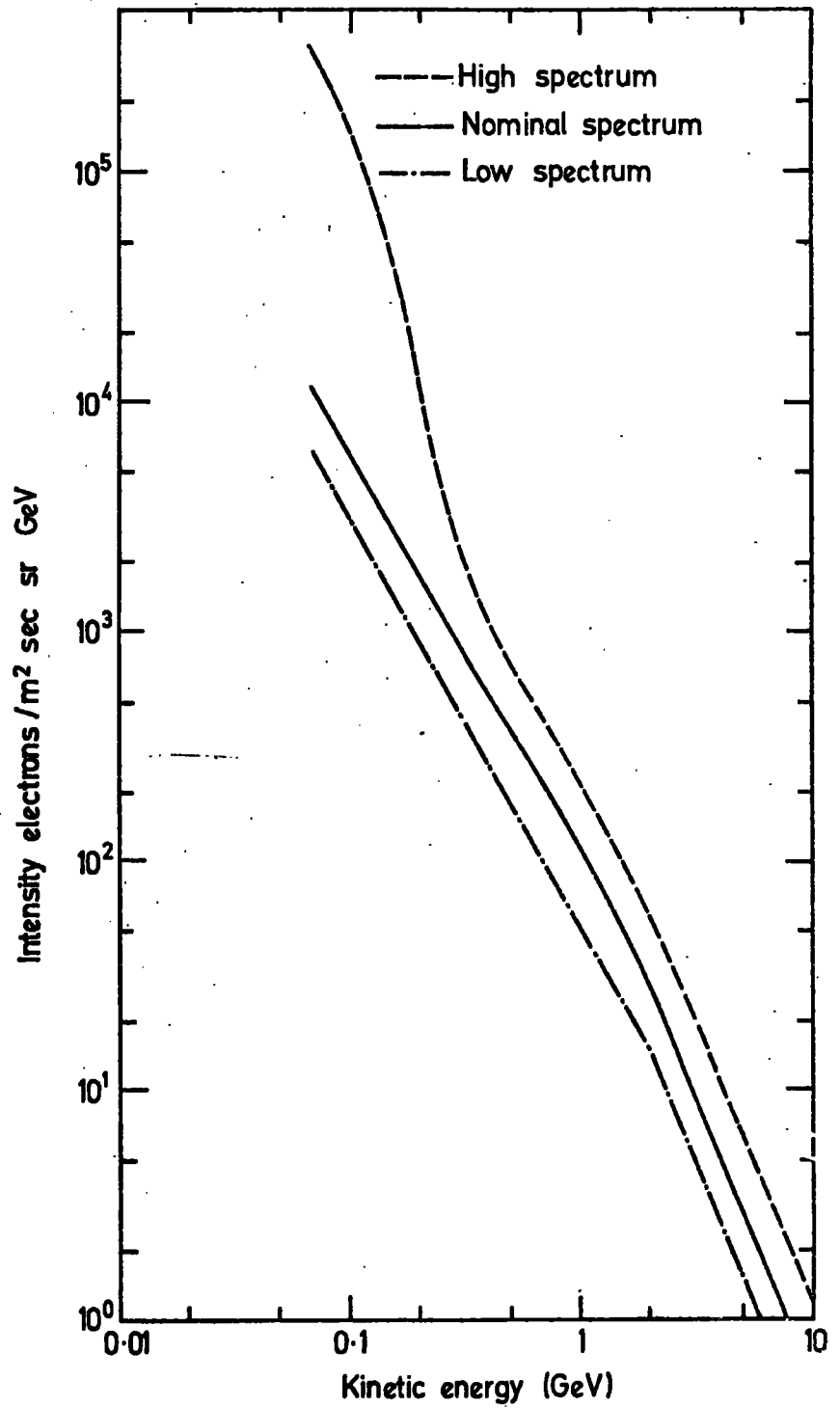
Figure 4. The differential electron spectra of Cummings et al (1973).
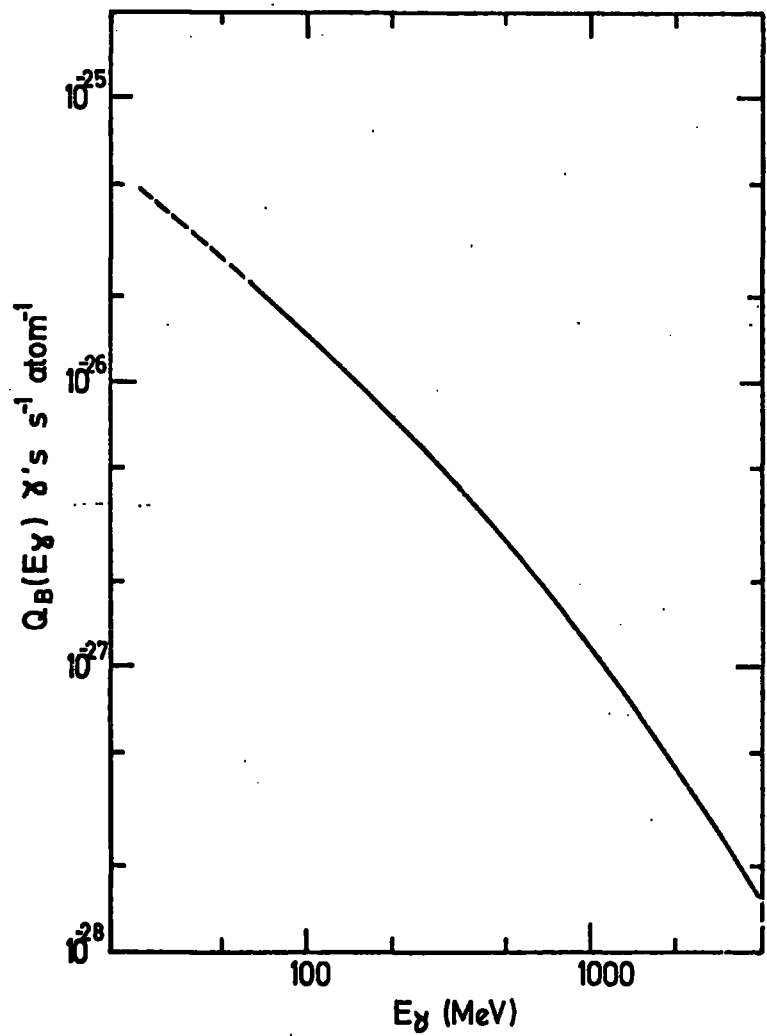
Figure 5. The integral energy spectrum of gamma rays from electron bremsstrahlung near the solar system. The dashed portion represents an estimate of the contribution at low energies.

and an interstellar medium with $\bar{M}$ = 1.4 (see

chapter 4). The emissivity at 100 MeV is 1.5 10^{-26}

γ's (H atom. s)$^{-1}$ and is 12% of the yield from π^c

production. The upper limit to the bremsstrahlung

rate was obtained using the Cummings et al. upper

limit to the electron spectrum and corresponds to 20%

of the π^o yield. The result is in very good agreement

with the calculations of Kniffen et al. (1975) who use

a similar electron spectrum. These authors also quote

an emissivity between 10 and 30 MeV of 1.17 10^{-25} γ's

atom^{-1} s^{-1}. Strictly there is no evidence for a

spectrum which continues with the same exponent down

to these low energies (Cummings et al. 1973). However,

if the integral spectrum of figure 3 is extrapolated

to 10 MeV a production rate for 10 - 30 MeV gamma rays

can be estimated and this is found to give q_B(10-30MeV)

= 7.9 10^{-26} γ's atom^{-1} s^{-1}.

7.3 The Distribution of Gamma Ray Emission in the Galaxy

The radial distribution of gamma-ray emissivity

in Galaxy has been derived by Strong and Worrall (1976)

from the intensity vs longitude results of Fichtel et al.

(1975). Their results are plotted in figure 6 as the

relative emissivity, W(R) as a function of Galactic

radius where the emissivity at 10 kpc is taken as the

datum.

Figure 6 clearly shows that the broad region of

high gamma ray intensity seen within 30° of the Galactic

centre originates in a ring of enhanced emissivity lying

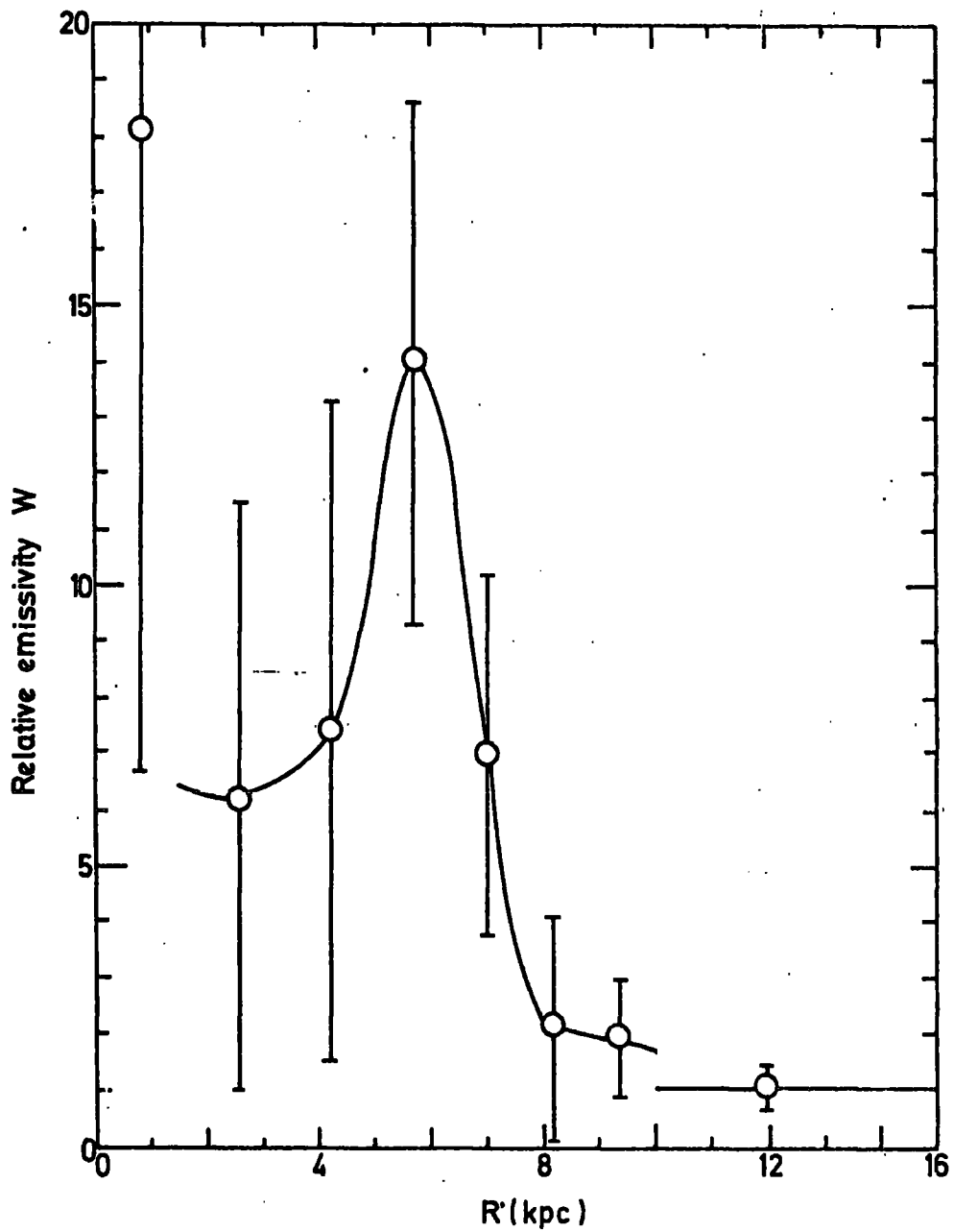within 5 and 6.5 kpc of the centre. The observations

Figure 6. The radial distribution of the relative emissivity
of gamma-rays as derived from the SAS II observations.

presented in this way are in a particularly convenient
form for comparison with the surface density of gas
in order to determine the radial distribution of cosmic
ray density.

7.4 The Distribution of Cosmic Rays

The results displayed in figure 6 are actually the
distribution of surface emissivity, $\Sigma_\gamma(R)$, as a function
of Galactic radius.   Thus if $Q_\gamma(R,z)$ is the volume
emissivity in gamma rays $cm^{-3} \ s^{-1}$ at distance R from
the Galactic centre and height z from the Galactic plane,
then $\Sigma_\gamma(R)$ is given by

$$\Sigma_\gamma(R) = \int_{-\infty}^{\infty} Q_\gamma(R,z)dz$$

Near the solar system the surface emissivity is 6.67
($\pm$ 2.3) x 10^{-5} gamma rays $cm^{-2} \ s^{-1}$.

The best evidence regarding the z distribution
of Q_γ suggests that it is dominated by the spread of
the gas in z.   Firstly the observed shape of the
galactic centre intensity vs latitude results of
Fichtel et al. (1975) is dominated by a very narrow
component only 1 - 2° in width.   This is the same
angular width as the gas layer at 5 - 6 kpc from the sun
and strongly suggests that the width of this feature
is determined by the thickness of the gas layer and
not by the cosmic ray layer.   Secondly, the observed
distribution in latitude of the non thermal radio
radiation is very wide implying that cosmic ray electrons
and the Galactic magnetic field extend to large distances
from the Galactic plane.   It seems almost certain that

the cosmic ray electrons which produce the radio emission ($E_e \simeq 1$ GeV) and the protons responsible for gamma ray emission ($E_p \simeq 3$ GeV) will have the same z distribution. If so, then the cosmic ray nucleons will have a constant density in the region occupied by the gas, and the z -dependence of the emission function $Q_\gamma(R, z)$ for Bremsstrahlung and pion production will be determined by the z - dependence of the gas.

Considering pion production alone, then, the surface emissivity $\sum_\gamma^\pi(R)$ becomes

$$\sum_\gamma^\pi(R) \quad = \quad \int_{-\infty}^{+\infty} q_\gamma^\pi(R) \, n_H \, (R, z) \, dz \qquad 4$$

If the simplifying assumption of a position independent proton spectrum is made then $q_\gamma^\pi(R)$ made be expressed as

$$q_\gamma^\pi(R) \quad = \quad \frac{w(R)}{w_\odot} \quad q_\odot^\pi$$

Where $w(R)/w_\odot$ is a function describing the density of cosmic rays at distance R from the Galactic centre relative to the solar value, and $q_\odot^\pi$ is the local gamma ray production rate per hydrogen atom which was calculated above.

In this case then the surface emissivity may be expressed as

$$\sum_\gamma^\pi(R) \quad = \quad q_\odot^\pi \, \frac{w(R)}{w_\odot} \, \sigma_H(R) \qquad\qquad 5$$

Where $\sigma_H(R)$ is the surface density of hydrogen. A similar expression may be written for the surface emissivity due to bremsstrahlung

$$\sum_\gamma^\mathcal{B}(R) = q_\odot^\mathcal{B} \cdot \frac{w_e(R)}{w_{e\odot}} \cdot \sigma_H(R) \qquad 6$$

Where now $\frac{w_e(R)}{w_{e\odot}}$ describes the variation of the cosmic ray electron density across the Galaxy, and as in the previous chapter the electron spectrum is assumed to have the same form throughout the Galaxy.

If now it is assumed that

$$\frac{w_e(R)}{w_{e\odot}} = \frac{w(R)}{w_\odot}$$

then $w(R)/w_\odot$ will be given by

$$\frac{w(R)}{w_\odot} = 3.47 \frac{W(R)}{\sigma_H(R)(q_\odot^{\pi^0} + q_\odot^B)}$$

where $\sigma_H(R)$ is in $M_\odot/pc^2$.

However, in writing down an expression for $w(R)/w_\odot$ in 8 two contributions have been neglected. Firstly the contribution from the inverse Compton effect has to be added. This gives a contribution

$$\sum_\gamma^{IC}(R) = q_\odot^{IC} t \frac{w_e(R)}{w_{e\odot}} \frac{\sigma_{st}(R)}{\sigma_{st\odot}} \qquad 9$$

Where t is the thickness of the electron disk which is taken as 1 kpc, and q^{IC} is the emissivity of IC gamma rays near the sun expressed as photons $cm^{-3} s^{-1}$.

A second contribution which must be included covers the variation of the ratio of primary electrons to seondary electrons across the Galaxy. In Chapter 2 it was pointed out that the same process which produces gamma rays through π^0 decay also produces secondary electrons and positrons through $\pi^\pm$ decay. As a result the secondary electron production $Q(\bar{r}, t, E)$ of equation 3.1 has the same spatial dependence as the gamma ray emissivity. It is clear that the seoondary part of the electron source function will have the same general structure as the gamma ray emission function in figure 4 i.e. a maximum between 5.0 and 6.5 kpc.

The distribution of secondary electrons is given by

$$\frac{w_e'(R)}{w_{e\odot}'} = \frac{\sigma_H(R)}{\sigma_{H\odot}} \frac{w(R)}{w_\odot} \qquad 10$$

here the double prime will be used to denote the
secondary electron part of the electron flux and the
single prime will denote the primary part.   In
obtaining 10 a constant value of T_e, the escape life-
time, was assumed over the whole galaxy.   Equations
6 and 8 may now be rewritten as

$$\sum_\gamma^B(R) = q_\ominus^B \left\{ \alpha \frac{w_e(R)}{w_{e\ominus}} \sigma_H(R) + \beta \frac{w_e(R)}{w_{e\ominus}} \sigma_H(R) \right\} \qquad 11$$

$$\sum_\gamma^{IC}(R) = q_\ominus^{IC} t \left\{ \mu \frac{w_e(R)}{w_{e\ominus}} + \nu \frac{w_e(R)}{w_{e\ominus}} \right\} \frac{\sigma_{st}(R)}{\sigma_{st\ominus}} \qquad 12$$

where

α= fraction of bremsstrahlung gamma rays produced by
primary electrons near the solar system

β= ditto .   . by secondary electrons

μ= fraction of inverse Compton gamma ray produced
by primary electrons near the solar system

ν= ditto ... by secondary electrons.

    In order to determine α, β, μ and ν the energy spectra
of the primary and secondary electrons are required.
These may be determined from the observations of flux of
positrons relative to the total flux of electrons and
from the physics of the $\pi^\pm$ production process.   Figure
7 shows the experimental results (Meyer 1975) on the frac-
tion $N_{e^+}/(N_{e^+} + N_{e^-})$ as a function of energy.   It can
be seen from figure 7 that the secondary electrons
have an energy spectrum between 100 MeV and 1 GeV which
is steeper than that of the primaries.   As a result α
has a value <0.3 the fraction of the electron flux at
100 MeV which is of secondary origin.   The values of α
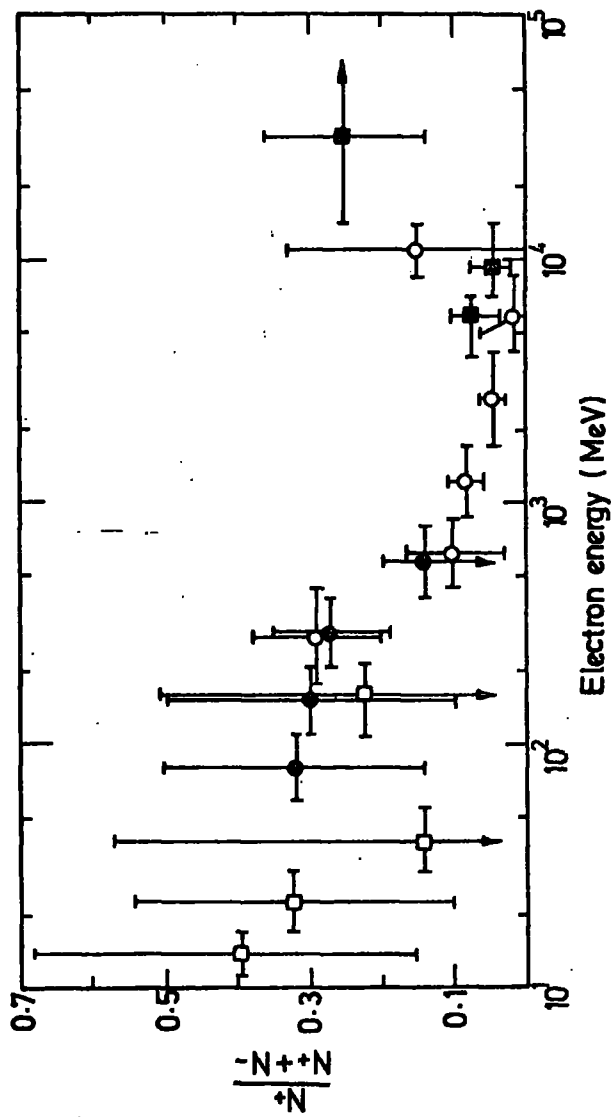
Figure 7.   The variation with electron energy of the fraction
of positrons in the electron flux.

and β were found to be 0.84 and 0.16 respectively.

The problem of the IC contribution is much simpler since the secondary spectrum has approximately the same slope as the primary spectrum above 1 GeV. The values of μ and ν are therefore 0.9 and 0.1.

Combining together the various terms for the surface emissivity given in equations 5, 10, 11 and 12, the values of α, β, μ & ν calculated above and the assumption $w_e'(R)/w_{e\odot}' = w(R)/w_\odot$ together gives $w(R)/w_\odot$. This is shown in figure 8. The error bars represent the errors in the unfolding alone and do not include the uncertainty in the gas density.

The cosmic ray distribution of figure 8 is very similar to both the pulsar and supernova remnant distributions and in the region $5 < R < 10$ kpc is consistent with the cosmic ray density being proportional to the stellar mass density.

The ratio of the energy densities in primaries and secondaries $w_e'(R)/w_e''(R)$ is determined by the density of hydrogen. Thus

$$\frac{w_e'(R)}{w_e''(R)} = \frac{w_{e\odot}'}{w_{e\odot}''} \frac{\sigma_H(R)}{\sigma_{H\odot}}$$

Since at 5 - 6 kpc $\sigma_H(R)/\sigma_{H\odot}$ is $\simeq 2$, the primary electrons dominate at 1 GeV and the spectrum of radio emission will be the same as the local spectrum, in agreement with the results of Stephens (1969).

7.5 The Sensitivity of the Conclusions to the cloud penetration probability
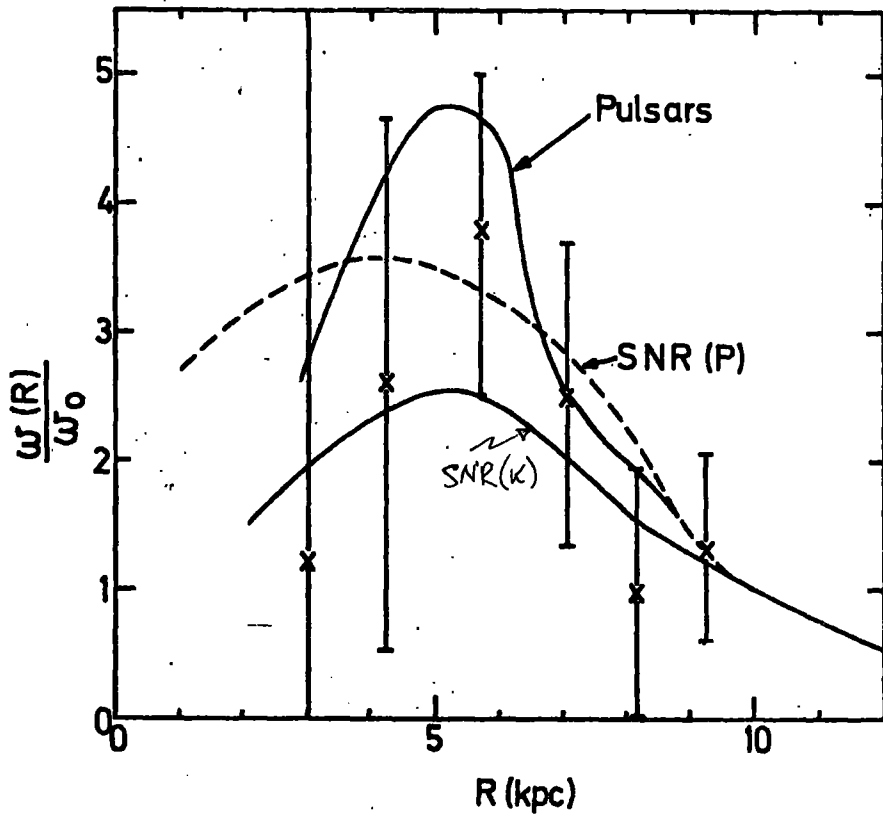
In the above calculations it was assumed, though

Figure 8.   The radial distribution of cosmic ray intensity, w(R)/w₀ as deduced from the gamma-ray observations. Also included for comparison are the radial distributions of pulsars and supernova remnants.

not explicitly stated, that the atoms of the hydrogen were distributed uniformly over the interstellar medium. However, this is not the case, since the molecular hydrogen is concentrated in clouds with typical diameters of 5 - 10 pc and densities of $\sim$ 3000 atoms cm^{-3}. The question which naturally arises is whether or not the cosmic rays are free to penetrate deep into the clouds. This problem will be discussed in this section.

The typical column density of a molecular hydrogen cloud is $\sim 10^{22}$ atoms cm^{-2}. This makes the cloud optically thin to cosmic rays and implies that unless some other mechanism screens the cloud centre then the density of cosmic rays at the cloud centre, n^c, and the density in the space outside the cloud, n^o are approximately equal. However, the small anisotropy in the cosmic ray flux at the cloud surface can produce Alfven waves which may, in the manner described in Chapter 3, scatter the cosmic rays, producing a cosmic ray mirror at the edge of the cloud. It is possible that this may screen the centre from the cosmic rays outside the cloud.

Consider the cylindrical cloud of figure 9. At the surface A the fluxes of coasmic rays in and out of the cloud are $\frac{n^o c}{4}$ and $\frac{n^o(1-\tau)}{4}$ c respectively. where c is the cosmic ray velocity, n^o the cosmic ray density outside the cloud and τ is the average optical depth for cosmic rays. Since the average velocity of the cosmic rays in the direction BA is $^c/2,$ τ is given by

$$\tau = 2R \, \sigma_{Inelastic} \, n_H$$

At the cloud surface A, cosmic rays stream into
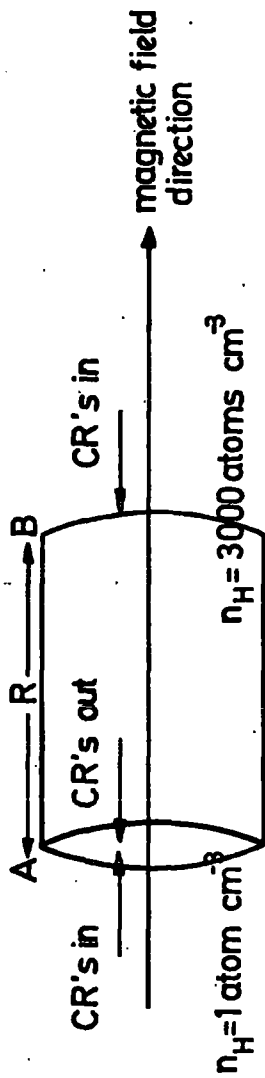
Figure 9.   The idealized interstellar molecular cloud considered in Section 7.5.

the cloud with velocity v_{st} where,

$$v_{st} = \frac{\tau n^o c}{4 n^o} = \frac{\tau c}{4}$$

At A, Alfven waves will be created and the energy density in the waves will grow if the growth rate due to the cosmic ray streaming exceeds the damping rate due to ion-neutral collisions. Following Dickinson (1975) the growth rate Γ_G and damping rate Γ_D are given by

$$\Gamma_G = \frac{1.69\ 10^{-10}}{(E/GeV)^{1.5}} \left(\frac{v_{st}}{v_A} - 1 \right)$$

$$\Gamma_D = 1.12\ 10^{-9} \left(\frac{n_H}{1cm^{-3}} \right) / \left(\frac{T}{1000\ K} \right)^{-1/2}$$

where v_A = Alfven velocity

Inside the cloud the situation is such that n_H = 3000, T = 10K and waves are rapidly damped. On the other hand outside the cloud n_H = 1, T = 100K and the condition for $\Gamma_G > \Gamma_D$ becomes $v_{st} > v_A$. In other words this requires the optical depth of the cloud to be a few times v_A/c. In the general ISM the value of v_A is 30 km s^{-1}, thus $v_A/c = 10^{-4}$, whereas the parameters of the cloud in figure 7 give $\tau = 2\ 10^{-3}$. Thus the conditions at A (and B) are such that the Alfven waves grow, and the streaming velocity becomes v_A.

As a result of this process the density of cosmic ray nuclei inside the cloud drops to a value n^c, where n^c is governed by the equilibrium between the rate at which cosmic rays are carried in through the surface and the rate at which they disappear inside the cloud due to inelastic collisions with the gas atoms. Thus

Rate of cosmic ray replacement = $n^o\ v_A$ ×Area

= Death rate = $n^c\ n_H\ \sigma_{In}\ c$ × Volume

$$\frac{n^c}{n^o} = \frac{v_A}{n_H \cdot \sigma cR} \cdot \frac{2v_A}{\tau c}$$

for the parameters given above

$$\frac{n^c}{n^o} \approx \frac{1}{10}$$

Such a reduction means a large reduction in the gamma ray yield from π^o decay.

A more detailed analysis (Skilling and Strong 1976) has shown that this process is very efficient below 1 GeV but that at higher energies the reduction is small. At 10 MeV the reduction is a factor of 80. These authors obtain significant gamma ray depletions when the column density of the cloud and/or the cosmic ray density are a factor of 10 larger. Thus this process works for protons for only the most massive clouds.

In their analysis, Skilling and Strong did not include the electron contribution to the gamma ray flux. At first sight the problem is a simple one. The electrons will be resonantly scattered by waves set up by the non-relativistic protons. For example a 100 MeV electron and a 4 MeV proton have the same Larmor radius. As a result the depletion of cosmic ray electrons inside the cloud is expected to be large. However, the analysis assumed no sources of cosmic rays within the cloud. In practice the cosmic ray nuclei with kinetic energies > 1 GeV/nucleon are not excluded very efficiently and secondary electrons are produced inside the cloud. These are prevented from escape by the waves set up by the low energy protons and consequently the secondaries build up inside. The equilibrium level is governed by a balance between

losses due to bremsstrahlung or ionization and creation
in nucleon-nucleon collisions.

Thus equibrium implies:

creation rate = destruction rate

$$\frac{n_1}{n_2} Q = n^c \frac{}{T_d}$$

Where Q is the secondary electron production rate
outside the cloud; n_1 and n_2 are the gas densities
in the cloud and outside the cloud respectively; n^c is
now the density of secondaries inside the cloud and T_d is
the lifetime of secondaries on the inside due mainly to
ionization and bremsstrahlung losses.

The equilibrium level outside the cloud is

$$n^o = Q T_e$$

where T_e is the escape lifetime.

Therefore

$$\frac{n^c}{n^o} = \frac{n_1}{n_2} \frac{T_d}{T_e}$$

If the typical paramters quoted above are substit-
uted the ratio is found to have the value $n^c/n^o \simeq 4$.

Clearly this is an important problem since it
implies that a large part of the gamma ray emission may
be due to bremsstrahlung by the secondary electrons. A
more detailed calculation Strong (Private Communication)
gives a depletion in the density of cosmic ray electrons
inside the cloud relative to the total density (primaries
and secondaries) outside. In the calculation by Kniffen
et al. (1975) the electrons were assumed to have free
access to the hydrogen. A more complete calculation
of the gamma ray yield requires more information on the
distribution of cloud masses.

7.6 Conclusions

The available evidence is in favour of a cosmic
ray density gradient between 5 and 10 kpc with approx-
imately the same distribution as that of the main cosmic
ray source candidates. From this it may be concluded
that the lifetime of cosmic rays in the galaxy is not
a strong function of R and that the cosmic rays do not
diffuse far from their sources. It is necessary, how-
ever, to examine again the possibility that the C R density
is uniform (in Extragalactic origin or Galactic plus long
diffusion paths) and to see under what conditions this
situation would pertain.

In order to reproduce the gamma ray observations
using a uniform cosmic ray density distribution it is
required that the hydrogen surface density at 6 kpc is
$51^{+}_{-17} M_{o}/pc^{2}$. Gordon and Burton (1976) give a density
at 6 kpc of 13 M_{o}/pc^{2} and Scoville and Solomon (1975)
give a density of 21 M_{o}/pc^{2}. There is a large uncert-
ainty attached to the quoted figures of the hydrogen
density. This arises because of the difficulties in
converting from the CO emission data to the column
density of molecular hydrogen and also because the layer
thickness is not known; both the Gordon and Burton and
the Scoville and Solomon results are based on only a
very limited number of observations of the layer thickness.
As a consequence of these problems the uncertainty in the
quoted figures for σ_{H2} may be as large as a factor of 2.

This fact suggests that the possibility of a uniform
cosmic ray density cannot be ruled out completely.

However, it will be seen in the next chapter that the
observations of the Galactic anticentre do not imply such
a uniform distribution.

REFERENCES

Comstock, G.M., Hseih, K.C. and Simpson, J.A., 1972.
Astrophys. J., 173, 691.

Cummings, A.C., Stone, E.C. and Vogt, R.E., 1973. Proc.
13th Int. Conf. on Cosmic Rays, Denver, 1, 335.

Dickinson, G.J., 1975. Ph. D. Thesis, University of Durham.

Fichtel, C.E., Hartman, R.C., Kniffen, D.A., Thompson, D.J.,
Bignami, G.F., Ogelman, H., Ozel, M.F., and Turner, T., 1975.
Astrophys. J., 198, 163.

Gordon, M.A. and Burton, W.B., 1976. Astrophys. J. to be
published.

Jenkins, E.B., 1976. GSFC Sympoisium on Gamma-Ray Astronomy,
to be published.

Kniffen, D.A., Bignami, G.F. Fichtel, C.E. and Thompson, D.J.,
1975. Proc. 14th Int. Conf. on Cosmic Rays, 1, 40.

Meyer, P., 1975. In 'Origin of Cosmic Rays', Eds. J.L.Osborne
and A.W. Wolfendale, D.Reidel, Dordrecht.

Pollack, J.B. and Fazio, G.G., 1963. Phys. Rev., 131, 2684.

Scoville, N.Z. and Solomon, P.M., 1975. Astrophys. J., 199,L105.

Skilling, J. and Strong, A.W., 1976. Ast. Astrophys. to be
published.

Stephens, S A., 1969. Ph.D. Thesis, University of Bombay.

Strong, A.W. and Worrall, D.M., 1976. J.Phys. A., 9, 823.

Waddington, C.J., 1974. The Nuclear Particles of the Cosmic
Radiation, University of Minnesota.

CHAPTER EIGHT

GAMMA RAY EMISSION FROM THE GALACTIC ANTICENTRE.

8.1 Introduction

In the last chapter it was shown that the evidence
from gamma ray emission and gas distributions indicated
that there was a gradient in the cosmic ray density
between 5 and 10 kpc from the Galactic centre. However,
no strong conclusion was possible because of many
problems associated with molecular hydrogen. In this
chapter attention is switched to a broad region centred
on the Galactic anticentre extending from 90° to 270°
in longitude.

In the anticentre direction the line of sight crosses
regions more distant from the Galactic centre than the
sun itself. Since the results of the CO emission
surveys of Gordon and Burton (1976) and Scoville and
Solomon (1975) showed that the dense molecular clouds
were concentrated to the region within 8 kpc of the
Galactic centre, their contribution to the hydrogen
column densities will generally be small. Hence the
atomic hydrogen column density may be used to give a
lower limit to the flux of gamma-rays to be expected as
a result of interactions between the cosmic rays and gas
and will allow comparison between predictions of
Galactic and Extragalactic models for cosmic ray origin.

In a sense the method proposed here is somewhat
similar to that put forward by Ginzburg (1972) for
the Magellanic Clouds. Ginzburg suggested using these
objects to test for the existence of extragalactic
cosmic rays by searching for the gamma rays which would

be produced by cosmic rays interacting with the hydrogen in the Clouds.

If no gamma rays are observed, then this would be definite proof of the Galactic origin of cosmic rays. Unfortunately, this proposal suffers from the disadvantage that the observation of gamma rays does not in fact rule out a Galactic origin. The present method is in principle much more sensitive than Ginzburg's because the difference in intensities between the Galactic and Extragalactic models should be greater than for the small signal to be expected from Magellanic Clouds. In addition this method should afford more possibilities for analysis through the l and b distribution of the gamma ray intensities. The method is also unambiguous, unlike Ginzburg's.

In the sections which follow two models for the distribution of cosmic rays are used to predict the latitude and longitude distribution of gamma rays around the anticentre direction. The available measurements are then used to attempt to identify the better model.

8.2 The Cosmic Ray Distribution
8.2.1 Galactic Sources

The radial dependence of the density of the cosmic ray source candidates was discussed in Chapter 3, and it was shown how the radial dependence of the cosmic ray density might be related to the source distribution. Here it is assumed that the escape lifetime for cosmic

rays is R independent and hence that on a Galactic

model for cosmic ray origin that the density of cosmic

rays is proportional to the density of sources.

In the outer regions of the Galaxy (i.e. R>10 kpc)

the distribution of sources is close to the distribution

of the surface mass density. This is represented in

the calculations by an exponenial function $W(R) = \exp$

$((10-R)/2.44)$ which approximately represents the

surface mass distribution given by Innanen (1973)

for the ou.er regions of the Galaxy.

In this calculation it is assumed that the z

distribution of the cosmic ray is rather wide so that

the cosmic ray intensity can be considered to be

constant over the region occupied by the hydrogen (a

few hundred pc). Thus, the surface density of the

sources is taken to give the relative cosmic ray

intensity. Justification for this assumption may be

derived from the distribution of synchrotron radiation

with Galactic latitude. Figure 1 shows the average b

distribution at 150 MHz towards the anticentre taken

from the compilation by Landecker & Wielebinski (1970).

Its width indicates a wide z distribution for both the

magnetic field and the cosmic electrons. It is reason-

able to assume that the z distributions of the GeV electrons

which produce the radio and the GeV protons which produce

the gamma rays are similar.

8.2.2 Extragalatic Sources

The model adopted here is of the Galaxy bathed
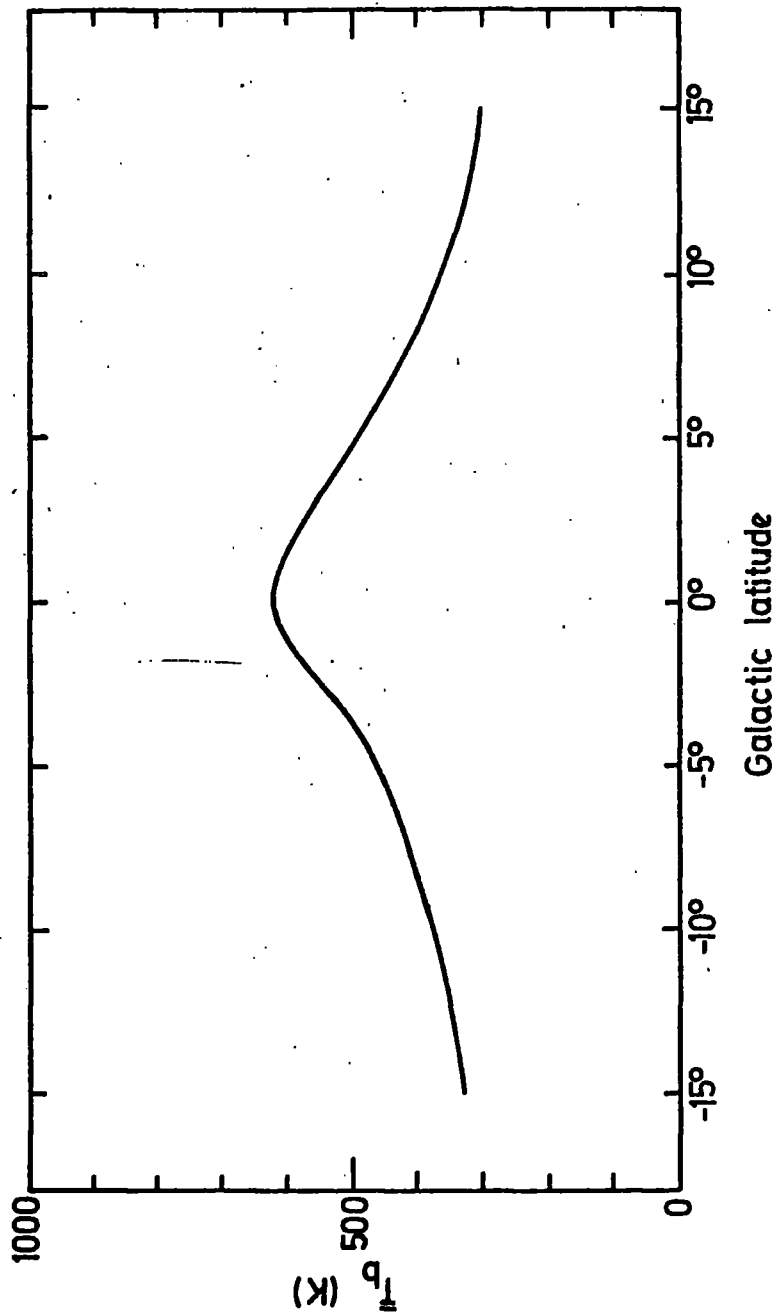
in a uniform flux of cosmic rays. Some propagation

Figure 1.   The latitude distribution of radio brightness
temperature (T_b) at 150 MHz, using the data of
Landecker and Wielebinski (1970).   The distribution
is averaged over the same longitude intervals as the
gamma ray observations in figure 5.

models e.g. Dickinson 1975 predict a uniform cosmic
ray density distribution even for Galactic origin
(see Chapter 5). Thus, even if agreement between
the predictions of the 'extragalactic' model and the
gamma-ray observations is found, a Galactic origin
will still not be ruled out.

8.3 The Distribution of Atomic Hydrogen

A convenient survey of the atomic hydrogen
distribution in this region is given by Lindblad (1966),
in the form of contour maps of the 21-cm optical depth
in velocity-latitude planes at 5° intervals of longitude.
The optical depth maps were constructed from the bright-
ness temperature maps (after correction for the various
instrumental effects such as antenna efficiency) by
assuming a spin temperature, T_{spin} of 125 K.

The optical depth-velocity profiles at various
latitudes were read from the contour maps given by
Lindblad. Figure 2 shows a typical optical depth-
velocity profile for l = 117.3 and b = 0.0. The
column density of atomic hydrogen is obtained from the
optical depth-velocity profile, thus

$$N_H = 1.823 \times 10^{18} T_{spin} \int \tau(v)dv \qquad 1$$

where v is in km s^{-1}.

Using the Galactic rotation velocity-radius relation,
and simple geometry the density of hydrogen as a function
of position may be derived from the optical depth.

$$n_H = 1.823 \, 10^{18} T_{spin} \tau(v)\frac{dv}{dr} \qquad 2$$
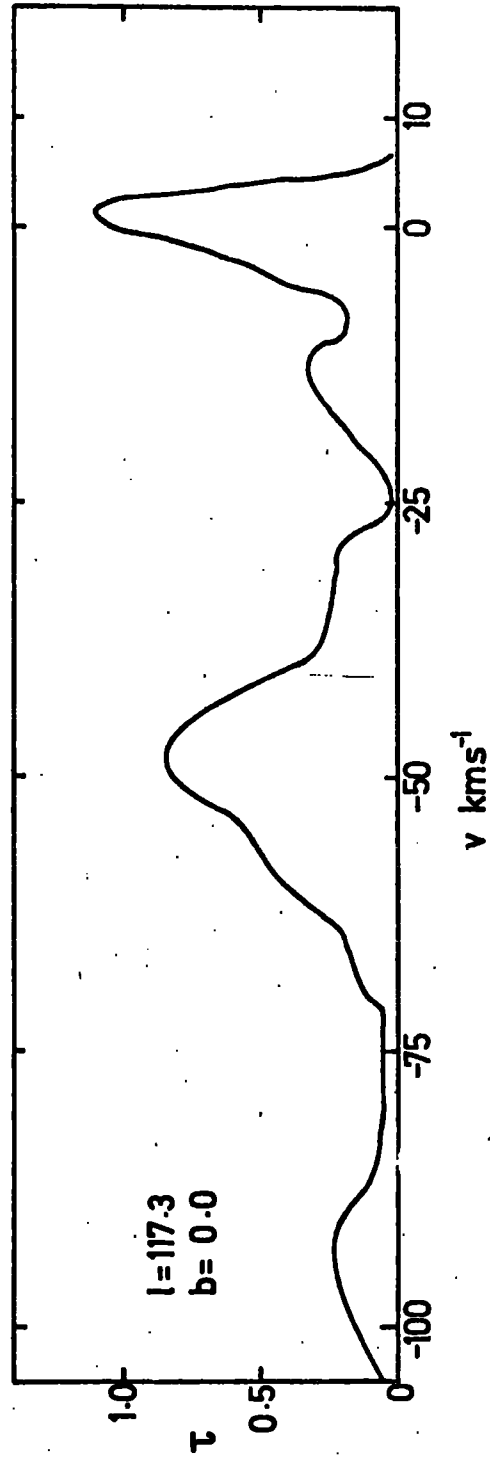
$$\text{atoms cm}^{-3}$$

Figure 2.   A typical optical depth (τ), velocity profile from Lindblad (1966).

The rotation curve used was that of Contopoulos and Stromgren (1965) and for computation this was represented by the interpolation formula given by Minalas and Routly (1968):

$$(R) = 67.76 + 50.06R - 4.0448R^2 + 0.0861 R^3$$
$$kms^{-1} \qquad R \text{ in kpc}$$

Comparison of the column densities obtained by integration under the profiles of $\tau(v)$ with those given in the compilation of column densities by Daltabuit and Meyer (1972) shows that the Lindblad data gives lower values at b = O.O. There are a number of observational difficulties which could have lead to this disagreement. In particular, when comparing two surveys made by different instruments it is not always certain that a common zero level and temperature scale have been used. This last problem has recently been tackled by Harten et al. (1975) who have compared the temperature scales of the main 21 cm survey instruments and give conversion factors for some surveys. For the early Leiden Survey used here the agreement of the temperature scale with that of the most modern instruments is to within 1%.

In this case the Lindblad data presumably represents a lower limit to the amount of hydrogen and this will be shown later to be adequate for the conclusions reached.

The z distribution of the hydrogen has been determined from 21 cm brightness temperature - velocity profiles by Jackson and Kellman (1974). These authors find that the thickness $z_{\frac{1}{2}}$ (defined as the distance

between half density points) generally increases

with increasing R in the longitude interval $200 \leqslant l \leqslant 300$

but that for $110 \leqslant l \leqslant 160$ the thickness remains fairly

constant. These results are shown in figure 3. This

departure from axial symmetry is the reason for employing

an empirical hydrogen distribution rather than the

averaged hydrogen density given by Gordon and Burton

(1976).

8.4 The Distribution of Gamma-ray Intensity around

the Galactic Anticentre

Using the atomic hydrogen distribution derived

from the 21 cm data as described in section 3, the

values of the gamma-ray intensity $j(l,b)$ can be

calculated for those regions where experimental data

exist. The SAS II data relates to the regions $90 \leqslant$

$l \leqslant 150$, $160 \leqslant l \leqslant 170$ and $200 \leqslant l \leqslant 260$, and the events

above 100 MeV have been summed to give the overall

b distribution (Fichtel et al. 1975).

The gamma ray intensity is given by

$$j(l,b) = \frac{1}{4\pi} \int_0^\infty Q_\gamma(r,l,b) \, dr \qquad\qquad 4$$

gammas cm^{-2} s^{-1} $ster^{-1}$

Where $Q_\gamma(r, l, b)$ is the emissivity of gamma rays with

E > 100 MeV in the direction (l, b) as a function of

r. This is given by

$$Q(r,l,b) = q_\gamma^{\pi+B} \, w(R) n_H(r,l,b) \qquad\qquad 5$$

Where $q_\gamma^{\pi+B}$ is the local gamma ray emissivity for both

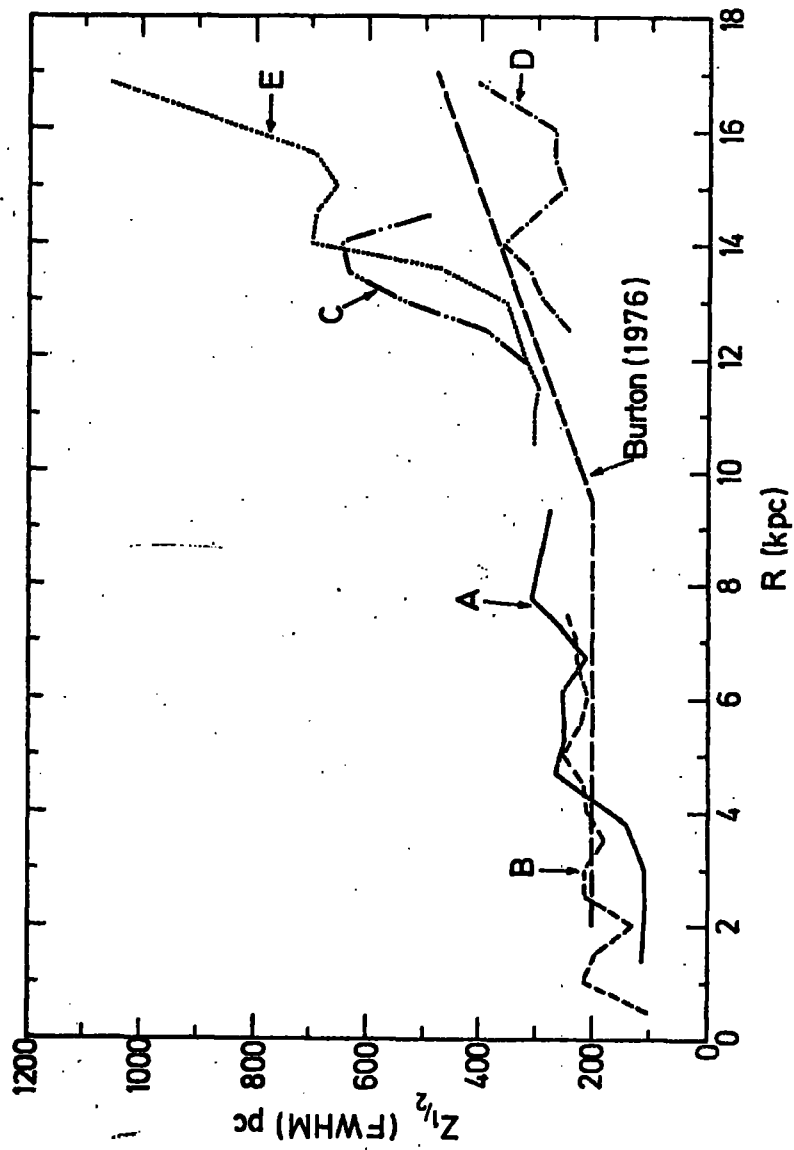bremsstrahlung and pion production combined, which was

Figure 3. The variation of $Z_{\frac{1}{2}}$ with Galactocentric radius R. Curves A-E are from Jackson and Kellman (1974) and refer to the longitude intervals; A, $0 < l < 90$; B, $270 < l < 360$; C, $160 < l < 205$; D, $110 < l < 160$; E, $200 < l < 300$. For comparison the results of Burton (1976) are also shown.

calculated in the last chapter, n_H (r, l, b) is the

hydrogen density distribution and W(R) represents

the relative intensity of the CR flux at distance

R from the Galactic centre with respect to the intensity

near to the Earth.

$$W(R) = \frac{I_{cr}(R)}{I_{cr}(10)} \qquad 6$$

In the calculations two forms of W(R) are used,

representing Galactic and Extragalactic origin respect-

ively.

For Galactic origin

$$W(R) = \exp \frac{10 - R}{2.44} \qquad 7$$

and for Extragalactic origin

$$W(R) = 1.0 \qquad 8$$

Figure 4 shows the predicted mean latitude distrib-

utions for $90 < l < 180$ and $180 < l < 270$. It is inter-

esting to note the asymmetry with respect to b = 0, in

opposite senses for the two directions. This effect

should be detectable when eventually the gamma ray

observations are presented in this form. Figure 5

shows the latitude distribution for the Extragalactic

and Galactic models, the predicted intensities in 5

being averaged over the same longitude intervals as

the data. In 5 the detector response function was

assumed to be a gaussian of width 3°. Figure 6

compares the longitude distribution of the gamma ray

line flux predicted by the models with the observations.

In figures 4, 5 and 6 the effect of the Galactic

model is to reduce the fluxes below the predictions of

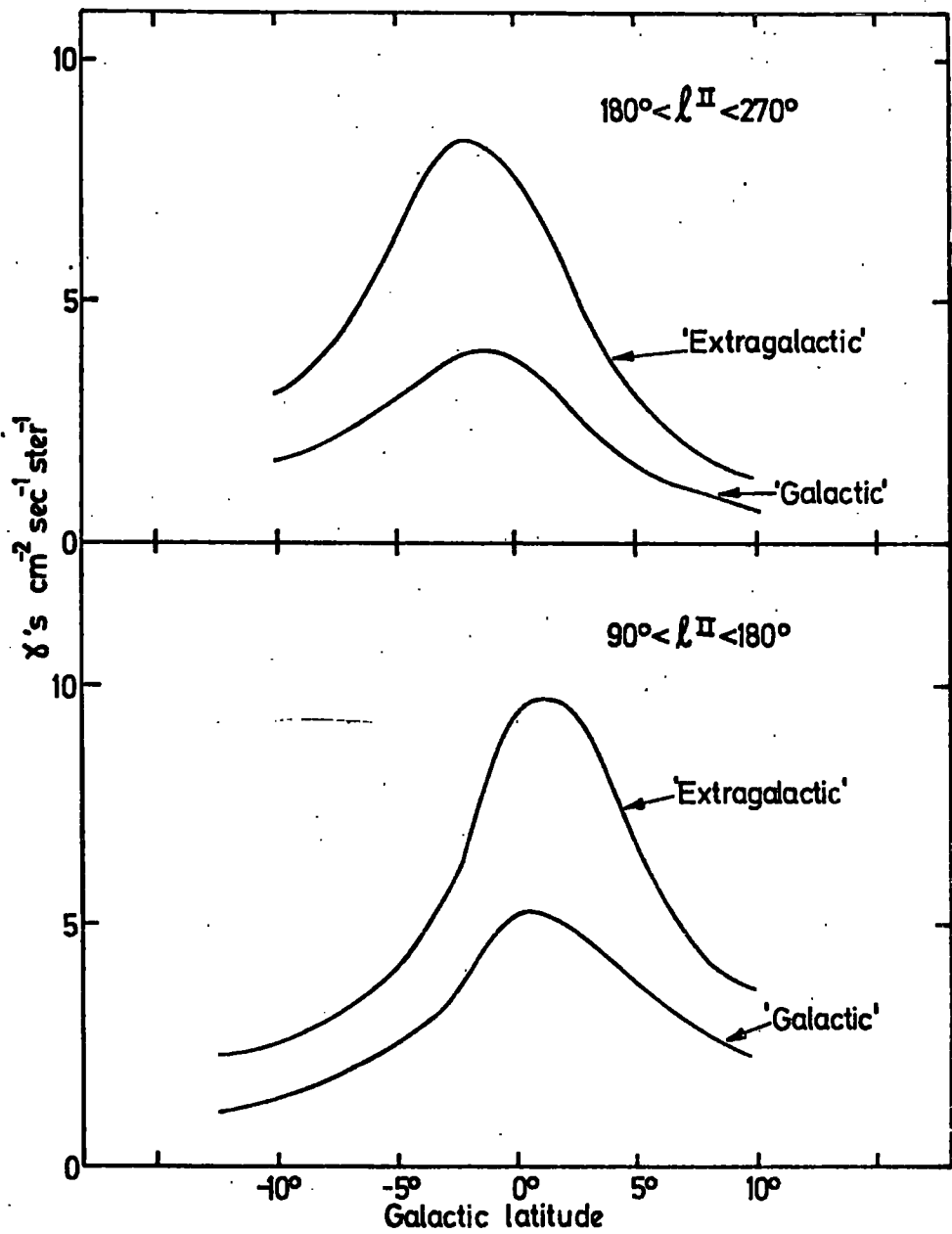the Extragalactic model by a factor which in figures

Figure 4. The latitude distributions of the predicted gamma ray
intensities averaged over a) l = 90°- 180° and
b) l = 180°-270°, for Galactic and Extragalactic models.
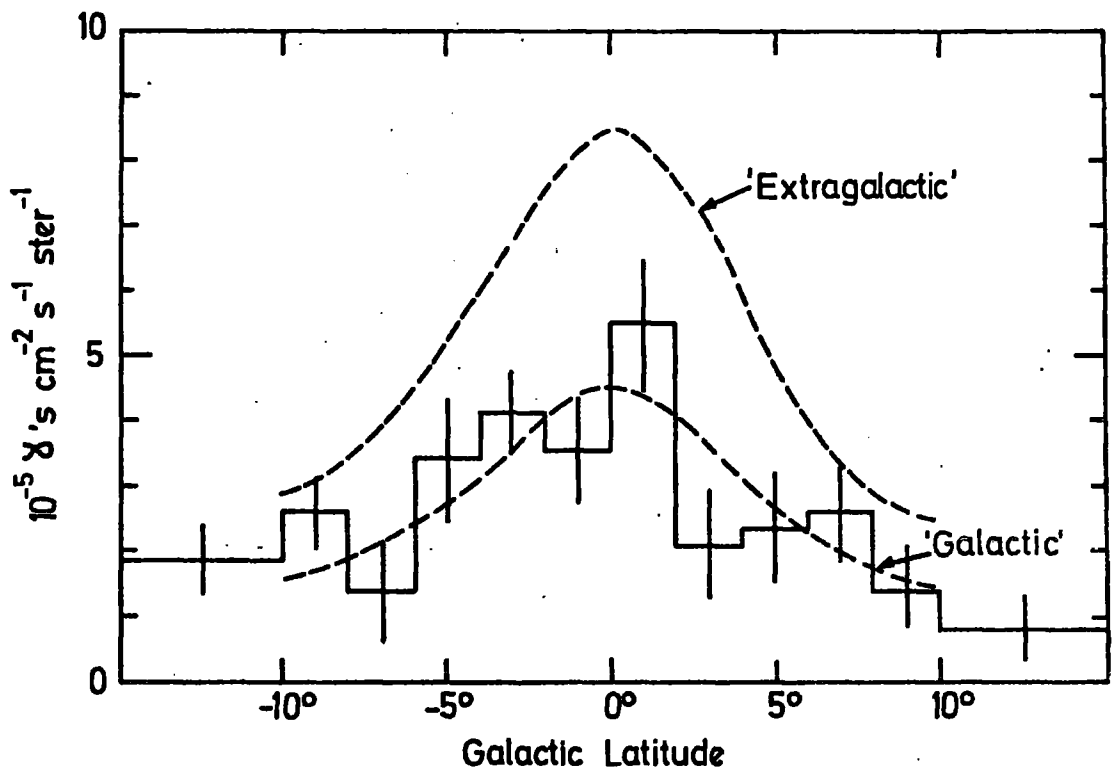
Figure 5.   Comparison of latitude distribution of gamma-ray
intensity on 'Galactic' and 'Extragalactic' models with
the SAS II data.   The predictions are averaged over
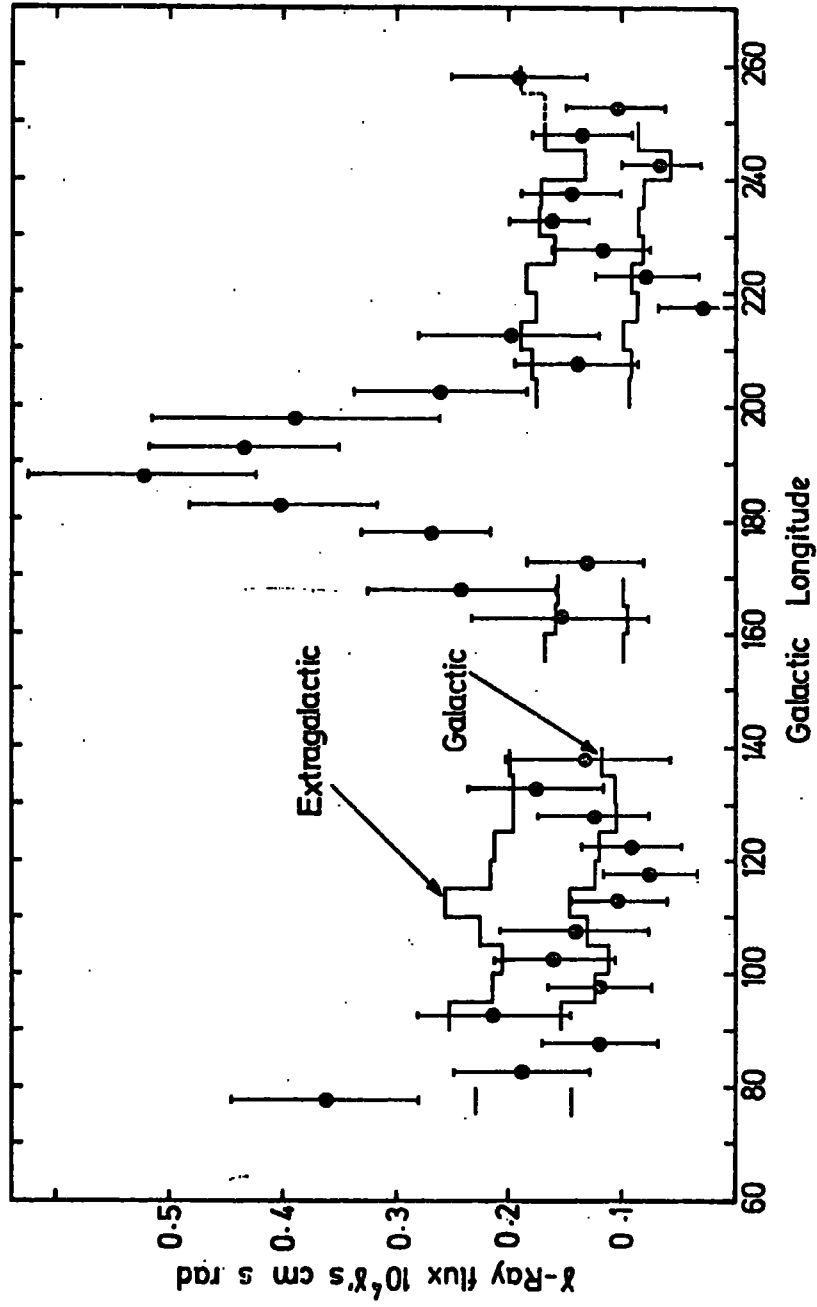the same longitude regions as the data.

Figure 6. Comparison of predicted longitude distributions of gamma-ray line fluxes for $-10° < b < 10°$ around the anticentre direction, on the Galactic and Extra-galactic models, with the SAS II data.

4 and 5 is virtually latitude independent; it does
not flatten the latitude distribution, as would be
anticipated for a Galaxy which is a flat slab.   The
rapid increase in the width of the Galactic gas shown
in figure 3 is responsible for this effect, which means
that even at b = 10 gamma rays are reaching us from
distances of a few kpc.

8.5 Discussion on the CR and gas distribution in the Anticentre

The most striking feature arising from the comparison
of the observations with the two models is that the Extra-
Galactic hypothesis predicts a flux about a factor of
two in excess of what is observed, while the Galactic
model does seem to give a good representation of the
observed distribution in latitude and also agreement
in the absolute flux levels.

It is important to examine the sources of errors
in these calculations.   For the hydrogen distribution
there are two main areas of uncertainty (excluding the
instrumental problems).

Firstly, the spin temperature of the gas has been
taken to be 125 K.   The evidence of 21 cm absorption
studies by Hughes et al. (1971) and Radhakrishnan et
al (1972) is for a temperature which is < 125 K.   Hughes
et al. quote a mean value of 71 K and for 90% of the
clouds observed find temperatures < 130 K.   The effect
of choosing 125 K as the temperature is to consistently
underestimate the optical depth of optically thick

features and hence to underestimate their column
densities.

Secondly, no allowance has been made for the
presence of molecular hydrogen in the interstellar
medium.   The evidence from the UV absorption measure-
ments (Spitzer 1973) is for considerable quantities of
molecular hydrogen in the denser clouds.   Jenkins (1976)
suggests a local density of hydrogen of 1.1 atoms cm^{-3}
of which 0.2 atoms cm^{-3} is molecular.

Both these factors act to increase the column
density.   Thus the above calculations have tended to
underestimate the hydrogen density implying greater
disagreement between the observations and the predictions
of the Extragalactic model.

The remaining uncertainty is in the Cosmic ray flux
near the Earth.   It is unlikely that the error in the
experimentally measured flux at 3 GeV can be as large
as a factor of two, since the effects of solar modulation
at these energies are small.   Another explanation is that
the local cosmic ray flux is not representative of the
average flux at this distance from the Galactic centre;
the average flux being at least a factor of two lower to
reach agreement with the gamma-ray observations.   This
is also unlikely since the very high isotropy at 10^{11}
eV makes the probability of being in a small local
excess very small (Dickinson and Osborne 1974).   Such
a local excess would in any case imply a Galactic origin
for cosmic rays.

All these factors weigh heavily against the Extra-

galactic model especially since the Galactic model adopted here agrees with the observations to within the experimental errors. This is consistent with cosmic ray origin in supernovae, supernova remnants, pulsars or any other source whose density falls off like the distribution of mass in the outer Galaxy; alternatively, this may be considered as indicating the existence of a cosmic ray disk which is of smaller radial extent than the hydrogen disk.

REFERENCES

Contopoulas, G.& Stromgren, B., 1965.   In Tables of plane galactic orbits', NASA Institute for Space Studies.

Daltabuit, E. & Meyer, S., 1972. Astr.Astrophys., 20, 415.

Dickinson, G.J. & Osborne, J.L., 1974. J.Phys. A., 7, 728.

Dickinson, G.J., 1975. Ph.D. Thesis University of Durham.

Fichtel, C.E., Hartman, R.C., Kniffen, D.A., Thompson, D.J., Bignami, G.F., Ogelman, H., Ozel, M.F. & Tumer, T. 1975. Astrophys. J. 198, 163.

Ginzburg, V.L., 1972. Nature Phys. Sci., 239, 8.

Gordon, M.A. & Burton, W.B., 1976. Astrophys. J. to be published.

Harten, R.H., Westerhout, G. & Kerr, F.J., 1975. Astr. J. 80, 307.

Hughes, M.P., Thompson, A.R. & Colvin, R.S., 1971. Astrophys. J. Suppl. No. 200, 23, 323.

Innanen, K.A., 1973. Astrophys. and Sp. Sci., 22, 393.

Jackson, P.D. & Kellman, S.A., 1974. Astrophys. J., 190, 53.

Jenkins, E.B., 1976. Goddard Space Flight Centre Syposium on Gamma Ray Stronomy, to be published.

Landecker, T.L. & Wielebinski, R., 1970, Aust. J. Phys. Astrophys. Suppl., 16, 1.

Lindblad, P.O., 1966. Bull. Astr. Inst. Netherl., Suppl., 1, 77.

Mihalas, D. & Routly, P.M., 1968. Galactic Astronomy, Freeman & Co., San Francisco.

Radhakrishnan, V., Murray, J.D., Lockhart, P. & Whittle, R.P.J., 1972. Astrophys. J. Suppl. No. 203, $\underline{24}$, 15.

Scoville, N.Z., & Solomon, P.M., 1975., Astrophys. J., $\underline{199}$, L105.

Spitzer, L., Drake, J.F., Jenkins, E.B., Morton, D.C., Rogerson, J.B. & York, D.G., 1973. Astrophys. J., $\underline{181}$, L116.

CHAPTER NINE

ON THE EVIDENCE FOR A GALACTIC ORIGIN FOR THE COSMIC RAY

NUCLEI BETWEEN 1 - 10 GeV

The observations of 100 MeV gamma rays from the Galaxy give us a useful way of studying the Galactic distribution of the 1 to 10 GeV cosmic ray nuclear component.   This is because the gamma rays appear to predominantly originate in collisions between the cosmic ray nuclei and the interstellar gas.   Comparison of the measured spectrum of gamma-rays between 10 - 1000 MeV from the Galactic centre (figure 3 Chapter 3) and the theoretical spectrum for this process (figure   Chapter 2) indicates that this is indeed the case and enables one to rule out a large contribution from electron Bremsstrahlung at, say, 100 MeV.   Furthermore, in Chapters 6 and 7 it was shown that the contribution from the cosmic ray electrons in Bremsstrahlung and inverse Compton scattering was considerably smaller than that from the cosmic ray nuclei. The fact that the π^o production and decay process apparently dominates is of great importance in simplifying the interpretation, especially since the electrons are already known to be of Galactic origin.

Assuming this fact, the Galactic distribution of the intensity of the cosmic ray nuclei may be deduced from the gamma ray observations using a map of the Galactic gas distribution.   This was carried out in Chapter 7 where it was shown that the flux of gamma rays from the broad region of enhancement around the Galactic Centre implied an increase in the cosmic ray intensity near the Galactic centre.   A comparison between the deduced cosmic ray and the source candidate distribution was made and some tentative conclusions were drawn about cosmic ray propagation.   Thus it was found

that the distribution of the cosmic rays and the source
candidates were very similar supporting the hypothesis of
cosmic ray origin in supernovae, their remnants or pulsars
and suggesting that cosmic rays diffuse no more than 1 - 2
kpc before escaping.

However, there are some difficulties with this interpretation
of the Galactic centre observations.   Basically, there are
two major problems which introduce considerable uncertainty
into the interpretation.

Firstly, as discussed in Chapter 7, the absolute
densities of molecular hydrogen are not known with any
confidence.   In Chapter 7 it was shown that to achieve
agreement with the observations using the atomic and
molecular hydrogen distributions of Gordon and Burton (1976)
the cosmic ray intensities at 5 - 6 kpc must be a factor
of 4 greater than the solar system values.   The form of
Scoville & Solomon (1975) molecular hydrogen distribution
is basically in agreement with that of Gordon & Burton;
yet using these authors' normalization, it is found that
the cosmic ray intensity required to explain the observed
gamma ray flux is only a factor of 2 up on the solar system
value.   Since it is generally agreed that the uncertainty
in converting from the carbon monoxide observations to the
molecular hydrogen density is the order of a factor of 2
this leaves open the possibility of explaining the
observations by a constant cosmic ray intensity.

The second problem is that of the contribution from
pulsars.

The simplest procedure to estimate the pulsar
contribution, given the Crab and Vela pulsars as examples

of gamma ray sources is to assume that the rate of gamma
ray production is proportional to the rate of total energy
loss, (obtained from the spin down rate), and use the Crab
or Vela pulsars as normalization.   This method was used
by Dahanayake et al (1976) using the pulsar catalogue of
Taylor and Manchester (1975).   The contribution was found
to be negligible except for the Crab and Vela pulsars.
Higdon and Lingenfelter (1976), however, have used much the
same method but concentrate on the contribution from as
yet unobserved young pulsars and their results suggest
that the gamma ray observations may be explainable by a
uniform cosmic ray intensity over the whole Galaxy plus
a contribution from 40 or 50 or so young pulsars.

Clearly, it is not possible to decide between the
Galactic and Extragalactic origins for cosmic rays by
using the Galactic centre observations, simply because
of the uncertainties in the interpretation.   Fortunately,
these problems do not complicate the interpretation of the
Galactic anticentre to the same degree.   Thus, in chapter
8 where the gamma ray flux from the Galactic anticentre
was examined in some detail, it was possible to rule out,
with some confidence, a uniform cosmic ray flux and hence
reject an Extragalactic origin for the majority of the
cosmic ray nuclei with energies around 1 - 10 GeV.   At
the same time a plausible model for the cosmic ray distrib-
ution based on the distribution of population I objects in
outer part of the Galaxy was found to give good agreement
with the observations.   Furthermore, it is important to
note that the existence of a significant quantity of

molecular hydrogen or a contribution from pulsars merely
requires that the cosmic ray gradient be steeper and
strengthens the conclusions.

There remain a number of questions to be resolved.
For example, in Chapter 7 it was shown that the intensity
of cosmic rays within dense molecular bearing clouds may
not necessarily be uniform across the cloud. The screening
process proposed may be very important for the gamma ray
yield from the Galactic centre but to include it in the
calculations requires more theoretical work on the process
and additionally an improved knowledge of the spectrum of
cloud sizes. Further, the problem of the thickness of
the molecular hydrogen layer requires more observations since
the present observations of the layer thickness are restricted
to very few directions. It is possible that the layer
thickness may vary across the Galaxy and hence the present
estimated molecular hydrogen content may be greatly in
error.

Finally, it is to be hoped that future observations
of the fluxes of the gamma rays from the Galactic plane
may help to resolve the question of the point source contri-
butions and enable the controversy of Galactic or Extra-
galactic origin for cosmic ray nuclei to be quite
definitely resolved.

REFERENCES

Dahanayake, C., Dodds, D. & Wolfendale, A.W., 1976.
Reprint.

Gordon, M.A., & Burton, W.B., 1976. Reprint.

Higdon, J.C., & Lingenfelter, R.E., 1976. Astrophys. J.,
208, L107.

Scoville, N.Z., & Solomon, P.M., 1975. Astrophys. J.,
199, L105.

Taylor, J.H., & Manchester, R.N., 1975. Astron. J.,
80, 794.

ACKNOWLEDGEMENTS